# Virtual sensor for air mass flow measurement in an SI engine

## Application of distributed lumped modelling in prediction of air mass flow into the cylinder of SI combustion engines

Sotirios Filippou

Submitted for the Degree of

Doctor of Philosophy

The Faculty of Engineering and Informatics

University of Bradford

2018

## Abstract

Sotirios Filippou

Virtual sensor for air mass flow measurement in an SI engine

Application of distributed lumped modelling in prediction of air mass flow into the cylinder of SI combustion engines



Keywords: Engine air mass flow, D-L modelling, transient engine testing



After undergoing an extensive study about engine air mass flow measurement approaches as well as engine modelling for air mass flow prediction, a major problem found to exist is that engineers have still not found a suitable technique to accurately measure the air mass flow entering the cylinder of an internal combustion engine. The engine air mass flow is the most important parameter needed during engine development so the fuel control can be accurately calibrated and as a result increase performance and reduce emission output of an engine. The current methods used to determine the air mass flow lead to inaccuracies due to the large amount of mathematical assumptions and also sensor errors and as a result the mapping and calibration process of a new engine family takes approximately 2 years due to extensive modelling and testing required overcoming the above drawbacks. To improve this, the distributed lumped modelling technique (D-L) of the inlet manifold was chosen, where the intake system is separated into very small sections which are distributed continuously throughout the volume of the intake until entering the cylinder. This technique is validated against a CFD model of the engine's intake system and real engine data as well as a 1D engine model.

## Acknowledgements

I am grateful to my supervisors, Dr Hong- Sheng Qi and Dr Jian- Ping Li for their support and useful advice during the writing up of this work and also for giving me the opportunity to complete it.

I am grateful to my external supervisor Professor K. M. Ebrahimi for his support and advice during this project and also for giving me the opportunity to work on this interesting project.

I am grateful to my family and parents who supported me during the course of this project and their continuous love and encouragement.

Also I would like to thank the University of Bradford and the HyperC laboratory in particular for providing their state of the art facilities where the majority of the experimental work was conducted and the faculty of engineering and informatics in general

Finally I am grateful to my employer, Ford Motor Co, Dunton technical centre for their continuous technical support during this project and for granting me permission to publish pictures and data from this work.

## List of publications

P. Schaal, S. Filippou et al, Robust methodology for fast crank angle based temperature measurement. SAE, 2016. ISBN: 10.4271/2016-01-1072

Ebrahimi K.M., Filippou S, Athanasiou P and Ahmedov, A., Port Based Modelling of Intake and Exhaust System, Submitted to IMechE Part D.

Table of contents

## List of figures

## List of tables

## Nomenclature

$V_{air}$ Volumetric flow rate of air $(m^3/s)$

VE Volumetric efficiency

$V_{cyl}$ Engine cylinder volume ( $m^3$)

n Engine speed (rpm)

$\rho_{air}$ Density of air (kg/$m^3$)

M molar mass of air (kg)

P Pressure (kPa)

T Temperature (K)

R Ideal gas constant (kJ/kg K)

M Mass (kg)

$C_d$ Discharge coefficient

$A_{th}$ Throttle area ($m^2$)

α (t) Throttle plate angle (deg)

t Time (sec)

L Length (m)

D Diameter (m)

C Speed of sound (m/sec)

## List of Acronyms

ECU: Electronic Control Unit

RAM: Random Access Memory

CPU: Central Processing Unit

UEGO: Universal Exhaust Gas Oxygen

D-L: Distributed Lumped

MAF: Mass air Flow

CFD: Computational Fluid Dynamics

MVEM: Mean Value Engine Model

HIL: Hardware In the Loop

SI: Spark Ignition

TDC: Top Dead Centre

BDC: Bottom Dead Centre

AFR: Air Fuel Ratio

MBT: Maximum Brake Torque

MAP: Manifold Absolute Pressure

EGR: Exhaust Gas Recirculation

GTDI: Gasoline Turbo Direct Injection

CAD: Computer Aided Design

RPM: Revolutions per Minute

API: Application Programming Interface

AMPRBS: Amplitude Modulated Pseudo Random Binary Signal

CA: Crank Angle

DoE: Design of Experiment

URANS: Unsteady Reynolds Averaged Navier- Stokes

# Chapter 1: Introduction

This project describes the development process of a virtual sensor for accurate air mass flow measurement in a spark ignition engine.

Nowadays automotive manufacturers consider the importance of emissions and fuel consumption very seriously when they release a new engine family into the market. The reason for that is that regulations related to emissions are so tight that in order to be competitive they need to develop very accurate engine control strategies in order to achieve maximum efficiency and also pass the emission tests set by the relevant organisations worldwide. The above can only be achieved if the engine control unit can provide the necessary amount of fuel for a clean and efficient combustion which in turn means that needs to accurately know (measure) the amount of air entering the engine. A clean combustion process results in a low emission, low fuel consumption engine with the highest possible power output under the whole engine operating range.

The current fuel system technology used in spark ignition engines is direct injection where highly pressurised fuel is delivered to a common fuel rail and injected directly into the combustion chamber of each cylinder. This setup gives engineers the ability to design very efficient engines but also is very challenging because the modern control strategies need to be able to measure the exact amount of air flow so the amount of injected fuel can be perfectly mixed with the air and result to a clean and efficient combustion process.

In this chapter there will be a brief description of the engine control unit and the basic functions it performs, followed by a short description of the inlet manifold and fuel control as well as current methods of air mass flow measurement and estimation. Towards the end of the chapter, the aims and objectives of this work will be stated and how this work can contribute to engine control improvement and last the structure of this thesis will be analysed.

## 1.1 Engine control unit

The complexity of today's cars demands the development of advanced control systems to increase safety, drivability and help reduce the fuel consumption and emission levels. The core of the various control subsystems is the engine control unit (ECU) or powertrain control module in case transmission control is required. The electronic control units were introduced on a larger scale with the introduction of three way catalytic converters in the late 80's for European market when the emission legislation became tighter for vehicles being sold worldwide. It was also clear at that time that future more complex engine systems e.g. turbocharged with variable valve timing and complex drivetrain would not be possible without the development of advanced control systems. [1]


Figure 1.1 Development ECU as used in engine test beds (Courtesy of Bosch)

Modern electronic control units comprise of standard microcontroller hardware such as RAM, CPU etc. and at least 1 additional piece of hardware, which synchronises the engine control commands with the reciprocating action of the engine. Early engine control units had very little processing power and RAM since the amount of inputs from the engine was small hence the commands to the engine was limited (mainly fuel and spark commands). Nowadays with modern vehicles becoming increasingly complex, the processing power of the ECU is increased with many of them having dual or even tri core CPU and increased RAM in order to cope with the amount of signals coming from the engine. The ECU software is typically a code written in programming language such as visual basic or C++ and in most cases is developed by the manufacturer of the ECU and sold to the automotive manufacturers together with the hardware. This software

contains the basic functionality of the ECU and using that the engine has to be calibrated in order to have the optimum performance. This topic will be analysed more in chapter 4.

```
/* begin ptwt_mode.trig */
if (  ( atmr1 > tkyon4 )          /* No more key-on BP updates */
   && ( bpinp_inf_ena == TRUE )    /* No harware failures */
   && ( tpp_theta_fin > lookup_2d(&fnbp_ntp_deg, n) )        /* high enough TP */
   && ( ect > ectbplo )           /* High enough ECT for warm engine  */
   && ( air_cip > bpinp_upd_min )  /* Limit learning to high enough air_cip  */
   && ( delta_air_cip > delmaplo ) /* air_cip not decreasing rapidly (delmaplo should have a negative value) */
   && ( delta_air_cip < delmaphi ) /* air_cip not increasing rapidly (delmaphi should have a positive value) */
   )
{
   /* determine air flow thru throttle body */
   bpptwt_flg = 1 ;                /* BP updated this BG pass */
   am_throt_tmp = ( F32Sqrt ( ( act + 460.0F )/(560.0F) )*( air_am_total - air_lk_tot ) );
   am_throt = f32clip( 0.0f, am_throt_tmp , 63.999f) ;
   bp_engoff_tmr = 0.0F;

   if ( inf_bp > p_epsilon_p) /* removed crkflg==FALSE for SIP/V11.000.000_BPINP
                              ** since when crkflg==TRUE, atmr1=ZERO_FLT;
                              ** when crkflg==FALSE, atmr1 can increase.
                              ** Then if atmr1>tkyon4, crkflg should already be FALSE
                              */
   {
      /* determine instantaneous inferred bp */
      am_throt_bp = am_throt / inf_bp;
      ibap_tmp = air_cip + inf_bp * lookup_3d( &fn1033_deg__A, tpp_theta_fin, am_throt_bp ) ;
      inf_ibap = f32min(ibap_tmp, bpmax) ;
   }

   inf_bp = rolav( inf_bp, inf_ibap, bpptwt_fk) ; /* filter instantaneous barometric pressure  */
}

else if (  ( eng_not_turning == TRUE ) /* Allow BP update when in Key-on, engine not turning  */
        && ( hev_ok_tmp == TRUE )
        && ( bp_engoff_sw != FALSE )  /* Applicatation must have a SIP or MAP sensor         */
        && ( air_cip > bpmin )        /* air_cip value is reasonable                         */
        && ( air_status_failed(air_ffg_status,AIR_CIP) == FALSE )  /* air_cip reading valid  */
        )
```

Figure 1.2 Example of ECU software code (courtesy of Ford Motor Co.)

## 1.2 Inlet manifold

The inlet manifold is a significant component of any modern internal combustion engine and is responsible for distributing the fuel-air mixture (or just air in direct injection engines) into the combustion chamber. A well designed intake manifold increases the performance of the engine significantly as it ensures even distribution of the combustion mixture (or just air) into the cylinders thus improving the combustion process. It is also being used for mounting various sensors measuring pressure and temperature which give additional information to the engine control unit and also crucial engine components such as fuel injectors and throttle bodies. Most inlet

manifolds use injection-moulded plastic or in high boost turbocharged engines aluminium is used for extra strength. Most of the components are also undergoing rigorous testing using simulation and finite elements software to ensure robustness during service and minimise tuning phenomena during engine operation, which can disrupt the airflow. It also has to stay cooler that the engine temperature during operation and ensure a perfect seal with the cylinder head otherwise the engine operation will be compromised due to additional air entering the engine for which the engine control unit is unaware of.

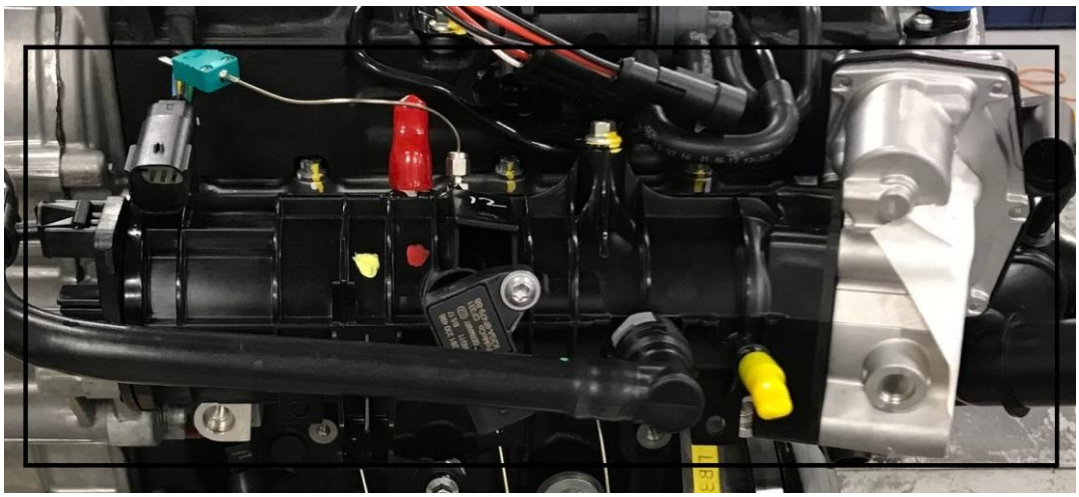

Figure 1.3 Inlet manifold on a development engine

### 1.3 Engine fuel control

One of the most important things within the ECU strategy is the determination of the required fuelling during engine operation. This is mainly because the combination of the correct prediction of the air mass (air charge) and fuel quantity can ensure maximum efficiency under all engine conditions and reduction of the emissions due to good combustion of the mixture. On modern engines, this is achieved by using closed loop control, which means

that certain sensors are providing feedback to the ECU and certain parameters are altered accordingly. Below you can see an example of a Lambda sensor or else called UEGO (for universal exhaust gas oxygen) which is the most critical one when it comes to closed loop fuel control. [2]

Figure 1.4 UEGO sensor (courtesy of Ford Motor Co.)

These kinds of sensors also have special heating elements inside to ensure the sensor stays at an optimum temperature at all condition so its accuracy is not affected.

### 1.4 Air mass flow measurement

The accurate measurement of the air mass entering the engine is very crucial as described earlier at the beginning of this chapter. At the moment during the mapping process of a new engine, the engineers use either mass airflow sensors or the speed- density equation, which is based on the ideal

gas law. The main reason they have to rely on these methods is that there is not currently a method with which the air mass can be measured directly just before entering the combustion chamber. That explains why it is important to be able to predict the air mass flow into the cylinder as accurately as possible and compare it with real engine testing data and simulations to make sure the necessary accuracy is achieved which in turn will lead to the right engine mapping and calibration process during engine development.

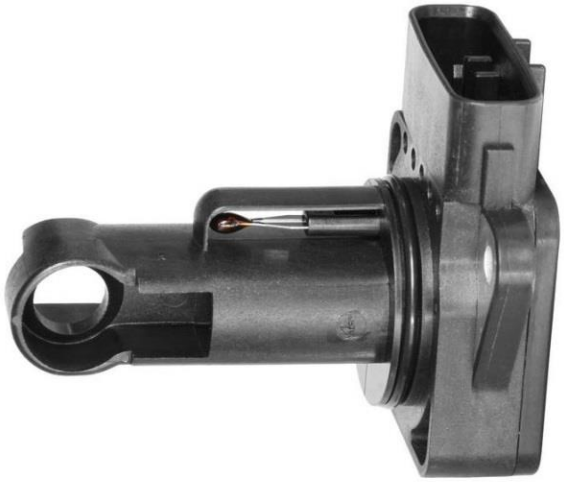

Figure 1.5 Mass airflow sensor (courtesy of Bosch)

### 1.5 Aims & Objectives

The aim of this project is to design a virtual sensor using distributed- lumped (D-L) modelling technique in order to predict the engine air mass flow at the inlet port of a spark ignited internal combustion engine. In addition to the D-L model development, special transient testing methodology was developed as well as a virtual engine model using WAVE software. These will be used to validate the D-L model against the real engine and the virtual engine data

which are at the moment the standard industry techniques for engine air mass flow measurement.

### 1.6 Contribution

After studying the SI engine air mass flow prediction literature, it was obvious that the current methods used to estimate engine air mass flow during engine mapping have flaws. In addition because they require a lot of mathematical calculations and as result assumptions, the accuracy is compromised. This project will present a novel method for predicting the engine air mass which could also run in real time thus minimising the need for extensive engine modelling and testing.

## 1.7 Structure of the thesis

The thesis consists of nine chapters. The literature review and background information to the air mass flow measurement are given in chapter 2. This is very essential as it helps understanding how essential this aspect of control and measurement is to modern internal combustion engines. Next is chapter 4 which describes the experimental setup and the testing methodology developed specifically for this work. It gives a thorough insight on state a state of the art powertrain testing facility and also describes the advanced methodology required for transient engine testing implementation. Chapter 5 analyses the engine test results ensuring that the data are high quality and suitable to be compared later on with virtual data as a validation platform. Chapter 6 describes the process of generating a virtual engine model in WAVE software as well as describing the main features and capabilities of the software. This software is used in industry by the sponsor (Ford) of this work and that is the reason it was preferred. Next follows chapter 7 which is very important as it describes the validation process between the virtual engine data and the real engine data. It is also a good indication if the virtual and real engine data correlate. In chapter 8 the D-L model and the technical details of this technique are presented and thoroughly analysed and the model is validated against a CFD model developed in ANSYS which is a widely used software in automotive industry. Finally chapter 9 is about the discussions and conclusions of this work and any future work that has to be undertaken either in an industrial or a research environment.

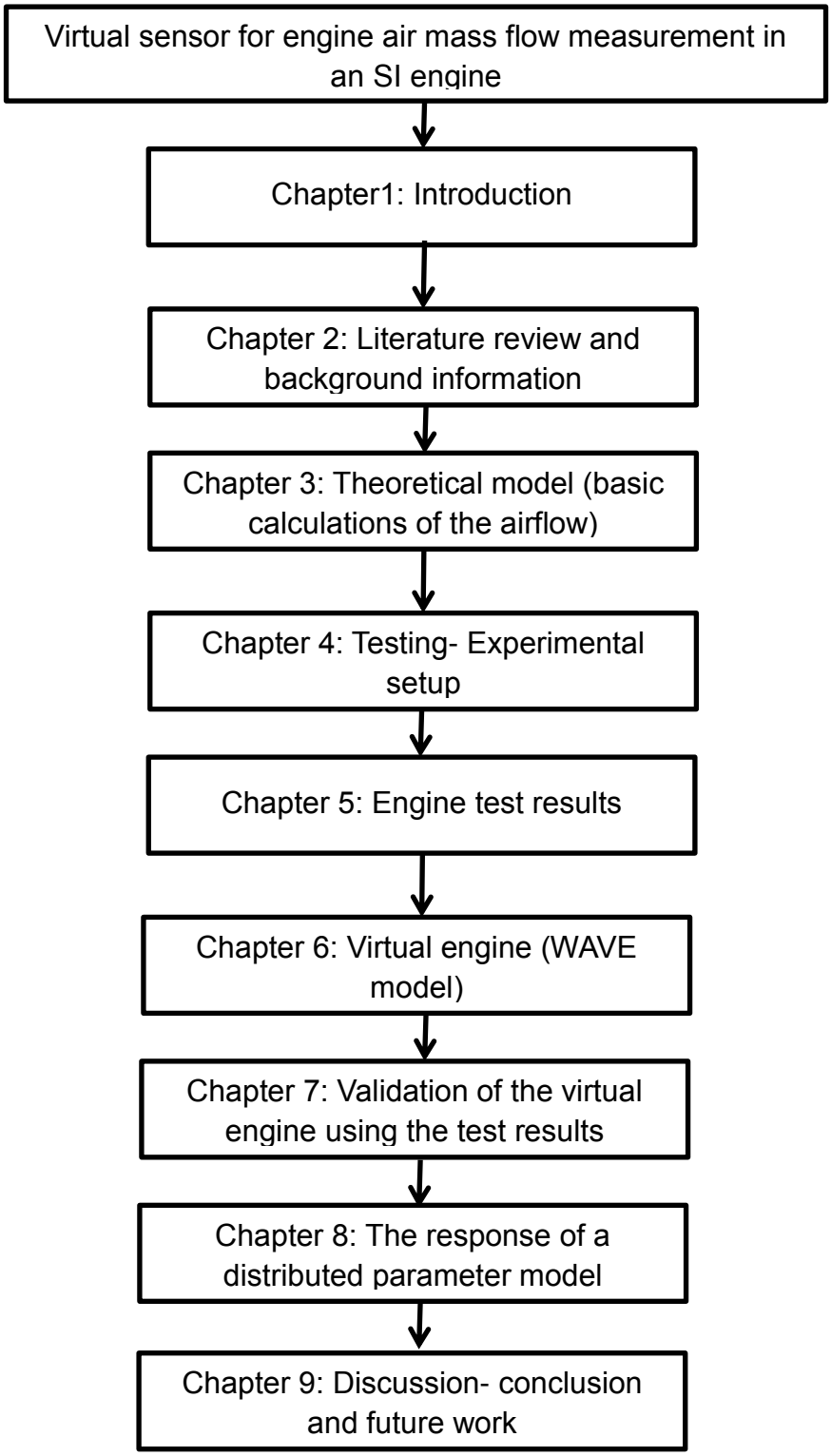


Figure 1.6 Structure of the thesis

# Chapter 2: Literature review and background information

This chapter is about the literature review and some background information on the history of engine control and airflow measurement, followed by some background information on the engine airflow measurement evolvement. Next the difference between the measurement, prediction and actual air flow are described. The next paragraph gives an introduction on to different types of engine modelling, followed by applications of engine modelling by engineers nowadays. In addition, the spark ignition engine operation and control is described based on the existing literature and towards the end of this chapter the importance of air mass flow measurement is explained, followed by the current air mass flow measurement and estimation techniques derived from literature.

## 2.1 History of engine control and airflow measurement

Since the introduction of the electronic control for engines in the mid 1970's, the engineers needed to find the right techniques to parameterise the software and ensure smooth operation and high power output of the engines. [3] This was not necessary while the engines were purely mechanical systems so it is apparent that the electronic engine control has significantly made the engine development process a lot more complicated. [4] At the beginning when the engines first adopted electronic control, the electronic control unit consisted of pre-configured look up tables for the fuel and spark control which were populated by the mapping engineers while the engines were tested on the dynamometer. As a result very basic sensors were installed on the engine mainly for reporting the engine speed and the coolant

temperature. At that point it is obvious that the ECU was running in open loop control without dynamically receiving feedback from the engine sensors. With the introduction of stricter emissions standards it was soon apparent that the above approach of parameterising the engine control unit was not adequate and engine developers should find a new way to accurately parameterise the fuel control of the engine in order to reduce emissions while maintaining the power output of the engine.[5] They soon realised that in order to dynamically provide the right fuelling during engine operation, the amount of air entering the engine needed to be determined. By knowing the amount of airflow into the engine the relevant fuel maps could be configured to provide the exact amount of fuelling to maintain stoichiometric air-fuel ratio. At that point engine control became a lot more complicated as many sensors needed to be added to the engine to support the closed loop engine control required to achieve such a level of accuracy. The most important of the sensors added was the mass air flow sensor (MAF) which could inform the ECU about the amount of air mass flow entering the engine. This would prove very beneficial as now engineers could more accurately parameterise the fuel control and make the engines more efficient and also environmentally friendly. Soon after it was apparent, that the above sensors were not very robust and could fail after only a few years in service due to sensor contamination especially in harsh environments with significant effects on engine performance and fuel consumption.[6] At that point a lot of research was going on in order to find alternative ways of air mass flow estimation such as the speed- density method which is analysed later on in

this chapter and also modelling techniques that could predict the engine air flow. [7]

## 2.2 Background of engine airflow measurement evolvement

As mentioned in the previous paragraph, the first implementation of air mass flow measurement on an internal combustion engine was the use of the mass flow sensor. By using this sensor the air fuel ratio control of the engine became more accurate and the engines could pass the upcoming strict emission regulations. These sensors are typically installed at the beginning of the air cleaner and are wired directly to the ECU. [8] After being used for a few years it became obvious that the high manufacturing costs of these sensors and their sensitivity on harsh environments made them less favourable among engine manufacturers. Furthermore, modern engines during their service life operate quite transiently and the response of these sensors is not high enough for accurate measurement during transient operation. To overcome the above disadvantages, researchers started experimenting with different type of sensors which measure the volume of the air entering the engine instead of the mass. [9] Such sensors are the vane meter and the Karman vortex sensors. These sensor types are not as accurate as the MAF sensor but they are more resilient in harsh operating environments and also have faster transient response. All the above sensor types are located at the beginning of the air cleaner which is normally a fair distance from the inlet port. The next evolution of the engine air mass flow is the development of the speed-density method. [10] With the emissions standards becoming more stringent, engineers realise that by using MAF of volumetric type sensors they were making a big trade- off between accuracy

and reliability. The speed-density method which is analysed later on in this chapter gave the opportunity to engine developers to estimate the air mass flow as a function of engine volumetric efficiency. The main advantage of this method is that the sensors required are located a lot closer to the inlet ports and also are not affected by pulsation occurring in the inlet manifold and thus providing more accurate readings. Most major automotive manufacturers use the speed- density approach nowadays to predict the engine air mass flow. With the advancement of computer technology, engine developers had the opportunity to develop engine models which could simulate the engine operation and predict the engine air mass flow. [11] These models can be either mathematical, physics based as explained later on this chapter or using computational fluid dynamics (CFD). [12] The main advantage of this technique is that the models can be used in conjunction with the measurement techniques to ensure accurate results while reducing the engine development time and as a result the costs. [13] Finally the most recent method used by engine developers for air mass flow prediction is the use of mathematical modelling in conjunction with observers. [14] The observers used for such studies can be based on constant gain extended Kalman filter theory to tune the observer or on speed – density principle. [15] They are very effective on predicting the engine air mass flow as they can filter the intake manifold pressure signal and also predict the manifold pressure during transients. [16] In order to calculate the air mass flow into the engine using an observer, the air intake system needs to be modelled. Normally this is includes a model of the throttle body for increased accuracy. [17], [18]

## 2.3 Difference between measurement, prediction and actual airflow

In the previous paragraph the ways of measuring or estimating the engine air mass flow based on the current literature were analysed. In reality the measured or estimated air mass flow is not the same as the actual air mass flow entering the cylinder. [19] Starting with the measured air mass flow it is worth noting again that the sensors are located at the beginning of the air path before the air cleaner. The distance between that point and the inlet port is quite significant and in between these two points there is a complex system of duct and pipes. While the engine is operating there are filling and emptying dynamics phenomena in the inlet manifold and the air path which means that what is measured at the air cleaner is not what enters the engine at the inlet port. [20] There is also pulsation phenomena in the intake manifold occurring from the valve timing of the engine which affects the reading of the sensors adding into inaccuracy. To make things more complicated, the sensors used for such an application deteriorate during their service life which means that there is an additional factor of possible false information into the ECU. On the other hand using the speed- density method has its disadvantages as well. This method uses complex mathematical calculations where many assumptions take place and thus reducing the accuracy of the method. Furthermore, it relies on volumetric efficiency tables which require parameterisation. [21] This is a very lengthy process which requires a lot of testing to be completed. Finally the main sensors feeding information for the speed- density calculations are located in the air path and not near the inlet port of the engine and as a result reducing the accuracy of this technique. Finally the modelling techniques although

they can predict the air mass flow reasonably accurately, are too complicated. As a result they can only be used as indication of the engine air mass flow because they cannot be implemented into real time inside the engine's ECU during operation. The reason for that is that the size of these models and their complexity would require a very powerful engine control unit which mean that it would be uneconomical for the automotive manufacturers to supply their engines with such a unit. [22]

A solution such as the one described in this work by using D-L modelling to measure the air mass flow at the intake port is ideal because not only it can accurately measure the airflow entering the engine but also being less complicated to the traditional modelling techniques, it can be directly implemented inside the control unit of the engine using rapid control prototyping software. This means that the fuel control can be accurately parameterised to ensure the optimum AFR control during engine operation and also during high transient operation.

### 2.4 Types of engine models

Generally there are two different types of models used to represent an internal combustion engine for control development and calibration [23]

- Look up table based engine models
- Physics based engine models

Both of these approaches use sets of equations to describe the engine within specific boundaries and assumptions. The main difference between them is that the look up table based models use equations that are related to measured input and output responses of different sub systems while in the

physics based models, the equations are representing actual variables within the engine. The parameters used in both of the above models are measured from a real engine. [24], [25]

### 2.4.1 Look up table based engine models

A look up table based engine model can describe the engine operation with very good detail. In order to generate a look up table model, experimental data tables are needed to describe the relation between the engine variables. Except from offering good detail, this sort of model is also very easy to generate and requires minimum CPU power. The main drawback of this modelling technique is that there is no flexibility as the engine data tables can describe only one engine configuration and if the engine design changes, then a different set of experimental data is required.

### 2.4.2 Physics based engine models

The physics basics engine models are the most popular type used for engine modelling and can be sub- divided into two main categories.

- Mean value engine models (MVEM)
- Crank angle based engine models

Starting with the mean value engine models and based on their name they express all the variables which are related to the engine's operation in a cycle to cycle basis considering only the mean values over a full cycle. [26] The mean value engine models are lumped parameter models using physical principles and they are capable of running in real time using relatively low computational power producing quite accurate results. [27] The main

disadvantage of this modelling technique is that a change in one of the engine's parameters will have no effect on the engine model until an engine cycle has been completed. Furthermore, it is impossible to observe how any engine parameter behaves during the course of an engine cycle and also what effects this parameter has to the overall engine system. [28] This type of modelling technique is generally preferred when simplicity and real time implementation is the target. In addition, it is the most flexible way of modelling an engine and also less demanding in computational power. [29] Finally it is worth mentioning that in mean value engine models, the engine torque, engine speed and any other parameter that is developed in time is described with a relevant time delay in order to mimic the engine's response to changes realistically. [30], [31]

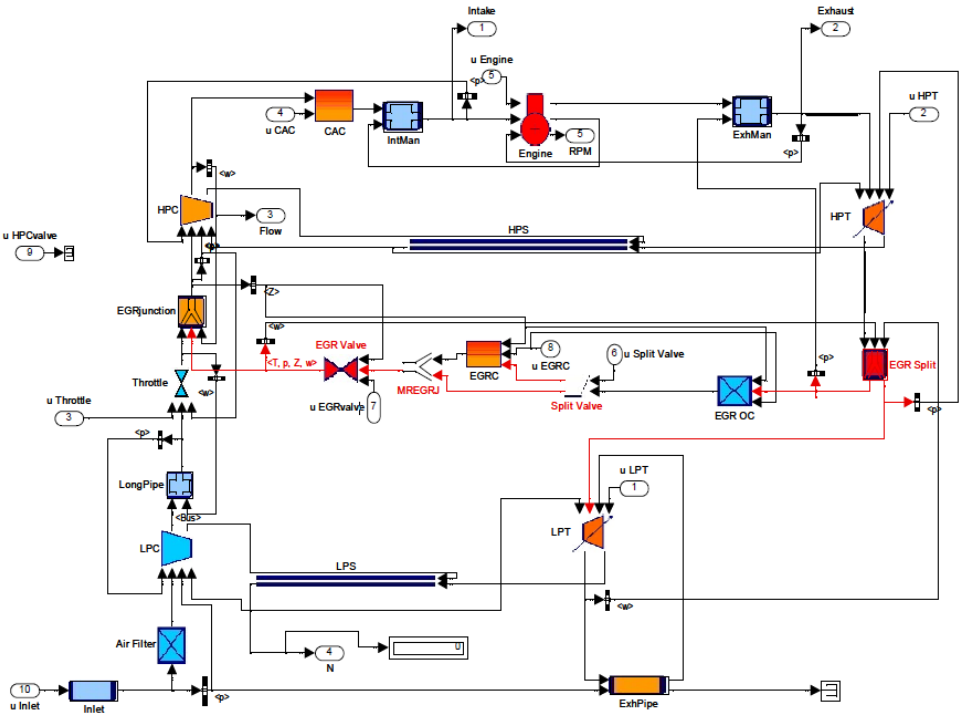


Figure 2.1 MVEM in Simulink

On the other hand, the crank angle based models can capture in great detail all the events taking place during every angle of the engine's rotation and also considering the progression of each engine parameter individually through each cycle. [32] Such modelling techniques offer more in depth analysis of the air intake dynamics which increases the level of their accuracy. This level of accuracy makes this type of models highly desirable during engine development as it is the most accurate way of simulating a virtual engine to the real engine. [33] A drawback of this type of modelling is that due to the high accuracy and complexity of the model and equations the computational power required for simulation is quite high and also the simulation speed is significantly slower compared to MVEM's. As a result this type of models is unsuitable for hardware in the loop testing where both the engine model and the engine hardware (ECU, sensors) are connected unless is specially converted from a MVEM. [34] To sum up it can be said that the each of the physics based models described above is suitable for certain applications and that determines which model type is chosen. For example in applications where simplicity and low computational power is preferred, the mean value model is preferred while whenever cyclic data and high accuracy is the target, the crank angle based model is preferred. [35]

## 2.5 Applications of engine modelling

The introduction of engine modelling during the 1970's has revolutionised the engine development process. This makes the applications where modelling can be used almost unlimited. Computer engine models are primarily used during the design process of a new engine family as they give the ability to engineers to simulate the engine which speeds up the development process.

[36] Another main advantage of engine modelling which makes it favourable among engine developers is that it reduces the actual testing time of the real engine and thus reducing the development costs significantly. Also engine modelling serves as a tool to understand and analyse the various phenomena occurring during engine operation and possibly develop diagnostic algorithms as well. [37] Finally engine modelling is widely used for engine control development as it can facilitate the development and testing of control algorithms in real time or not. Recently with the advancement of electronics and computer technology a new type of simulation which combines software and hardware is used. It is the so – called HIL (hardware in the loop) where engine hardware such as ECU or throttle motor and throttle position sensor are connected to a mathematical model running for example in Simulink. [38] This HIL application is very beneficial during engine control development as it gives the opportunity to the developers to test the real engine hardware connected to a representative model and identify possible issues such as signal noise level, hardware reliability etc. before the hardware is connected to the real engine. [39]

## 2.6 SI engine operation and control

The internal combustion engines have been chosen over the year as a propulsion method for most of the different vehicle types due to their relatively high efficiency and low production cost. They can be divided to many different categories mainly based on their capacity, number of cylinders, valve train type but the most important classification is based on the type of fuel they are burning. There are two main types of internal combustion engine, the spark ignition (SI) and the Diesel engine. Both types

of internal combustion engines have carried on developing through the years. Originally at the early stages the target was to increase performance and reliability while the last thirty years with the development of the electronic control strategies the objective is to reduce emissions and fuel consumption without compromising the performance at the same time.

### 2.6.1 SI engine operation

The SI engine operates following a repeated cycle of four strokes which are the intake, the compression, the expansion and the exhaust stroke. [40]

Intake stroke: During that stroke the piston is at TDC (Top Dead Centre) and the intake valve(s) is open. While the piston moves towards the BDC (Bottom Dead Centre) fresh air-fuel mixture is drawn to fill the cylinder. In case of a direct injection engine where the actual fuel is injected inside the cylinder, only air is drawn inside the cylinder during the intake stroke.

Compression stroke: During that stroke, the inlet valve closes just after the piston hits the BDC and the air – fuel mixture is trapped inside the cylinder. The piston moves from BDC to TDC compressing the mixture and thus the temperature of the mixture. During that stroke in theory there should not be any flow out of the cylinder if the engine is in good order but in most cases there is some flow escaping through the piston rings to the crankcase referred to as blow- by. [41]

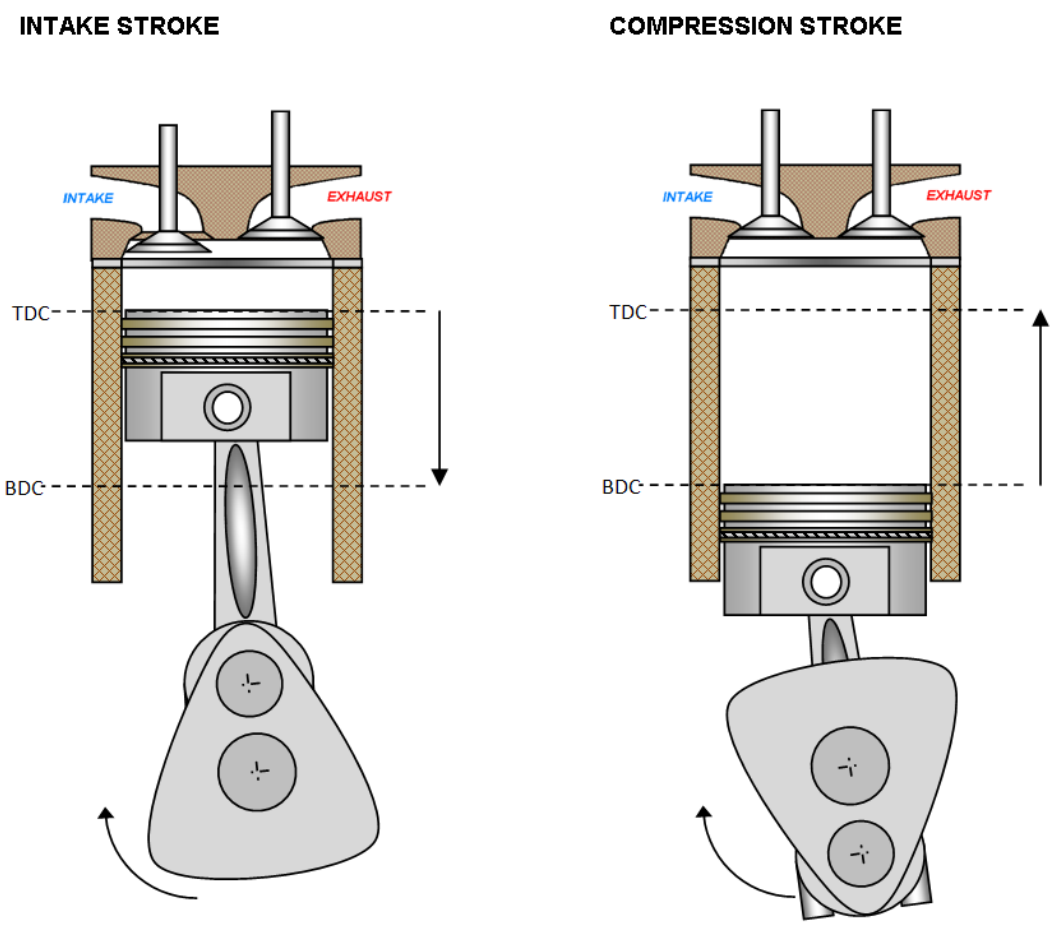


Figure 2.2 Intake and compression strokes

Expansion stroke: Towards the end of the compression stroke the spark plug is energised which results in ignition of the air – fuel mixture which is under pressure. This means that the combustion process has started and the gas pressure pushes the piston towards TDC. This stroke is the only one producing work and this is why it is commonly referred as power stroke.

Exhaust stroke: During that stroke the exhaust valve(s) opens just before the piston reaches BDC and while the piston moves up again towards TDC it pushes all the gases out from the cylinder towards the exhaust manifold.

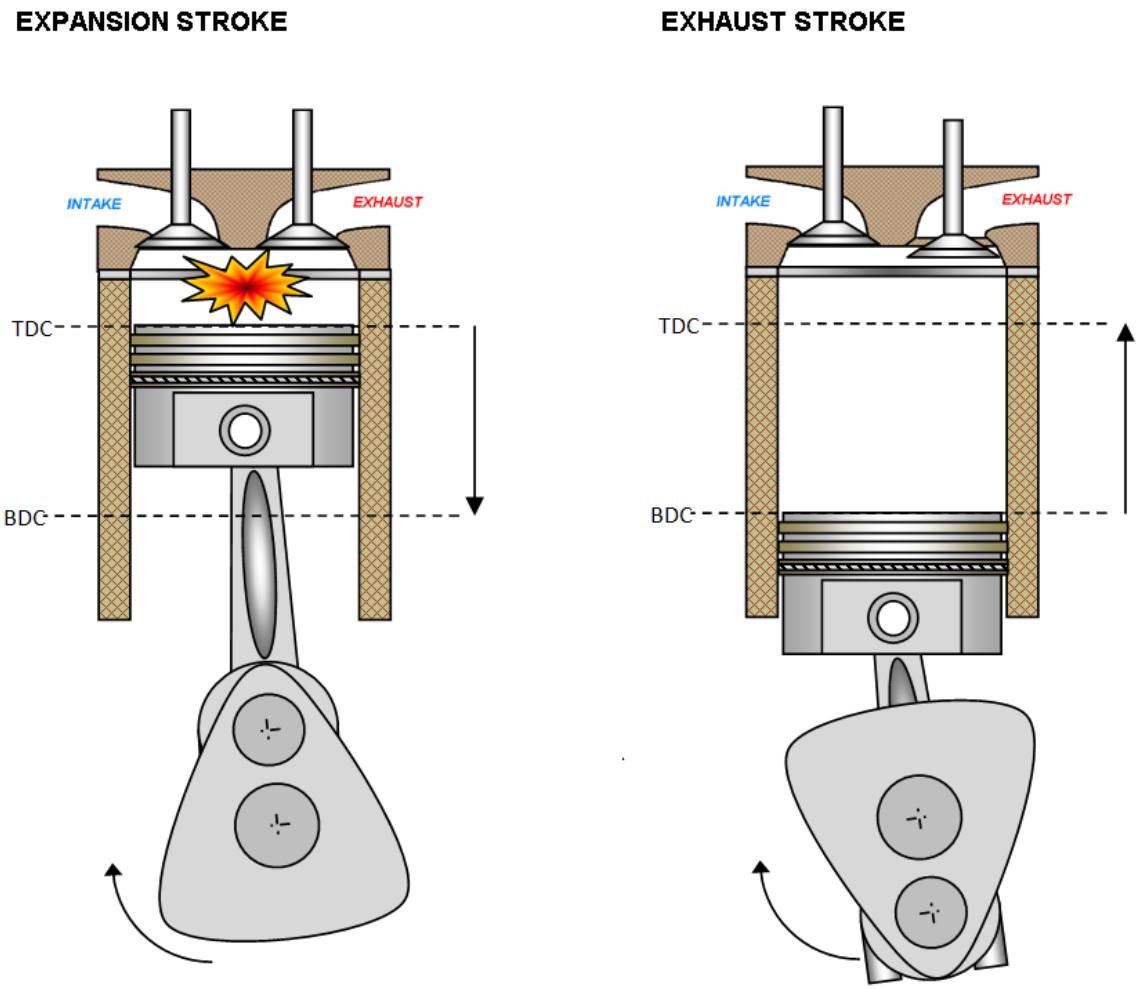


Figure 2.3 Expansion and exhaust stroke

### 2.6.2 SI engine control

The SI engine when firstly appeared was a purely mechanically controlled system where various subsystems where mechanically connected and controlled to assist the engine operation. With the emission standards becoming stricter every year and the need to reduce fuel consumption without affecting performance, this resulted into the engine being evolved to a very complex electronically controlled system. Most engines nowadays incorporate complex control systems such as variable valve timing, spark

timing and fuel control algorithms, exhaust gas recirculation etc. in order to achieve high efficiency and smooth operation while maintaining the maximum power output. In this paragraph only the fuel and spark control will be described as they are the ones found in every modern engine.

Fuel Injection: Over the years many different injection systems have been used on SI engines. During the transition from carburettors to injection systems the most common system was the single point injection system. In that configuration there was a single throttle butterfly valve with a single injector distributing the air- fuel mixture in all cylinders. Their main advantage at that time over the carburettors was that the engineers gained some very basic control over the fuel timing and also these systems could be easily fitted on existing engines running on carburettors. The next system that followed was the multi point injection system. This is used very commonly even on modern engines and basically comprises of one injector per cylinder placed directly on the intake manifold next to the inlet port. A central throttle body at the beginning of the manifold is controlling the air flow of the engine. Depending on the engine, the injectors can be fired simultaneously or sequentially. Finally the latest injection system is the direct injection system where the fuel is directly injected inside the cylinder. This technology allows control engineers to accurately control the spraying of the fuel and in combination with the very high pressure of the system a perfect mixture of air and fuel can be achieved. The main objective of the fuel injection system is to control the air- fuel ratio (AFR) as accurately as possible to the stoichiometric value (14.7 kg of air/ kg fuel) where the catalyst operates at its highest efficiency. [42]

Spark timing: Another very important control parameter of an SI engine is the spark timing. The combustion process inside the engine requires a specific amount of time to complete thus the timing of when this process starts is very crucial and is controlled by the spark timing. Every time the spark plug is energised, the flame starts next to its tip and propagates fast through the combustion chamber. This is the so- defined flame speed. During the combustion process the temperature and pressure increase rapidly. If in an area of the combustion chamber the un- burnt mixture temperature exceeds a certain limit, it will self-ignite. That means that there are large pressure and temperature oscillations which can damage the engine. From all the above it is obvious why the spark timing control is so crucial for the engine operation. The maximum pressure and temperature have to be kept below the knock limit which is only possible by altering the spark timing. The spark timing is also called spark advance and is measured in degrees of crank angle before TDC. There is a value of spark timing for every engine operating condition which results in the maximum brake torque (MBT) produced by the engine. By reducing (retarding) the spark timing the torque output of the engine is reduced and by increasing (advancing) the spark timing knock can occur. [43]

ECU: As described briefly in chapter 1 of this work, the ECU is the core element controlling the engine including the spark and fuel which were described earlier in this paragraph. Its main target is to control the engine actuators and achieves that by monitoring various engine sensors and making the right actuation during engine operation. At this point it is worth noting the most common sensors which can be found in every modern

engine and are monitored by the ECU in order to ensure efficient operation of the engine.

- MAP and MAF sensors which are used for measuring the manifold absolute pressure and mass air flow to the engine respectively. These sensors are described analytically later on this chapter as they are a crucial part of this project.
- Lambda sensor which provides a signal to the ECU related to the amount of oxygen which is present in the exhaust gases. From that signal the ECU can determine if the burnt mixture was rich or lean and adjust the fuelling accordingly.
- Air temperature sensor which is used by the ECU to determine the temperature of the air entering the engine and thus the density of the air. The importance of this sensor is described later on in this chapter.
- Coolant temperature sensor which is used to determine the engine's components temperature such as the cylinders and the engine block. Based on this sensor, the ECU can adjust various actuators to make the engine operating smoothly and efficiently from cold start until it is fully warmed up.
- Crankshaft position sensor which informs the ECU about the speed of the engine and also at what point the engine pistons are at TDC. This signal is very important for the spark timing actuation
- Knock sensor which outputs a high frequency signal to the ECU when knocking occurs and as a result the spark timing can be adjusted to restore the normal operation of the engine.

Finally it is worth mentioning that the ECU algorithms are separated into two main categories, open loop and closed loop control. A closed loop control structure is where the actuation parameters are evaluated constantly by monitoring various engine sensors as a feedback to the ECU. Based on that feedback the ECU makes the right actuations. An open loop control is when the ECU makes the necessary actuation but uses no feedback to determine if the goal has been achieved. [44], [45]

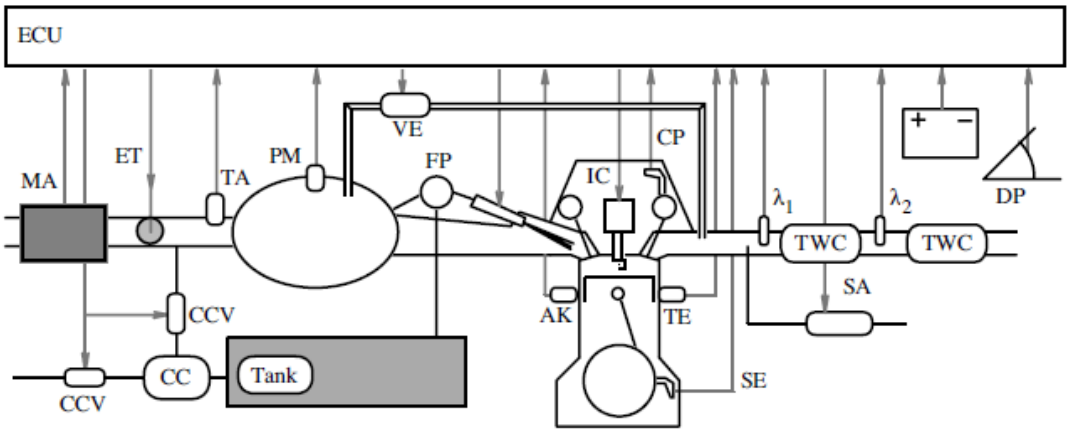


| | | | | | |
|---|---|---|---|---|---|
| AK | knock sensor | PM | manifold pressure sensor | VE | EGR valve |
| CP | camshaft sensor | ET | electronic throttle | SA | secondary air valve |
| IC | ignition command | TA | intake air temperature sensor | TWC | 3-way catalyst |
| MA | air mass-flow sensor | TE | cooling water temperature sensor | ECU | controller |
| SE | engine speed sensor | CC | active carbon canister | CCV | CC control valves |
| FP | fuel pressure control | $\lambda_{1,2}$ | air/fuel ratio sensors | DP | driver pedal |

Figure 2.4 Schematic representation of sensors found on modern SI engines [44]

## 2.7 Importance of air mass flow measurement

By reading all the above paragraphs of this chapter it is easily understood that the SI internal combustion engine has evolved into a very complex electronically control system with various complicated subsystems. Basic engine design and testing is not enough anymore to ensure a successful and

efficient engine and it has to be combined with advanced mathematical modelling and hardware in the loop testing to develop the necessary control strategies in the ECU. In the recent years the SI engine has to face increasing competition from other methods of propulsion such as electric motors and hybrid powertrains. This makes the need for efficient and accurate control imperative. The recent years, engine development has been focusing on improving engine efficiency and emissions in order to maintain the advantage of the SI engine against other means of propulsion. The most important element to achieve that is for the ECU to accurately measure the engine air mass flow. The ECU requires knowing the exact air mass flow in order to set the required fuel duration and timing for each condition and the correct spark timing so the maximum torque can be achieved. If the engine air mass flow is not measured or calculated by the ECU that has serious consequences to the engine operation. In such case the wrong fuelling will be triggered which makes the engine inefficient and will increase the emissions and also the wrong spark timing which will cause significant loss of torque or even knock events. From all the above it is very obvious why the engine air mass flow is so important and also why engineers are trying constantly to find new ways to measure or estimate it so the best possible engine efficiency and performance can be achieved. In the next paragraph the current methods of measuring or estimating the engine air mass flow will be presented and analysed.

## 2.8 Engine air mass flow measurement and estimation techniques

In this paragraph the air mass flow measuring techniques will be presented as well as some methods currently used by engineers to estimate the air mass flow.

### 2.8.1 Hot wire sensor

This is the most widely used sensors by automotive manufacturers and measures directly the air mass flow of the engine. It is normally connected on the air box assembly and its principle of operation is based on the hot wire anemometer. In figure 2.2, a hot wire air mass flow sensor can be seen.

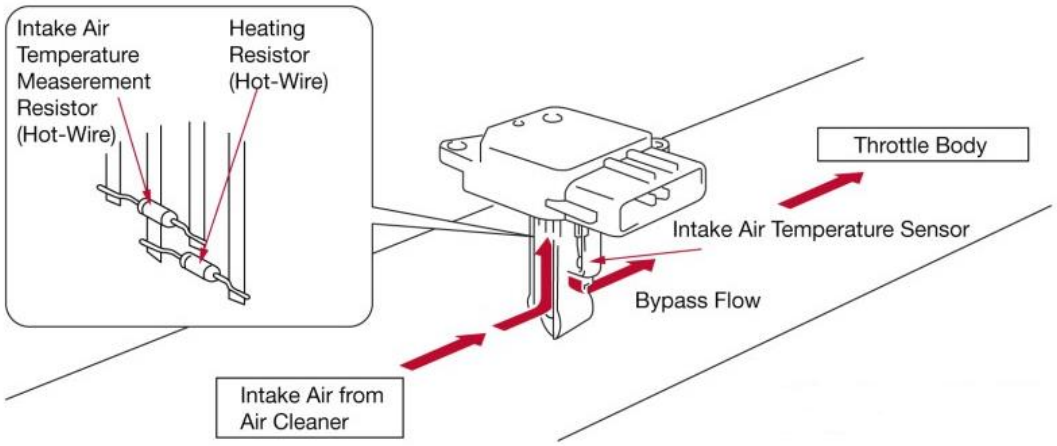


Figure 2.5 Hot wire air mass flow sensor (courtesy of Denso)

Those sensors contain an element with a thin wire, which holds an electric current. This wire being electrically charged increases its temperature gradually and as such its resistance. When airflow passes through the sensor this temperature drops and its resistance. At each resistance, the sensor outputs a relevant voltage as configured by the manufacturer. This relationship between the resistance and the voltage output is the calibration

of the sensor, which is inserted into the engine strategy, and as a result, the ECU by getting the voltage output from the sensor translates that directly to mass airflow. [46]

### 2.8.2 Vane meter

The vane meter type of sensor is another very popular way of measuring the airflow into the engine. It is an older design of sensor and was mainly used on the early injection systems but has now been replaced by more modern and faster sensors. The principle of operation is based on the moving spring loaded vane, which is contained within the sensor and connected to a variable resistor or else called potentiometer. Because the vane is in the middle of the airflow it moves proportionally to the airflow and at the same time, a voltage is applied by the engine-wiring loom to the potentiometer. Because the vane is connected to the potentiometer ever time is moved a proportional voltage appears as an output from the potentiometer, which relates to the angle of the vane. It is easily understandable that the vane moves because of the drag between that and the airflow against it. However, this measuring technique has some disadvantages because the vane is directly in the middle of the airflow and that causes disruption in the airflow, which can cause engine performance issues. The sensor also consists of many electrical and mechanical contacts, which can wear out limiting the accuracy of the sensor. [47]

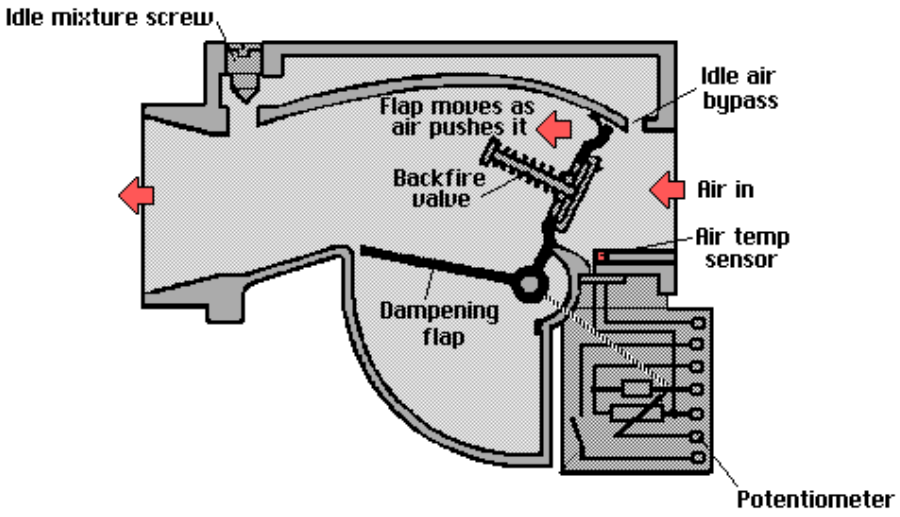


Figure 2.6 Vane meter main components

### 2.8.3 Karman vortex sensor

Another type of sensor used for air mass flow measurement is the Karman vortex sensor. The main principle of operation of this sensor is disrupting the airflow by using a bow perpendicular to the flow. This will cause the creation of oscillatory Karman vortices with a frequency proportional to the air velocity. There is an additional pressure sensor within the main sensor, which can sense these pulses and can generate an output, which can be read by the ECU and thus know the air mass flow to the engine. [48]

### 2.8.4 Lucas – Dawe air mass flow meter

This type of sensor was originally intended for use on engines but it is more suitable for a laboratory environment as it is explained later. In figure 2.4, a schematic representation of the sensor can be seen.

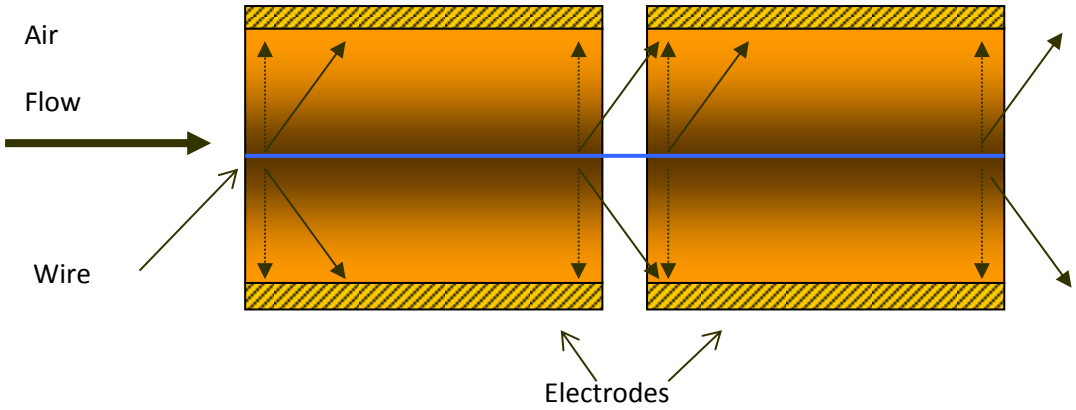


Figure 2.7 Lucas- Dawe air mass flow sensor

The principle is illustrated by figure 2.4 where the central electrode (blue) is charged with 10 kV, which causes a Corona discharge. When air flows through the sensor, this causes an imbalance to the current flowing to the electrodes on the sides of the duct. That difference in the current flow is proportional to the air mass flow rate passing through the sensor. Because the principle of this sensor is based on the current flowing to the collector electrodes, that gives it an extremely low response time of about 1ms however that also makes it very sensitive to humidity changes and that is why it is more suitable for a laboratory environment where the conditions are more stable than a vehicle. [49]

### 2.8.5 Ultrasonic air mass flow sensor

This method of measuring air mass flow is the most modern and its principle of operation is described in chapter 4 of this thesis. It is the main sensor used for measuring the engine air mass flow during engine testing in this project and its accuracy is very good. Due to the nature of this sensor, being too big and expensive is only used in laboratory environment and thus is not suitable for using on a vehicle setup

2.8.6 Speed – density equation (manifold absolute pressure sensor)

The second method that is widely used on modern engines for estimating the air mass flow is the speed – density equation. In this case, there is no air mass flow sensor but instead there is a manifold absolute pressure (MAP) sensor. In this method, the speed – density equation is used which contains the engine speed, the volume of the intake and the density of the air to calculate the air mass flow entering the engine. The first step is the calculation of the intake volume described in equation 2.1 below.

$$V_{air} = \frac{VE * V_{cyl} * n}{2}$$ Equation 2.1 [50]

Where VE is the volumetric efficiency of the engine, $V_{cyl}$ is the cylinder volume and n is the engine speed.

The next requirement is to calculate the air density, which is described by equation 2.2

$$\rho_{air} = \frac{m}{V} = \frac{nM}{\frac{nRT}{P}} = \frac{MP}{RT}$$ Equation 2.2 [50]

Where M is the molar mass of air, P is the intake manifold pressure measured by the MAP sensor, T is the inlet air temperature measured by the IAT sensor, and R is the ideal gas constant.

Combining equations 2.1 and 2.2, the air mass flow entering the engine can be calculated, which is described by equation 2.3 [50]

$$\text{m} = V_{air} * \rho_{air} = VE * V_{cyl} * \frac{M}{R} * \frac{n}{2} * \frac{P}{T}$$ Equation 2.3 [50]

The advantages of using speed – density equation instead of measuring the air mass flow directly are that the sensors used are very reliable and inexpensive and they do not pose any restriction to the airflow like some of the sensors described earlier. On the other hand, the speed – density equation requires complicated calculations by the ECU, which means that more processing power is, required making the ECU more expensive and the volumetric efficiency tables stored in the ECU take a long time to be parameterised during the early stages of engine development.

Finally, it is worth mentioning that the engine that will be used in this project for experimental testing uses the speed – density equation with a MAP sensor instead of measuring the air mass flow directly. The MAP sensor has two different chambers inside separated by a flexible diaphragm. The first chamber is sealed and measures the ambient pressure and the other one towards the inlet manifold that measures pressure – vacuum depending on engine operating condition. There is also a built in pressure sensitive circuit that monitors the movement of the diaphragm and translates it to a voltage output.

## 2.9 Summary

In this chapter, first the history of the need for airflow measurement on IC is presented and explained, followed by background information on the evolvement of the air flow measurement and estimation. This is a crucial part as it helps understanding all the research that has been implemented on this topic and is based on the current literature. Next the difference between the actual airflow entering the cylinder and the measured- estimated is

explained. This also presents the drawbacks of the current methods used by engineers. The following paragraph focuses on the different types of engine modelling used currently to assist engine development and also their possible applications. In addition, the basic operating principles of the SI engine are described as well as the control principles of modern SI engines. This is essential as it helps understanding how modern engines operate and what is needed in order to achieve engine control. Finally the importance of air mass flow measurement is explained and justified, followed by all the methods used by engine developers to measure or estimate the engine air mass flow as it appears on current literature.

# Chapter 3: Theoretical model – basic calculations of the airflow

In this chapter at first a literature review on induction systems is presented while the next paragraph analyses the main sub systems from which the induction systems consist of and the last paragraph is a brief theoretical analysis about the phenomena and equations that govern the induction system operation.

## 3.1 Induction system

The main function of the induction system is to provide to the engine the required amount of clean air which later is going to be mixed with the correct amount of fuel. The induction system of an engine performs three main operations. The first is to ensure that the air entering the engine is clean free of debris or any kind of micro particles which is very essential for the ideal mixture of the air with fuel. In addition the induction system must be designed in such a way by the automotive engineers which ensures the best volumetric efficiency of the engine or in other words that the air entering a particular engine is the maximum possible at any engine speed. This is important because on spark – ignition engines, SI the combustion process and the torque output of the engine are mainly determined by the air charge in the cylinders. As it can be seen in a following paragraph the flow efficiency has a direct impact to the power that will be produced by an engine. Last but not least the acoustic performance must be taken under consideration while designing an induction system as current regulations put a limit to the maximum mass air flow level that vehicles can make during test. The speed of air generated by the induction system can play a major role so the

acoustic performance is an important parameter at the design of an induction system. Figure 3.1 shows finite element analysis to confirm structural rigidity and to analyse the acoustic performance of the induction.

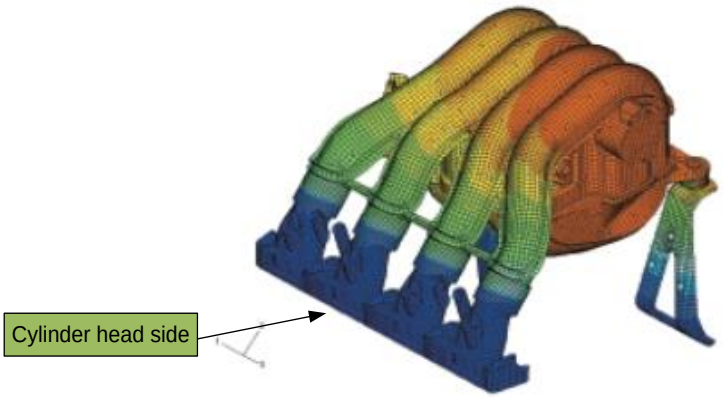


Figure 3.1 FEA analysis of the induction system

The majority of the induction systems are made of plastic when used in naturally aspirated engines as plastic is cost effective and also helps engineers to keep the overall weight of the engine at low levels. Furthermore plastic retains a smoother inner surface after injection moulding so it does not require any further machining. Also it is very important the materials that are used to be recyclable and plastic is one of those materials. Figure 3.2 shows a plastic inlet manifold which is the main part of the induction system. [51]

When the pressure in the induction system exceeds the atmospheric pressure like in turbocharged engines then aluminium is used for the induction system. The reason for that is that aluminium can handle the additional pressure supplied by the turbocharger, also because the air entering the engine is compressed has increased temperature and aluminium can dissipate heat effectively and last but not least aluminium is

the most cost effective material after plastic which enhances the overall lightness of the engine. Figure 3.3 shows an aluminium inlet manifold.

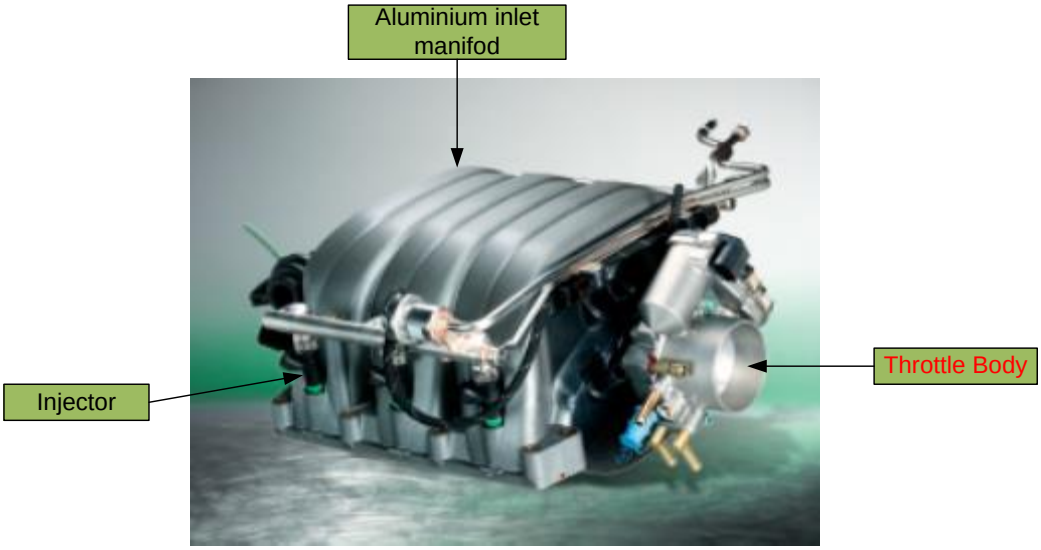


Figure 3.2 Aluminium inlet manifold

With the advancement of technology computational fluid dynamic software has been developed and it is considered to be the most cost effective solution to determine and analyse the volumetric efficiency and the flow through the induction system. Such software can also predict the ideal induction system shape and also analyse all the phenomena while air is passing through the induction system.

### 3.2 Induction subsystems

The induction system consists of various mechanical and electronic parts except from the inlet manifold itself. All these components are the subsystems of the intake system of an engine and their main role is to transmit signals to the ECU related to the air mass flow towards the engine. There are also additional pipes and hoses required to run ancillary devices of the engine.

### 3.2.1 Air cleaner assembly

The first sub system of the induction system is the air cleaner assembly. This is the first component the air has to go through on its way to the engine and as the name implies its main purpose is to ensure the air is free of dust, pollen and other contaminants. This is achieved by using a very dense filter element which in most cases is made of paper. This is a serviceable item and its role is very vital as contaminated air entering the engine can cause premature wear to vital engine components. Also if the filter element is not inspected and changed regularly this can cause restriction in the air path which in turn increases the pressure drop across the air cleaner and reduces engine performance and economy. In addition to its primary role, the air cleaner assembly is also used in most cases for mounting crucial air path sensors such as inlet air temperature sensor (IAT) and mass air flow sensors. In figure 3.3 an air cleaner assembly can be observed. It is also obvious where the air filter element is located in between the upper and lower part of the air cleaner box. The lower part duct is the one that drives the air to the filter from the environment and the upper part duct takes the filtered air to the throttle body assembly towards the inlet manifold. [52]

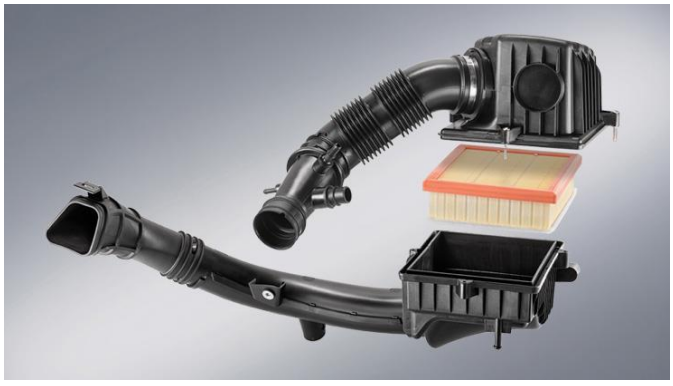

Figure 3.3 Air cleaner assembly (Courtesy of MANN – HUMMEL)

### 3.2.2 Sensors

As mentioned in chapter 2, depending on the way the ECU determines the engine air mass flow there are some sensors required. These can be either the IAT sensor if the speed – density method is used or the MAF sensor if the mass flow rate is measured directly. Both these sensors are located in the air cleaner assembly or just after it towards the engine and are very crucial for the efficient operation of the engine. Another critical sensor is the manifold absolute pressure sensor (MAP) which was described in chapter 2 as well. This sensor is used when the ECU estimates the engine air mass flow using again the Speed – Density equation and provides information about the pressure in the inlet manifold. This sensor is located directly in the middle of the inlet manifold. [53]

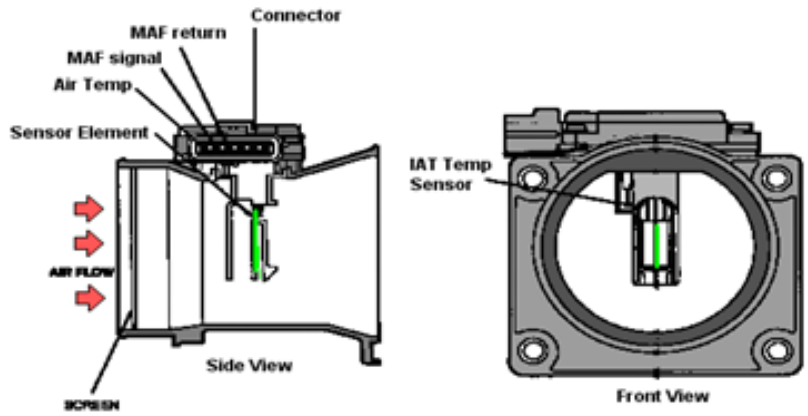


Figure 3.4 MAF sensor (Courtesy of Ford Motor Co)

### 3.2.3 Throttle body assembly

A very important subsystem of the intake system is the throttle body assembly. The throttle body is an electromechanical valve which comprises of the main housing and the butterfly valve plus some additional sensors. Its

main role is to control the air flow into the engine by adjusting the opening and closing of the valve. The butterfly valve is electronically connected (drive by wire) with the accelerator pedal where the driver's demand is translated by the ECU into a relevant valve position so the demand can be achieved. On the side of the butterfly valve there is a potentiometer directly attached to it which informs the ECU about the exact position of the valve. In figure 3.5 a throttle body assembly can be seen. The throttle body is always attached in the beginning of the inlet manifold assembly so it can accurately control the airflow. [54]

Figure 3.5 Throttle body assembly (Courtesy of Continental A.G)

### 3.2.4 Variable intake runners

Apart from the main induction system and its subsystems there are also other technologies which are adopted by the induction system or collaborate with it in order to increase volumetric efficiency and reduce emissions and fuel consumption.

Modern induction systems adopt variable intake runners which can improve the air charging in engines by adjusting the length of intake manifold. Of course that depends on the engine speed and by adjusting the length of the intake manifold, performance and torque can be optimized. At high engine speeds where the velocity of air is high, a short intake runner improves performance while at low engine speeds where the kinetic energy of the air is low, long intake runners are used. In order to switch the intake manifold geometry a flap system is used. This is controlled by the engine management system and is driven by an electric motor. Figure 3.6 shows how a variable intake manifold changes its length. [55]

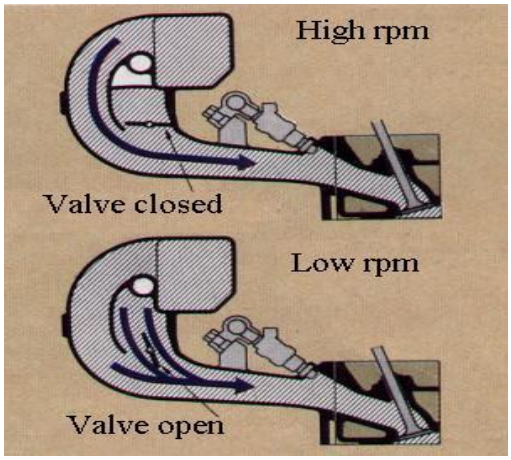


Figure 3.6 Variable length intake runners

### 3.2.5 Exhaust gas recirculation (EGR)

Another system that is used in collaboration with the induction system is the exhaust gas recirculation (EGR)**.** EGR is designed to reduce the amount of oxides of Nitrogen (NOx) created in high combustion temperatures. NOx is reduced by recirculating small amount of exhaust gases into the induction manifold where it mixes with the air charge. EGR is controlled by a valve

which regulates the exhaust gas flow to the induction and is strictly related to the engine speed, load and temperature. Figure 3.7 shows a schematic representation of how EGR works. [56]

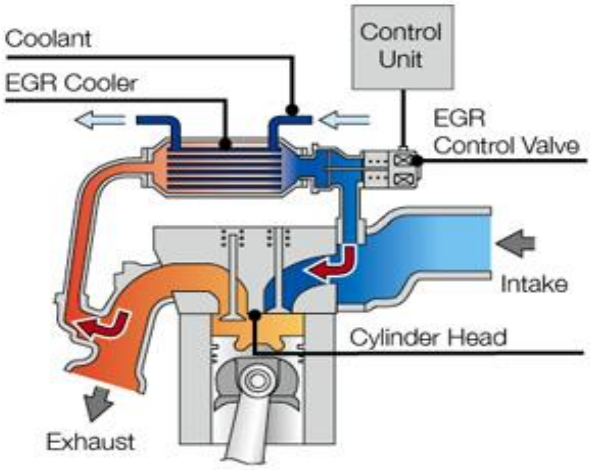


Figure 3.7 Schematic representation of EGR system

### 3.3 Theoretical analysis (dynamics of the intake manifold)

In figure 3.8 a schematic diagram of an intake manifold can be seen with all the sensors required to calculate the air mass flow into the cylinders.

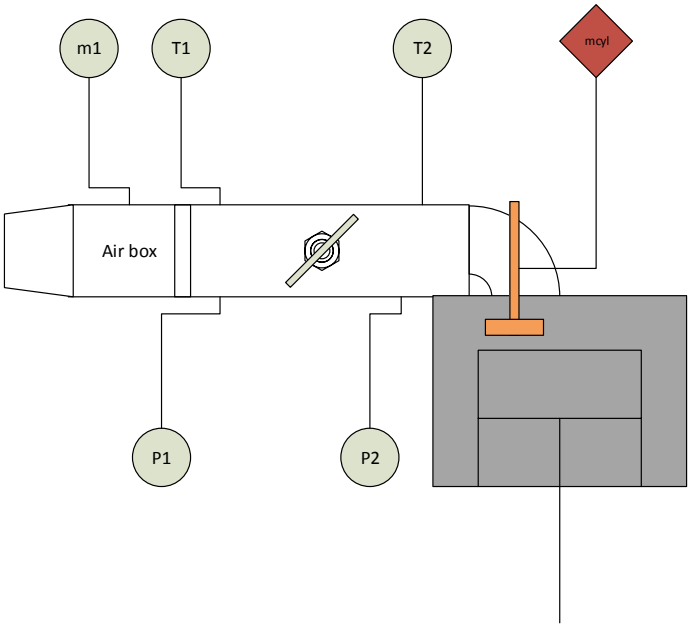


Figure 3.8 Intake System with sensors

Assuming that the engine works as a pump which sucks air then the mass for one cylinder in theory can be described by equation 3.1,

$$mair, cyl, th = P2Vair, cyl, th = \frac{P2}{RT2} Vair, cyl. th \qquad 3.1[57]$$

Where the volume of air flow for one cylinder for a 4 stroke engine can be described by equation 3.2,

$$Vair, cyl, th = \frac{1}{2} Vd\, n \qquad 3.2\ [57]$$

Where $Vd$ is the displacement of one cylinder and $n$ is the engine speed in RPM. The above equations describe the theoretical air flow in one cylinder

which in reality is different and in fact smaller because in an engine phenomena such as pumping loses due to the throttle restriction, valve timing tuning, restrictions at the inlet port etc. exist. Hence it is necessary to define the volumetric efficiency of an engine which is described by equation 3.3,

$$nv = \frac{mair,cyl}{mair,cyl,th} = \frac{mair,cyl}{\frac{1}{2}nVd\frac{P2}{RT2}} \qquad 3.3\ [57]$$

The volumetric efficiency is determined experimentally as a look up table and depends on the engine speed $n$ and the throttle butterfly position $a$.

Another characteristic quantity for the air mass flow entering the cylinder is the air mass passing through the throttle which can be described by equation 3.4

$$mthrottle = Cd\ Ath\frac{P1}{\sqrt{RT1}}AFC \qquad 3.4\ [57]$$

Where $Cd$ is the coefficient of discharge for the flow, $Ath$ is the throttle butterfly actual area which is described by equation 3.5 below,$T1$ , $P1$ is the temperature and pressure before the throttle and AFC is the condition of the airflow (sonic or subsonic) as described by equations 3.6 and 3.7 below.

$$Area(t) = \frac{\pi}{4}d^2{}_{th}\left[1-\cos(a(t))\right] \qquad 3.5\ [57]$$

Where $d$ the throttle butterfly diameter and $a(t)$ is the throttle plate angle.

Furthermore as described in equation 3.4 there are different air flow conditions depending on the speed of the engine which have to be defined. These conditions are divided into sonic and subsonic flow. Under specific

manifold pressure sonic flow is observed and at that point any further increase at the air flow cannot be seen. For that reason at sonic flow the pressure at the inlet manifold is insignificant and even if it becomes extremely low it cannot create any further increase in the air flow. Sonic flow is commonly found during engine deceleration so when the throttle is closed or partially closed and equation 3.6 describes a sonic at any point below a critical pressure limit.

$$S_{sonic} = \sqrt{k\left[\frac{2}{k+1}\right]^{\frac{k+1}{k-1}}} \qquad 3.6\ [57]$$

Where $k$ is the ratio of the air specific heat. Flow changes to sonic at about 0.54bar of manifold pressure and for $k$=1.4. On the other hand subsonic flow is found in higher manifold pressures or in other words with wide open or partially open throttle plates, as long as the manifold pressure is higher than the critical point that was mentioned previously. At subsonic conditions the air flow increases depending on the pressure ratio and the throttle angle and any drop on the manifold pressure could make the air flow o increase. Air flow under subsonic conditions can be expressed by equation 3.7.

$$S_{Subsonic} = \left(\frac{P_m(t)}{P_{atm}(t)}\right)^{\frac{1}{k}} \cdot \sqrt{\frac{2k}{k-1}\left[1-\left(\frac{P_m(t)}{P_{atm}(t)}\right)^{\frac{k-1}{k}}\right]} \qquad 3.7\ [57]$$

Where $Pm$ refers to the manifold pressure in $N/m^2$ which practically can be measured using a MAP sensor or additional pressure instrumentation. [57], [58], [59]

### 3.4 Summary

This chapter starts with a description of the induction system and the main job which performs. It is very important to understand all the technical characteristics of the induction system as its role is vital to the SI engine operation. The next paragraph goes through a detailed description of the various subsystems the induction system comprises of and what role each one has. Finally the last paragraph describes the theory and the calculations behind the induction system as used when a mathematical model of the induction system needs to be developed.

# Chapter 4: Experimental setup– Testing methodology

This chapter is about the experimental setup required to perform the necessary tests and also the testing methodology specifically developed for the engine data collection. At first the unit under test is described analytically and some of the unique features of this engine are described. This is important as it plays a very important part in this project and also has a very innovative engine design which sets it apart from the competition. Next the testing facility layout is described pointing at the key equipment that allows for efficient powertrain testing followed by the measurement and data acquisition system. In addition the measured signals are described and their location on the engine is shown and justified. Last but not least an extensive description of the testing methodology is presented explaining what makes it different to what most automotive manufacturers currently use.

## 4.1 Unit under test

The engine under test in this project is a Ford fox upgrade GTDI (gasoline turbo direct injection) and is the latest generation downsized internal combustion engine from the above manufacturer. It is currently at the final stages of the development and is expected to be put into production towards the end of 2018. Below you can see a table with the most important technical details of this engine.

| | |
|---|---|
| Maximum power | 125 PS (92 KW) @ 6000 RPM |
| Maximum Torque | 200 Nm @ 2000 – 2500 RPM |
| Bore | 71.9 mm |
| Stroke | 82.0 mm |
| Total engine capacity | 999 $cm^3$ |
| Connecting rod length | 137.00 mm |
| Compression ratio | 10.5: 1 |
| Firing order | 1-2-3 |

Table 4.1 Technical details of the engine under test

The past few years most automotive manufacturers have adopted a new concept of engine by downsizing them and adding a turbocharger. This makes the engines lighter, smaller in size, more efficient and with far less emissions. This particular engine used in this project is the latest in downsizing technology from Ford and is an upgrade of the current engine available on the market but with many improvements and innovations. The most important feature is that although under normal conditions is a three cylinder engine, under certain speed and load conditions it can deactivate cylinder number 1 and run on 2 cylinders. This is achieved by an electrohydraulic actuator in the valve train of cylinder 1 which when commanded it disables the valves and no combustion can be achieved. At the same time the ECU disables the spark and the fuelling for that cylinder. During that mode the spark timing and the fuelling on the two remaining cylinders is slightly increased and the turbocharger produces more boost to compensate for the inactive cylinder but the overall fuel consumption of the engine is decreased. When the engine needs to switch mode and run on three cylinders because the load/speed is increased, the valves are activated again and after compression is built back (a few cycles) then the spark timing and fuelling are enabled. In reality it is not so easy to implement the above technology as this present significant control engineering challenges. Engineers have to take under consideration the duration that the engine operates under cylinder deactivation mode as this can significantly affect the performance and emissions of the engine. For example if the cylinder remains inactive for too long then it cools down which makes it not ideal when the clean combustion process and low emissions is the target. Another

important factor is the drivability the customer experiences during mode switching as it is obvious that when 33% of the engine capacity is deactivated this will have a significant effect on the torque produced by the engine. All the above indicate that the timing of the whole process and the engine conditions under which the deactivation is performed are crucial to ensure that this transition is hardly noticeable by the driver and also seamless to ensure that the whole gearbox/driveline is not stressed unnecessarily.

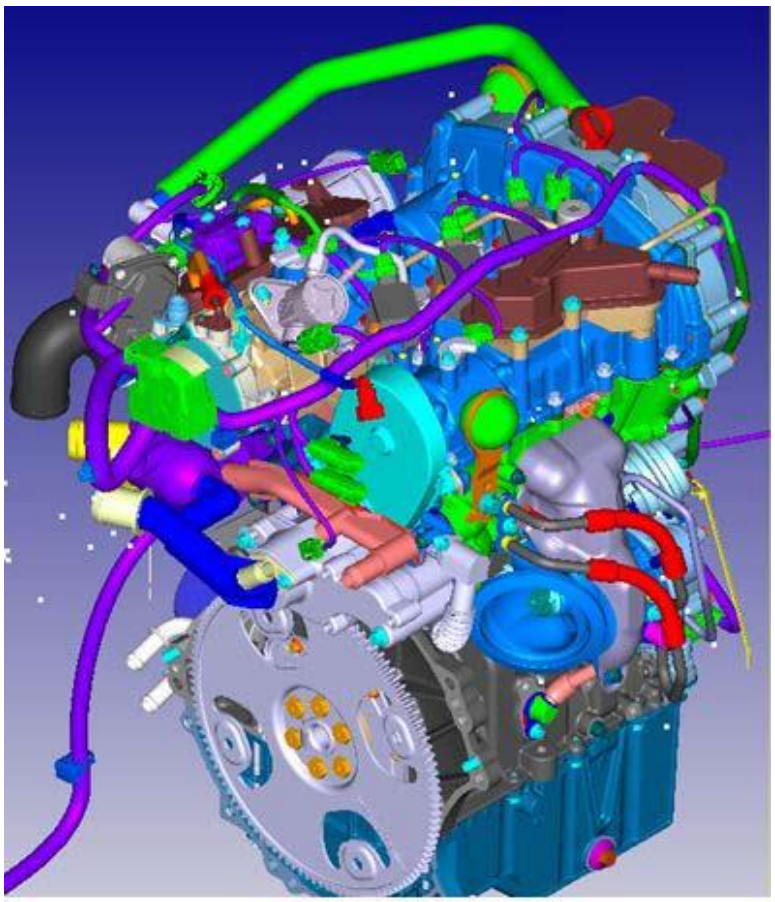

Figure 4.1 3D CAD Drawing of the engine (courtesy of Ford Motor Co)

In addition to the above feature this engine also incorporates the latest in variable valve timing technology in both inlet and exhaust camshafts (Ti-VCT) to ensure maximum drivability and quick response under all operating

conditions. It also has very advanced spray guided direct injection system to increase combustion performance and ensure that the relatively high compression ratio for a turbocharged engine can be achieved. The turbocharger is a low inertia small size unit to minimise turbo lag while it can spin up to 240000 RPM to ensure it can provide the necessary boost. It is both water and oil cooled to increase its reliability. Finally it is worth mentioning that being a high output engine it has piston cooling jets to reduce the temperature of the pistons and also a variable geometry oil pump to ensure the optimum lubrication is provided with the minimum friction losses. In figure 4.2 it is noticeable that although the engine incorporates the latest in engine engineering and control it still maintains a very compact design which makes it suitable for any vehicle size and a very low mass. [60]

## 4.2 Test cell layout

The testing facility used for the experiments is a state of the art palletised room capable of handling both steady state and also highly dynamic powertrain tests including drive cycles and real driving emission simulations. The software and hardware used within this facility is engineered mostly by AVL which is a world leader in powertrain testing and simulations.

### 4.2.1 AC Transient dynamometer

The dynamometer used for the experiments was a foot mounted asynchronous unit capable of handling 220 kW and 550Nm of torque. Being an AC electric motor means that it cannot only absorb (brake) the engine but also motor it simulating any possible condition or drive cycle. The main advantages of such a unit are that it can have very high speed gradient due

to low and optimised inertia which makes it ideal for transient testing and the torque measurement is performed either with the traditional load cell setup for increased accuracy or by using an in line torque flange and elastic coupling on the shaft to reduce torque oscillations where this is required. It is also worth mentioning that inside all the bearing cases there is oil circulation which reduces friction thus enhancing the measurement characteristics and response of the unit. The maximum speed that the dynamometer can operate is 12000 RPM meaning that it can basically handle almost any engine design available nowadays. [61]

Figure 4.2 Back view of the AC dynamometer rested on its mount

### 4.2.2 Fuel mass flow measurement

It is very important for the engineers to be able to measure the fuel consumption of the engine under test because by using these data they can

verify that the fuel demand calculated by the engine strategy is accurate and also they can perform various calculations together with the emission analysers to ensure that the engine is performing efficiently and clean. In this particular facility where the tests were performed a very advanced measurement device is used which can also condition the fuel and supply it to the engine at an optimum temperature to enhance repeatability of the results. The measuring principle of this device is gravimetric and that means that the fuel consumed by the engine is taken from a continuously weighted measurement vessel which has all the properties of the vehicle tank. From time to time the device automatically calibrates itself by using a calibration weight thus improving the accuracy.

### 4.2.3 Air mass flow measurement

The device used for the air mass flow measurement is probably the most important within the testing facility as it is the one that provides us with the experimental data from the engine which will be compared against the simulated and modelled data in a later chapter. This device is the latest technology available for measuring air mass flow in an engine and the measuring principle is based on the ultrasonic transit time differential method. The figure below will help explain how this device works.

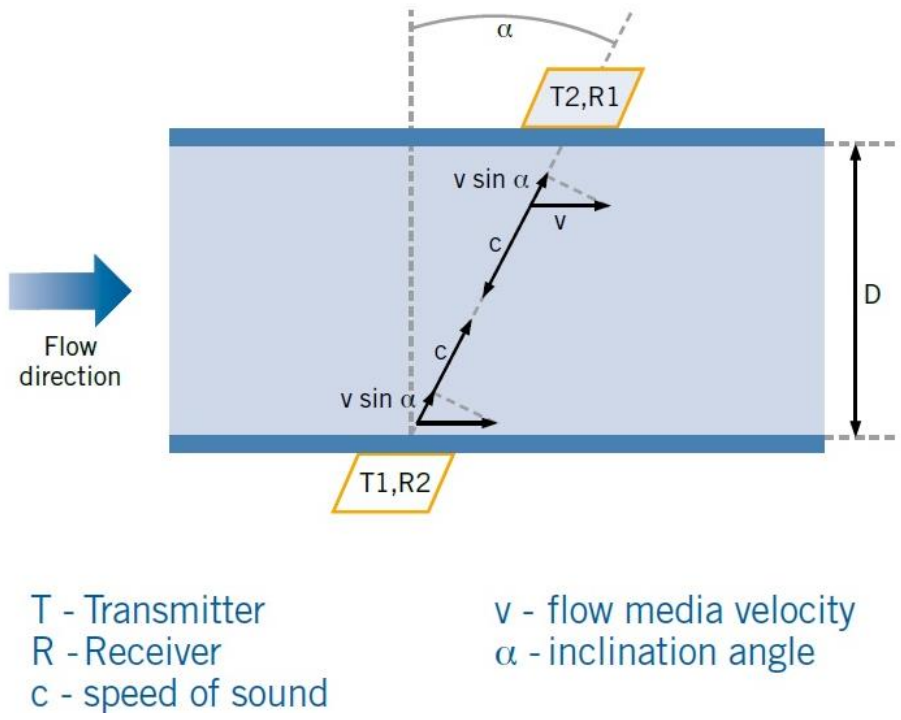


Figure 4.3 Schematic representation of the air mass flow measuring principle

In this method two ultrasonic pulses are sent simultaneously from two transmitters installed in the measuring head (T1, T2) through the flowing air. One pulse is sent into the flow direction and the other one against. The interaction between the speed of sound c and the velocity of flow v accelerates the pulse in one direction and decelerates the pulse in the other direction. This means that the signals at the 2 receivers on the measuring head (R1, R2) arrive at different speeds. Below the initial required equations will be explained which will lead finally to the calculation of the air mass flow. First the equations that calculate the transit time of the ultrasonic pulse in both directions are needed which will be described by equations 4.1 and 4.2

$$t1 = \frac{L}{c + v\sin a} \qquad 4.1[62]$$

And also

$$t2 = \frac{L}{c - v\sin a} \qquad 4.2\ [62]$$

Where t1 and t2 is the transit time of ultrasonic pulse in flow direction and against flow direction respectively.

Also equation 4.2 describes the sound path at an inclination angle

$$L = \frac{D}{cosa} \qquad 4.3\ [62]$$

Where D is the tube diameter and α is the inclination angle as both shown in figure 4.4. Then equations 4.1 and 4.2 can be used to determine the flow velocity which is described by equation 4.4

$$v = \frac{L}{2sina}\left(\frac{1}{t1} - \frac{1}{t2}\right) \qquad 4.4\ [62]$$

And the speed of sound can also be determined as described in equation 4.5

$$c = \frac{L}{2}\left(\frac{1}{t1} + \frac{1}{t2}\right) \qquad 4.5\ [62]$$

The volume flow can be calculated as well as shown in equation 4.6 by including the calibration factor K and also using the flow velocity calculated by equation 4.4

$$V = K\frac{\pi D^2}{4}v \qquad 4.6\ [62]$$

And finally by using the density of the medium $\rho_a$, the temperature of the medium $T_a$

and the pressure value from the built in sensor $P_a$ then the corresponding air mass flow can be calculated as described by equation 4.7 [62]

$$Q_m = \frac{\mathrm{P}_a}{R\mathrm{T}_a}\mathrm{V} = \frac{k\rho_a}{c^2}\mathrm{V} \qquad 4.7\ [62]$$

In the figure below the actual setup of the device is shown inside the engine test cell

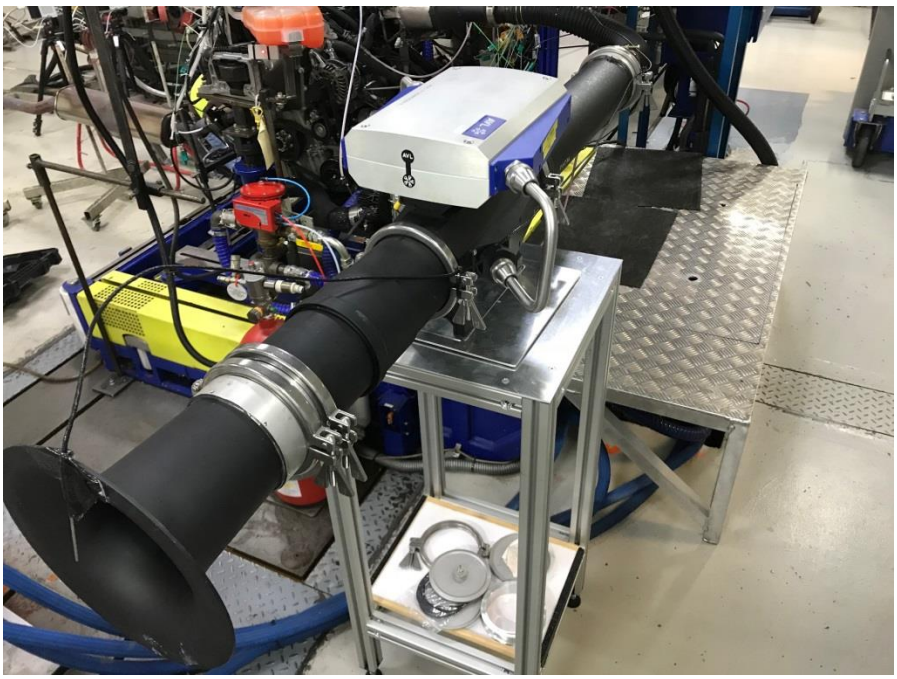

Figure 4.4 Installation of the air mass flow measurement instrument

### 4.2.4 Emissions measurement devices

Another important element of the engine testing facility is the emission analysers. They are used to constantly measure the exhaust gases while the engine is running and they report the % of the pollutants such as $CO_2$, THC, $NO_x$ and CO during engine development process. Their role is crucial because on development engine when the ECU is mapped and calibrated the engineers need to know that their settings will not affect the emissions of the engine and as a result it will be able to pass the emission tests which are becoming increasingly tight. Normally the measuring probes are positioned

before and after the catalytic converter which makes sure that the correct operation of the catalytic converter can be checked and verified. Another important element in this setup is the distance between the probes and the device. Ideally it has to be not more than 10 metres as this ensure that there is not significant measurement lag due to gas travel distance. [63]

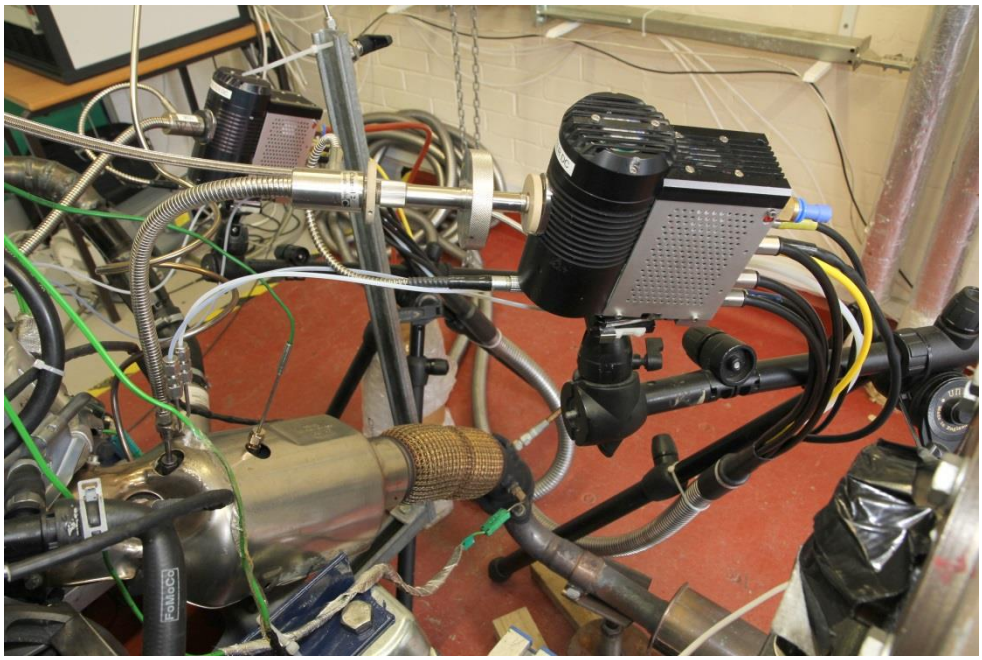

Figure4.5 Pre catalyst emission probe for CO, CO2 measurement

4.2.5 Environmental controls

The term environmental control refers to the infrastructure used to control and condition various fluids which are used to control various engine subsystems temperatures. These subsystems are the engine coolant which is used to keep the engine at an optimum temperature, the oil cooler which maintains the engine oil temperature at an optimum temperature to ensure the best possible lubrication of the engine, the intercooler which control the boosted air temperature into the engine and lastly the combustion air where the temperature of the air the engine is breathing can be controlled. All the

above play a major role on the repeatability of the data produced by any testing facility because temperature variations can affect the way an engine operates. Also by having accurate environmental control the safety of the engine can be ensured and also gives the flexibility to the engineers to simulate different operating conditions which can be found at different parts of the world where the engine will have to operate. [64]

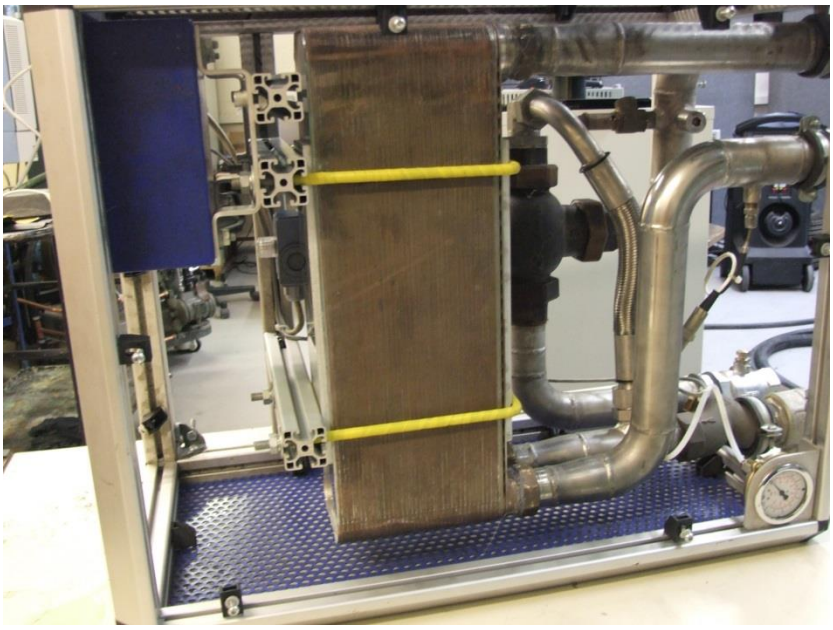

Figure 4.6 Heat exchanger for engine coolant temperature control

## 4.3 Engine test automation software

The term test automation software means all the individual software packages that make the operation of the testing facility possible. These software control each individual component of the facility including the engine and also the various data acquisition systems that provide data.

### 4.3.1 Puma automation platform

The Puma automation platform is a software package which is designed and developed by AVL and its primary role is to control the whole testing facility and its subcomponents. All the signals from the facility are connected to a central hub and the software control this hub and as a result the dynamometer, various data acquisition systems, measuring devices and the environmental controls can be managed. The systems also extended capability as it allows the engineers to create automated tests necessary for powertrain development and also complicated scripts and calculations which can trigger additional actions during engine testing. All the subsystems connected to the software use standard communication protocols found in industry such as TCP/IP, CAN which means that additional devices can be connected any time. It also incorporates an advanced limit protection monitoring where the engineers can configure certain limit parameters and develop logic so the software can act on its own when automated testing is performed to ensure the ultimate engine protection and data quality. Also through the above software platform the environmental controls of the testing facility can be managed through PID controllers and look up tables which use closed loop control for enhance control accuracy. It is also important that it support also server installation which means it can be used for controlling more than one testing facility as found nowadays in most automotive development centres. Below in figure 4.7 a typical Puma screen can be seen with non-running engine. [65]

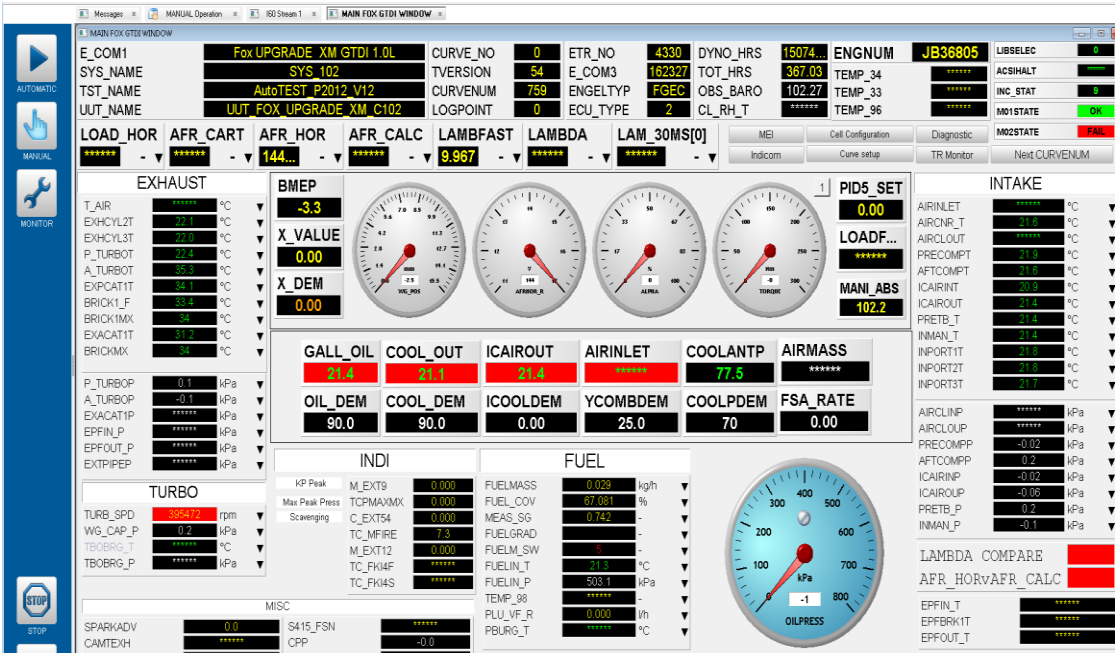


Figure 4.7 Puma automation software

### 4.3.2 ECU calibration software

The engine used in this project as mentioned earlier is a development engine and as such is connected to a development ECU where the engineers have full access to obtain and modify calibration parameters. For that purpose ATI Vision software was used which is an integrated development, calibration and measurement system specifically designed for engine development. This software gives the ability to the engineers to obtain real time parameters from the engine such as cam timing, spark timing, fuel control and modify these while the engine is running and examine the effect they have on engine performance. It can also be used together with Matlab to create complex models about engine control systems and download them directly to the ECU without needing to alter the source code (strategy). The basic calibration toolkit consists of the ECU interface which is an emulator installed within the ECU to allow the user full access to it, the PC software and a USB

link between the ECU and the PC where the software is installed. The data acquisition kit used in this project is also connected to the calibration software but this will be analysed later on in this chapter. In figure 4.8 below the screen of the calibration software can be seen. It is worth mentioning the large number of ECU parameters that can be found in this screen. [66]

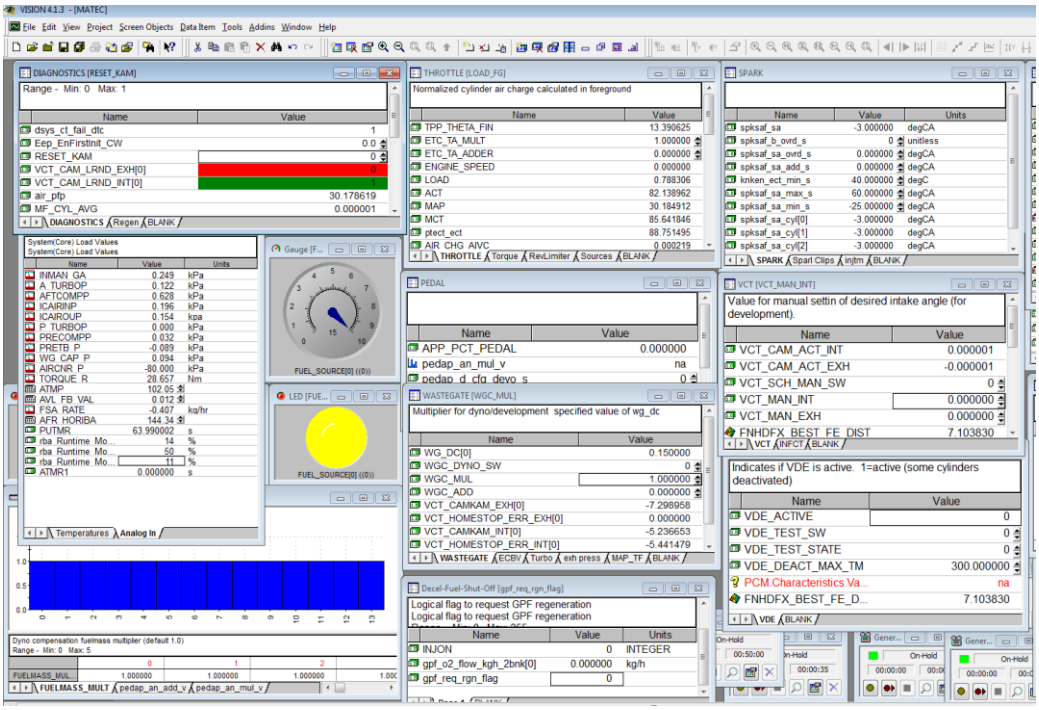

Figure 4.8 ECU calibration interface

### 4.3.3 Combustion indicating software

It is very important during engine testing and development the combustion process to be monitored and recorded as this mainly indicates any inefficiency during engine operation. For this project the IndiCom combustion indicating software was used which is developed by AVL and provides the user with crank angle data acquisition for cylinder pressure, spark timing and real time calculations. It also allows the development of very advanced knock and misfire algorithms which can detect these phenomena and take action to

ensure maximum engine protection is achieved. Also additional calculations and signal filtering can be configured and calculated either crank angle based or time based depending on the requirement. The software is connected via Ethernet to the real time hardware and the sensors and this topic will be analysed later on in this chapter. Lastly it is worth mentioning that during testing the indicating software is in communication with the automation platform and the ECU calibration network in a private network and they all share data with each other mainly for engine protection- limit monitoring and data logging. In figure 4.9 below various measurements can be seen during engine operation including the cylinder pressure traces and mean effective pressure. Also in the right graph data from the knock algorithm can be seen which is used for knock detection. [67]

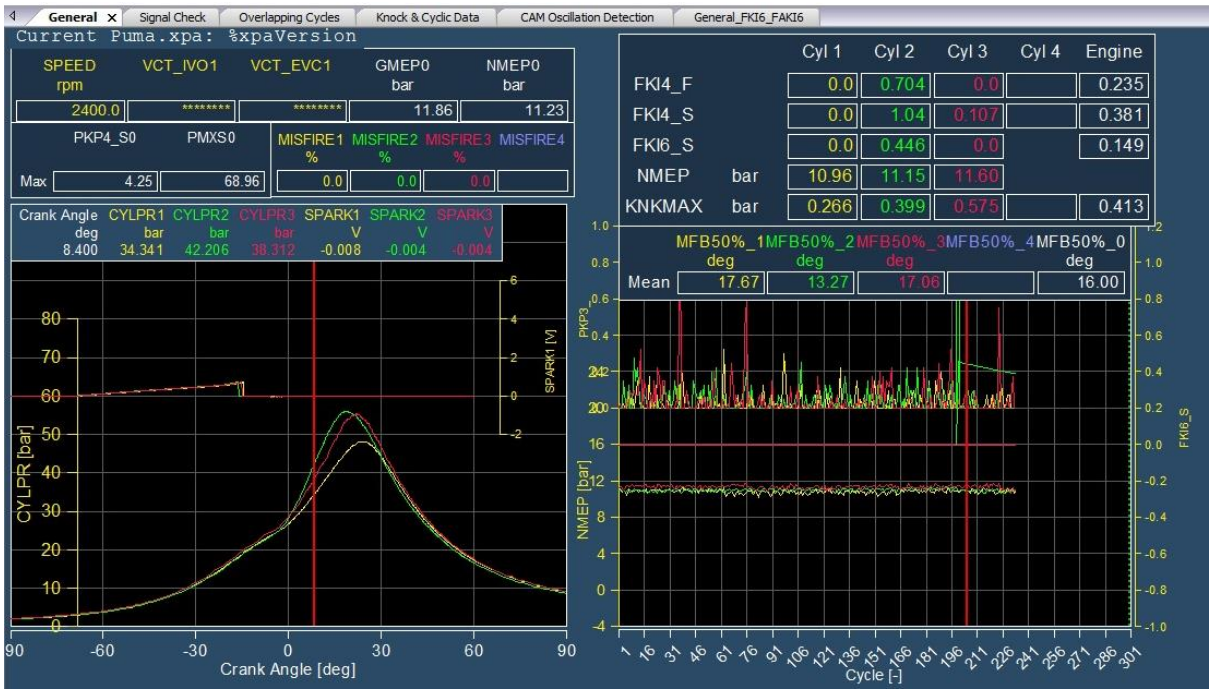


Figure 4.9 IndiCom combustion indicating software

## 4.4 Measurement and data acquisition systems

In every testing facility the measurement and data acquisition devices are the ones that provide the engineers with the necessary data for engine development and normally are located within close proximity to the engine. They are control and parameterised through the various software which were analysed earlier on this chapter.

### 4.4.1 Engine sensor signals

This is the first part of the instrumentation which was used in this project and as the title describes it uses the actual engine sensors which are installed on the engine to obtain data during testing. These sensors are connected to the engine wiring loom and transmit their readings to the ECU which in turn allows us to access these readings since there is direct access to the ECU through the calibration software. The engine sensor technology is so advanced nowadays that engineers can rely on these sensors since the readings they provide are very accurate. Examples of these sensors used in this project are the manifold absolute pressure sensor (MAP), engine speed sensor, air fuel ratio (Lambda) sensor, variable cam timing sensors etc. These sensors are adequate for engine operation but during development additional external sensors are required to cover locations where engine sensors do not exist. In figure 4.10 a CAD drawing of the engine under test is shown where most of the engine sensors can be seen and also how they are connected with the engine wiring loom.

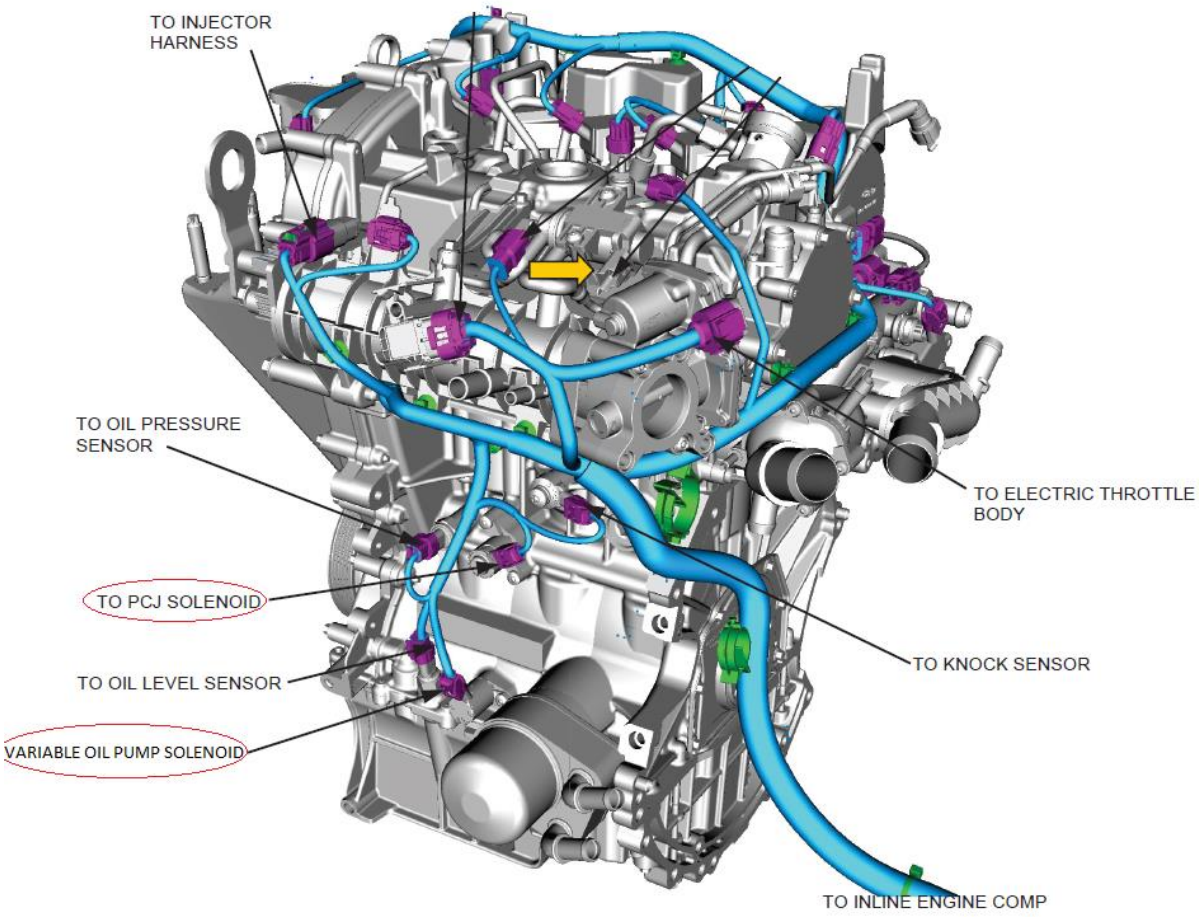


Figure 4.10 Engine sensors and wiring loom [60]

### 4.4.2 External sensors

The term external sensor refers to all the sensors used on the engine and are added on top of the existing sensors and their data is logged independently from the ECU. In this project many different types of external sensors were used mainly for pressure, temperature, combustion analysis and turbocharger instrumentation. The pressure sensors used in this project are manufactured by General Electric and they are specifically designed for engine and vehicle development. That gives them a significant advantage

because they firs can withstand the harsh environment of a testing facility (temperature, vibrations) and also provide the necessary accuracy required in such a project (error up to 0.2%). Normally on development engines pressure sensors should be present in all the critical areas of the engine such as the intake manifold, the whole air path from the compressor outlet to the throttle body and also the exhaust before and after the catalyst. The location of the sensors is critical not only because engineers need the data from these points but also because the right instrumentation points can show slight malfunctions of the engine which otherwise would be hardly noticeable. The principle of operation of such sensors is a silicon sensing element which is installed inside a high integrity pressure module constructed from stainless steel. Any pressure difference excites this sensing element and this excitation is translated into a voltage output which engineers can read. This voltage output is translated into a pressure reading based on the calibration certificate of the sensor and the final pressure reading is obtained. In figure 4.11 such a sensor can be seen.

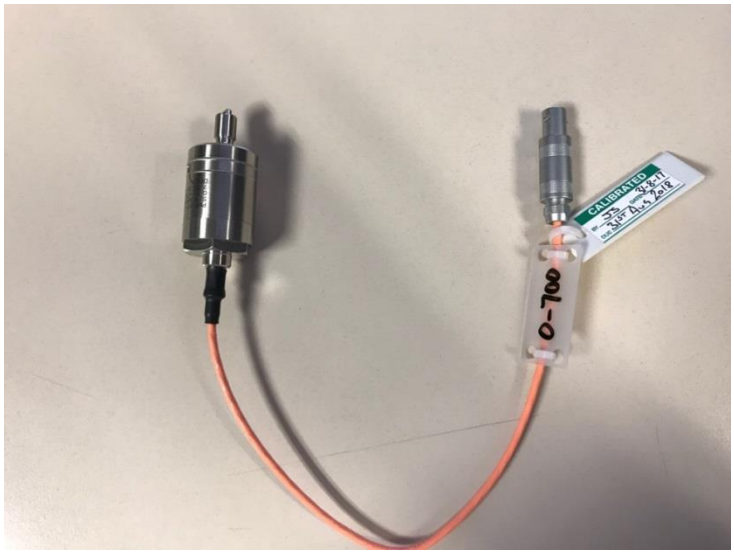


Figure 4.11 External pressure sensor GE PMP317

As it will be described later the engine tests performed for this project are highly dynamic which means that the pressure pick up point is as close to the sensor as possible to ensure the maximum dynamic pressure difference is obtained. It is also worth mentioning that these sensors need to be professionally calibrated every 6 months to ensure maximum accuracy.

The next type of external sensors used is the thermocouples for temperature measurement. Thermocouples are made of two different electrical conductors which form an electrical junction at differing temperatures. As a result a temperature dependent voltage is produced which can be interpreted as a temperature reading. There are many types of thermocouples available but for this project the type K was used which is the most common. Also a different type of thermocouple was developed specifically for this project which is extremely thin at 0.08mm since a very low response time was needed to capture the rapid temperature change during testing. The other two sizes used were 1.5mm and 3mm. The thicker ones were used on the exhaust side of the engine where any other thinner thermocouple would not last due to the high temperatures reaching up to 1000 degrees Celsius. [68]

Figure 4.12 Specially developed thermocouple 0.08mm thickness [68]

In the above figure the super thin thermocouple can be seen installed in a standard thermocouple fitting and ready for installation to the engine. The thermocouples were installed on every location where a pressure sensor existed as on many calculations it is very handy to have a pressure and temperature reading available at the same point. In figure 4.13 a typical engine instrumentation setup can be seen as used on the engine under test. The measuring point is at the inlet and outlet of the compressor.

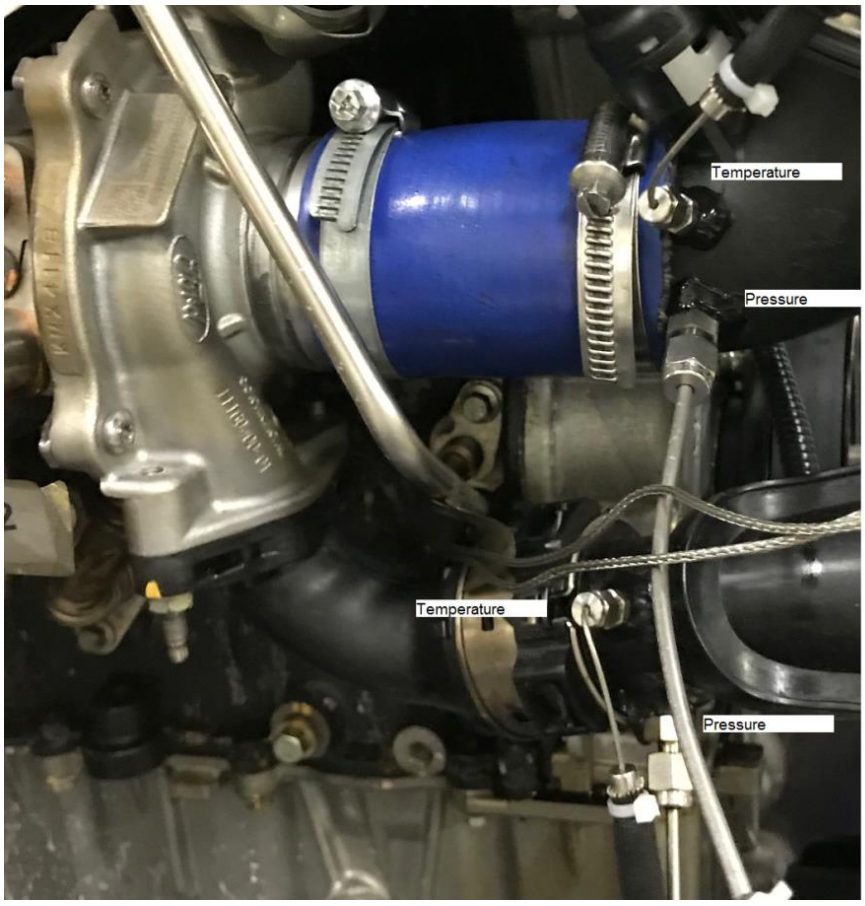


Figure 4.13 Compressor inlet-outlet instrumentation [60]

Another very important element of the instrumentation is the combustion pressure sensors. There are 2 different types of sensors available. The first is a combination of a spark plug and a pressure transducer all in one unit and the second is a standalone pressure transducer mounted on the cylinder

head where the combustion chamber is located. For this project the second type was selected due to the accuracy advantage due to higher sensitivity. These sensors are piezoelectric which means that the pressure element creates a voltage every time there is a change in pressure. It is obvious that the number of the sensors in this engine is equal to the number of the cylinders and these sensors are directly connected to the real time combustion analysis hardware which obtains their reading. The particular sensors used in this project are manufactured by Kistler and they have been specifically designed with high tolerance to knock and detonation. These events during engine operation can significantly deteriorate the ability of the sensor to react on pressure changes.

### 4.4.3 Data acquisition systems

For this project two main data acquisition systems were used. One designed for analogue inputs and temperatures and the second one is the real time processing hardware which was used for combustion indicating data with crank angle resolution.

The first data acquisition kit is the EMX series and is designed and developed by Accurate Technologies and is the same company that develops the ECU calibration software. The EMX series is a range of modular data acquisition devices which can be connected and configured directly to the ECU calibration software. The data acquisition rate is 1 kHz for analogue inputs and 500 Hz for thermocouples which makes it one of the highest available on the market today. The above modules have been designed specifically for engine and vehicle development which means that

they can withstand the harsh environment of a testing facility. In figure 4.15 the EMX data acquisition system can be seen installed


Figure 4.14 EMX data acquisition system

The main reason this acquisition system was chosen for this project is that it can directly be connected to the ECU calibration software which means that while testing the data from the engine sensors and all the external sensors, thermocouples can all be time aligned and recorded in a single recorder file which makes data post processing a lot easier and robust. Also because these devices are fully programmable through the software, the engineers can apply digital filtering, anti-aliasing settings and complex calculations on recorded channels which offers a lot more flexibility and ensures higher data quality. This system uses CAN protocol to communicate with the software through a central hub where also the ECU is connected and that ensures

very high and reliable data transfer rate. It is also worth mentioning that during the course of this project some slight imperfections in the operation of the devices was noticed and collaboration with the development company was established to further improve the product so it suits our requirements. [69]

The second data acquisition system is the X-ION high speed data acquisition platform. It is a modular acquisition system that can be easily adapted to different units under test and environments and that gives it the advantage to be able to manage the growing powertrain complexity. It is the most advanced combustion indicating hardware at the moment and it can also handle analysis of electrified powertrains. In figure 4.15 below you can see the modular design of the system.

Figure 4.15 AVL X-ION acquisition platform

The cylinder pressure transducers are directly connected to this device from the engine and it provides them with the necessary signal amplification so the engineers can obtain the readings. The hardware connects to the indicating software via a Gigabit Ethernet link which is the fastest private network connection available. Another advantage of this system is that it

supports cascading of up to six units with time synchronisation in case there is large number of signals. The hardware also offers time based acquisition with real time crank angle transformation (through an engine encoder) with a resolution of up to 0.01 degrees crank angle and that allows simultaneous availability of data in both time and crank angle domain. Once the sensors are physically connected to the hardware then the parameterisation is done programmatically as shown in figure 4.16.

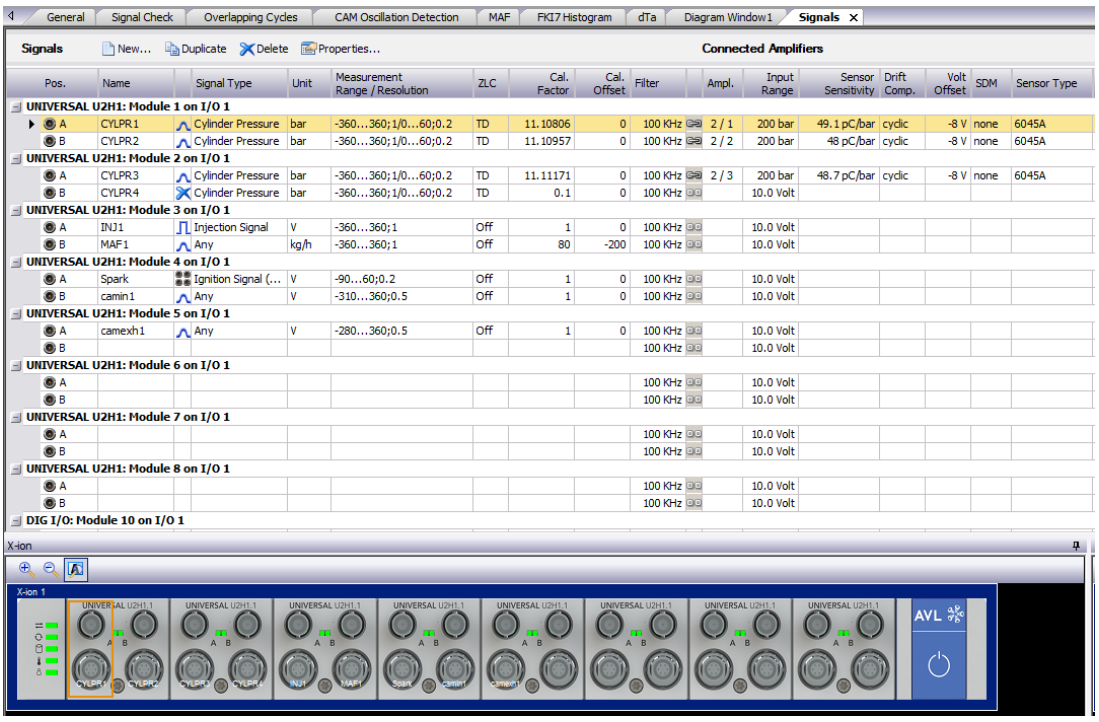


Figure 4.16 Parameterisation of X-ION data acquisition system

The above figure is a good example which shows the flexibility of the system as it shows that not only combustion related signals can be obtained but also various other engine signals such as spark timing or injection timing. [70]

## 4.5 Testing methodology

For this project a new engine testing methodology was developed which is quite different from the ordinary tests that are performed during engine testing. The main purpose of this different type of testing is to excite the system (engine) as much as possible in the shortest period of time which as a result provides us with a very rich index of data. [71], [72] The tests were divided into three main categories based on the engine actuator which was excited. The first and main test is the rapid air charge sweep, and then the torque test was performed where the engine spark was excited and last is the turbo controls test where the turbo waste gate actuator was excited. All the tests were performed by using advanced programming interface (API) algorithms using Matlab directly controlling the ECU calibration software hence the ECU. The application programming interface comprises of subroutine definitions, protocols and tools for building an application using specific software. Basically it allows different software to communicate with each other by using pre-defined methods of communication. Normally when software is written the developer provides an API guide with the software including a list of other software that can communicate with it so engineers can develop applications based on these information. [73], [74]

### 4.5.1 Air charge sweep

Before starting explaining this test it is worth mentioning that with the term air charge sweep it is implied that with the engine running at a constant speed the inlet manifold pressure of the engine is ramped up from the minimum to the maximum achievable point. This can be done either by actuating the

throttle pedal directly and let the ECU control the actuators or in our case by writing an algorithm which allows us to directly change the actuator settings as desired. The second method was chosen for our tests because of the way the ECU strategy works. In other words by actuating the throttle pedal the ECU tries to achieve a maximum torque by constantly changing the throttle and the waste gate but this causes nonlinear readings of the air mass flow since the actuators are not working linearly. By ramping up the actuators directly and bypassing the ECU control strategy it is ensured that the maximum manifold pressure can be achieved in the most linear way. Below in figure 4.17 an example of the air charge sweep test algorithm in Matlab can be seen.

```
%throttle ramp
throttle_ramp_start = 10;            %[degrees] start of ramp
throttle_ramp_delta = 30;            %[degrees] increase in throttle
throttle_ramp_max = 41;              %[degrees]  maximum allowed throttle position

%wastegate ramp
wg_ramp_start = 0;             %[degrees] start of ramp
wg_ramp_delta = 0.30;            %[degrees] increase in throttle
wg_ramp_max = 0.31;              %[degrees]  maximum allowed throttle position

repeats = 1;                % times to repeat the loop
ramp_time = 60;             %[seconds]

% test for instruction cycle time
tic;
ETC_TA_ADDER.TargetValue = throttle_ramp_start;

for i = 1:100
    ETC_TA_ADDER.TargetValue = ETC_TA_ADDER.ActualValue + 0.1;

end

time_avg=toc/100;

% complete the ramp test 'repeats' times rf
iterations = ramp_time/time_avg;        %number of iterations to complete
throttle_increment = throttle_ramp_delta/(iterations/2);
wg_increment = wg_ramp_delta/(iterations/2);

tic

for i = 1 : repeats

    ETC_TA_ADDER.TargetValue = throttle_ramp_start;

    pause(10);
    for j = 1 : iterations/2
        if ETC_TA_ADDER.ActualValue < throttle_ramp_max
            ETC_TA_ADDER.TargetValue = ETC_TA_ADDER.ActualValue + throttle_increment;

        else

        end
    end


    for j = 1 : iterations/2
        if WGC_ADD.ActualValue < wg_ramp_max;
            WGC_ADD.TargetValue = WGC_ADD.ActualValue + wg_increment;
```

Throttle actuation

Wastegate actuation

Figure 4.17 Air charge sweep test algorithm

Another part of the algorithm which is not displayed is handling the recording of the data channels and auto saving the data file at the end of the test. After the maximum manifold pressure is achieved the engine is kept at that point

for a few seconds until is stabilised and then the same process is repeated to ramp down the manifold pressure to the point where the test initially started. This test is repeated at different engine speeds and camshaft timing positions.

### 4.5.2 Torque test

The torque test uses the same API interface for changing the spark like the previous test but the method with which that is achieved is different. For this test, sweep methods to adjust the spark are not being used but instead an amplitude modulated pseudo random binary signal (AMPRBS) is created and then injected into the spark adder within the ECU. The AMPRBS is generated using a special algorithm which gives us the ability to control the limits, duration and hold time of this signal. [75]

```
%% randomly generated signal


start_time = 0;
end_time = 20;          %seconds
duration = end_time - start_time;
sample_time = 0.05;

time = [start_time:sample_time:end_time];

min_val = 0.15;
max_val = 0.5;

min_hold = 0.1;
max_hold = 1;

n = duration/min_hold;

%generate hold times
holds = (max_hold-min_hold).*rand(n,1) + min_hold;
cumholds = cumsum(holds);

%generate amplitudes
amps = (max_val-min_val).*rand(n,1) + min_val;
total = sum(amps);

%align amps with holds
count = 1;

for i = 1:length(time)              %checks to see if time(i) has been exceeded
    if time(i) < cumholds(count)
        value(i) = amps(count);
    else
        count = count + 1;          %if it has the counter is incremented
        value(i) = amps(count);
    end
end
```

Signal properties

Signal Limits

Signal hold time

Figure 4.18 AMPRBS Signal generation algorithm

After the AMPRBS signal is generated it is fed into the main algorithm so the engine can be excited and the main purpose of this test is to examine the changes in air mass flow of the engine when the spark is modulated. The advantage of using this sort of signal compared to ordinary sweeps is that because the hold time can be very small (0.1s, extreme spark limits (advanced – retarded) can be achieved that in any other case would not be possible due to knock or misfire. Before the test starts the engine is at a constant speed/load position with the throttle locked (bypassing the ECU strategy) and then the spark signal is fed into the ECU. This results into fluctuations of the torque generated by the engine and as a result the air

mass flow into the engine changes accordingly. Similarly to the air charge test, in this test the recording and storage of data is handled automatically through the test algorithm.

### 4.5.3 Turbo controls test

This test uses the same algorithm to generate the AMPRBS signal like the previous test but in this case the signal is fed into the waste gate adder calibration parameter. The engine is kept at a constant speed/load point similarly to previous test and then the signal is fed into the actuator. This results into sudden increase and drop of the inlet manifold pressure which causes big differences in the engine's air charge which in turn means the air mass flow changes as well. In this test it is very critical to choose the correct actuator limits for each speed/load point as wrong configuration of the test algorithm can lead into excessive boost pressure which can damage critical engine components or the engine itself. In figure 4.19 part of the Matlab algorithm can be seen used for the turbo controls test.

```
% Throttle setting

   ETC_TA_ADDER.TargetValue = 10;

   pause (2);

   ETC_TA_ADDER.TargetValue = 15;

   ETC_TA_ADDER.TargetValue = 20;

   pause (2);

   ETC_TA_ADDER.TargetValue = 40;

   pause (2);

%    ETC_TA_ADDER.TargetValue = 40;
%
%    pause (5);
```

```
%% randomly generated signal

amps = {0.1, 0.6};
holds = {0.1, 1};

[time, value] = amprbs (60, amps, holds);

sample_time = time(2) - time(1);        %time vector must be uniform
tic;


for i = 1:length(time)  %careful with sample time (est min is 50 msec)

    if i == 1
        WGC_ADD.TargetValue = value(1);


    elseif i >= 2
        while toc  < i * sample_time
            %do nothing

        end

        WGC_ADD.TargetValue = value(i);

    end
```

**Signal limits**

**Signal duration**

**Wastegate excitation**

Figure 4.19 Turbo controls test algorithm

## 4.6 Summary

This chapter starts with a description of the technical characteristics of the unit under test which is important as it represents the engine used for testing on the dyno and consequently the data collection. The next paragraph describes analytically the testing facility used for the test and its main elements emphasizing on the principle of operation of the main instrument used for measuring the engine air mass flow. The following paragraph gives an analytic description of the software used for controlling the testing facility and various hardware, followed by an analysis of the various measurement and data acquisition systems used for data collection. It is crucial to understand the above as this sort of testing facilities are very complicated and consist of various pieces of software and hardware. Finally the last part of the chapter gives an in depth description of the testing methodology specially developed for this project with examples of the actual code running the experiments.

# Chapter 5: Engine test results

This chapter is about presenting and analysing the experimental data collected during engine testing. At first the recorded channels are described due to their large number and also the complexity due to the many locations the readings were picked up from. Next the daily check data collection is described and justified, followed by the air charge data collection analysis. Next is the torque data collection and description and ending up with the turbo controls data collection and analysis. At the end of this chapter a short summary of the data collection will be discussed.

## 5.1 Recorded channels description

As mentioned in the previous chapter, during the engine testing experiments the data obtained are from different sources but they are all recorder in a same recorder created within the ECU calibration interface. The main reason for that is that it ensures all the data are time aligned and also being saved all in a single file it makes post processing a lot easier and efficient. In figure 5.1 all the recorded channels and a short description which explains what exactly is measured on the engine can be seen. It is also worth mentioning that there are three different acquisition rates depending if the channel is pressure, temperature or calibration parameter from the ECU. The channel names look a bit difficult to understand but they are set up in a way that the minimum amount of characters is needed to describe what kind of measurement they refer to. [76]

| Channel Name | Description | Units | Acquisition rate |
|---|---|---|---|
| A_TURBOP | Pressure after turbo | kPa | 500 Hz |
| ATURBO_T | Temperature after turbo | Deg C | 500 Hz |
| ACT | Air charge temperature | Deg F | 100 Hz |
| AFR_HORIBA | Air fuel ratio | - | 100 Hz |
| AFTCOMPP | After compressor pressure | kPa | 500 Hz |
| AFTCOMPT | After compressor temperature | Deg C | 500 Hz |
| AFTCOMPT_FAST | As above with special thermocouple | Deg C | 500 Hz |
| AIRCNR_P | Air cleaner pressure | kPa | 500 Hz |
| AM | Air mass | Kg/hr | 100 Hz |
| ATMP | Atmospheric pressure | kPa | 500 Hz |
| ATMT | Atmospheric temperature | Deg C | 500 Hz |
| AVL_FB_VAL | Fuel flow | Kg/hr | 100 Hz |
| ECT_DEGC | Engine coolant temperature | Deg C | 100 Hz |
| ENGINE_SPEED | Engine speed | rpm | 100 Hz |
| FSA_RATE | Air mass flow | Kg/hr | 500 Hz |
| ICAIRINP | Intercooler inlet pressure | kPa | 500 Hz |
| ICAIROUT | Intercooler outlet temperature | Deg C | 500 Hz |
| ICAIROUP | Intercooler outlet pressure | kPa | 500 Hz |
| INMAN_GA | Inlet manifold pressure | kPa | 500 Hz |
| INMAN_T | Inlet manifold temperature | Deg C | 500 Hz |
| LAM_30MS | Engine lambda sensor | - | 100 Hz |
| LBMF_INJ_0 | Fuel injector mass flow | Kg/hr | 100 Hz |
| LOAD | Normalised cylinder air charge | - | 100 Hz |
| MAP | Manifold absolute pressure | In Hg | 100 Hz |
| MCT | Manifold charge temperature | Deg C | 100 Hz |
| P_TURBOP | Pre turbo pressure | kPa | 500 Hz |
| P_TURBOT | Pre turbo temperature | Deg C | 500 Hz |
| PRECOMPP | Pre compressor pressure | kPa | 500 Hz |
| PRECOMPT | Pre compressor temperature | Deg C | 500 Hz |
| PRETB_P | Pre throttle body pressure | kPa | 500 Hz |
| SPKSAF_SA | Final spark angle | deg | 100 Hz |
| SPKSAF_SA_ADD_S | Spark angle adder | deg | 100 Hz |
| TORQUE_R | Raw torque measurement | Nm | 500 Hz |
| TPP_THETA_FIN | Throttle butterfly valve | deg | 100 Hz |
| TQE_BRK_LED | Calculated torque | Nm | 100 Hz |
| TQE_BRK_REQ | Required torque | Nm | 100 Hz |
| TURBO_N_INF | Turbine speed | rpm | 100 Hz |
| VCT_CAM_ACT_EXH | Exhaust camshaft position | deg | 100 Hz |
| VCT_CAM_ACT_INT | Intake camshaft position | deg | 100 Hz |
| WG_CAP_P | Waste gate capsule pressure | kPa | 500 Hz |
| WG_DC_0 | Waste gate duty cycle | - | 100 Hz |
| WGC_ADD | Waste gate duty cycle adder | - | 100 Hz |

Table 5.1 Recorded data channels

## 5.2 Daily check data collection

The term daily check refers to a process that takes place daily before the actual engine testing commences and produces statistical data. It is not directly related to this project but it is worth mentioning due to the importance of this procedure. The testing sequence is defined by the development engineers and normally consists of a series of operating points all different to each other where various engine actuators such as camshafts, spark timing are set to simulate different engine operating conditions. In our case these operating points are four and the test is fully automated and data are collected and stored according to their collection date and can be plotted in a way that shows the whole history of the engine since testing was commenced. The most important advantage of the daily check procedure is that the engineers can plot al the historical data of each instrumentation channel of the particular engine and can immediately spot malfunctioning sensors or instrumentation or even more importantly engine operation issues. In figure 5.1 the data from the fast ultrasonic air mass flow sensor plotted and in the x axis the dates can be seen. The operating point for this particular graph is 2000 rpm and 200 kPa brake mean effective pressure. It is very obvious that there are no large deviations on the sensor readings which ensure that the repeatability of this sensor is very good and also there is no malfunction on the engine since the air mass flow measured is constant. All the channels described in the previous paragraph are included in the daily check data collection which means that by checking this data regularly the quality of the data produced by the engine can be maximised and also less valuable testing time is wasted.

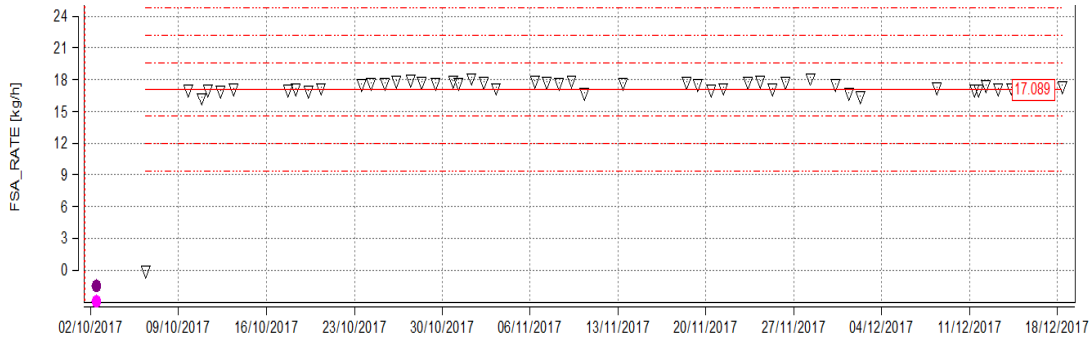


Figure 5.1 Daily check point example

## 5.3 Air charge test results

This paragraph first talks about the operating point that was chosen for this particular test and the engine settings followed by justification of these choices and then the air charge data will be presented and analysed using graphs generated by Matlab.

### 5.3.1 Engine test operating point

During engine development and more specifically air charge calibration, the engine is operated at a number of speeds starting from idle to the maximum operating speed of the engine. This ensures that the whole operating range of the engine is covered and the engine can be mapped appropriately. Also because all modern engines have variable valve timing it is very important that the valve timing is known every time an air charge sweep is performed since valve timing has a major effect on engine breathing. For that reason camshaft indexes are generated for every engine which have all the possible cam timing settings that the engine could have during service. For this particular engine in this project there are 15 camshaft indexes.

The operating point that was chosen for the data collection that will be presented in the next paragraph was 2905 RPM and the camshaft index was 0 which indicates that the camshafts are in the locked position and the inlet valve opens 20 degrees after top dead centre (ATDC) and the exhaust valve closes at 0 degrees which is the top dead centre (TDC). This engine speed was preferred because it is within the maximum torque range of the engine and also is high enough for the turbocharger to generate high boost pressure which has a direct effect on the air charge of the engine. Also it is a very stable operating speed during high boost conditions such as this test which as a result gives higher quality data with minimum oscillation especially on the measured air mass flow into the engine as it can be seen later. The cam timing was set to locked position (index 0) because the engine operates quite efficiently at this point and also ensures there is no blow through (scavenging) condition which could lead to pulsation in the inlet manifold and again could affect the measured air mass flow. Before moving to the data analysis it is worth mentioning that during the air charge data collection, the engine was operated in almost every speed and camshaft index but the above operating point was selected based on the author's judgement and existing literature. [77]

### 5.3.2 Engine test results and analysis

Before moving to the test results presentation and analysis it is important to mention that the whole duration of this air charge test (sweep) is 6 minutes. Normally during air charge calibration the sweeps last a lot longer (up to 20 minutes) but in this project due to very fast data acquisition systems the sweep was performed a lot faster without sacrificing data quality. Also the

inlet manifold pressure rate is 1 kPa/second which is controlled by the automation software.

During air charge calibration one of the most important prerequisites is the accurate control of the engine coolant temperature during testing. The coolant temperature can seriously affect engine operation as the ECU is programmed to operate differently when the engine is not in the optimum operating temperature. This as a result can affect the combustion process which also has a direct effect on the air charge characteristics of the engine. For this particular engine the coolant temperature demand is set at 88 degrees Celsius with maximum tolerance of ± 5 degrees and the test cell PID controller takes over to maintain this temperature throughout the test.

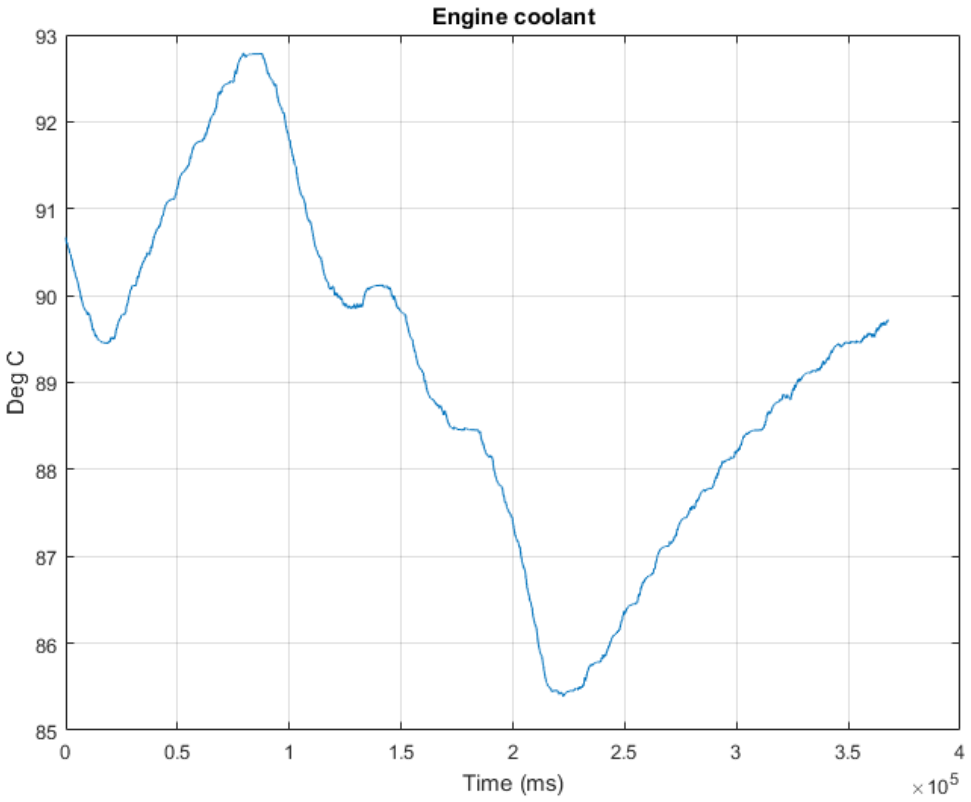


Figure 5.2 Engine coolant data

In figure 5.2 the engine coolant temperature recorded data can be seen for a particular air charge test. It is noticeable that the temperature deviation at any point is not exceeding the maximum tolerance of 5 degrees from the set point of 88 degrees Celsius. By looking at the graph it can be seen that the test started with a temperature of about 90 degrees and the first 100 seconds it rose to almost 93 degrees. After that the PID controller reacted and the temperature gradually dropped to 85.5 to increase again at about 90 degrees towards the end of the test.

The next very important element that needs to be analysed during an air charge test is the actuator settings. As described earlier at a previous chapter in order to perform this test, the throttle butterfly is moved from the minimum to the maximum allowed angle followed by the waste gate duty cycle until the maximum intake pressure is achieved.

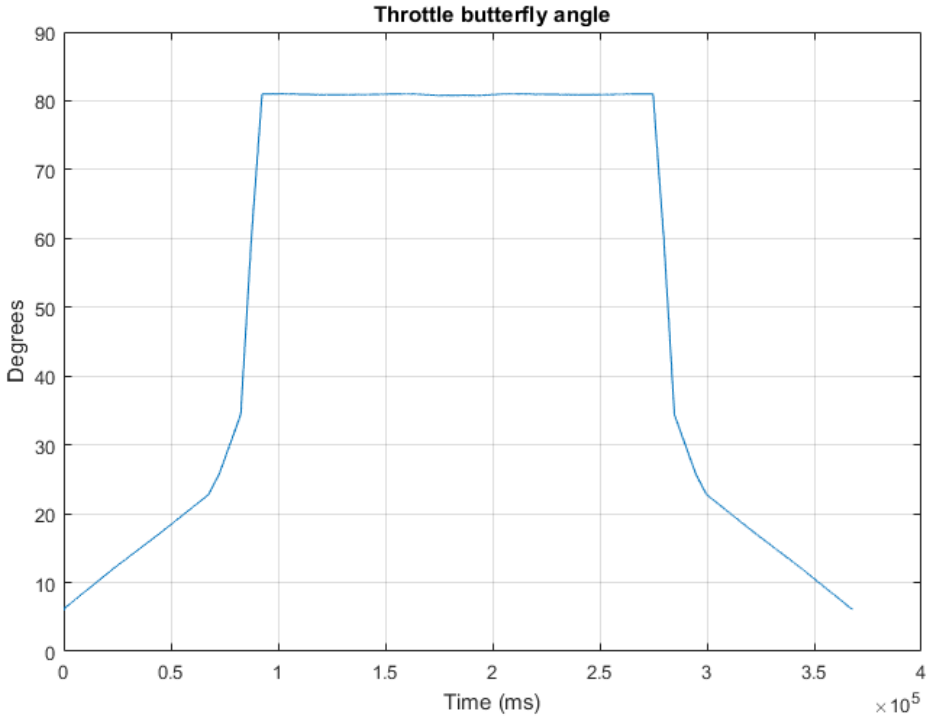


Figure 5.3 Throttle butterfly data

In figure 5.3 the throttle butterfly actuation during the test can be observed. The graph shows that the test started with the butterfly just below 10 degrees follower by a linear increase up to 25 degrees the first 70 seconds and then a steep increase to the component limit of 81 degrees which occurred at about 100 seconds since the test started. It is noticeable that the line of the graph changes and becomes steeper after25 degrees and that is because after that point the throttle butterfly has less effect on the boost pressure of the engine and as such the automation software ramps up the throttle faster to maintain the required boost pressure increase rate.

Below in graph 5.4 the waste gate duty cycle data can be seen. The duty cycle is unit less and its range is from 0.15 – 1 where 0.15 translates to fully open and 1 fully closed (maximum boost).

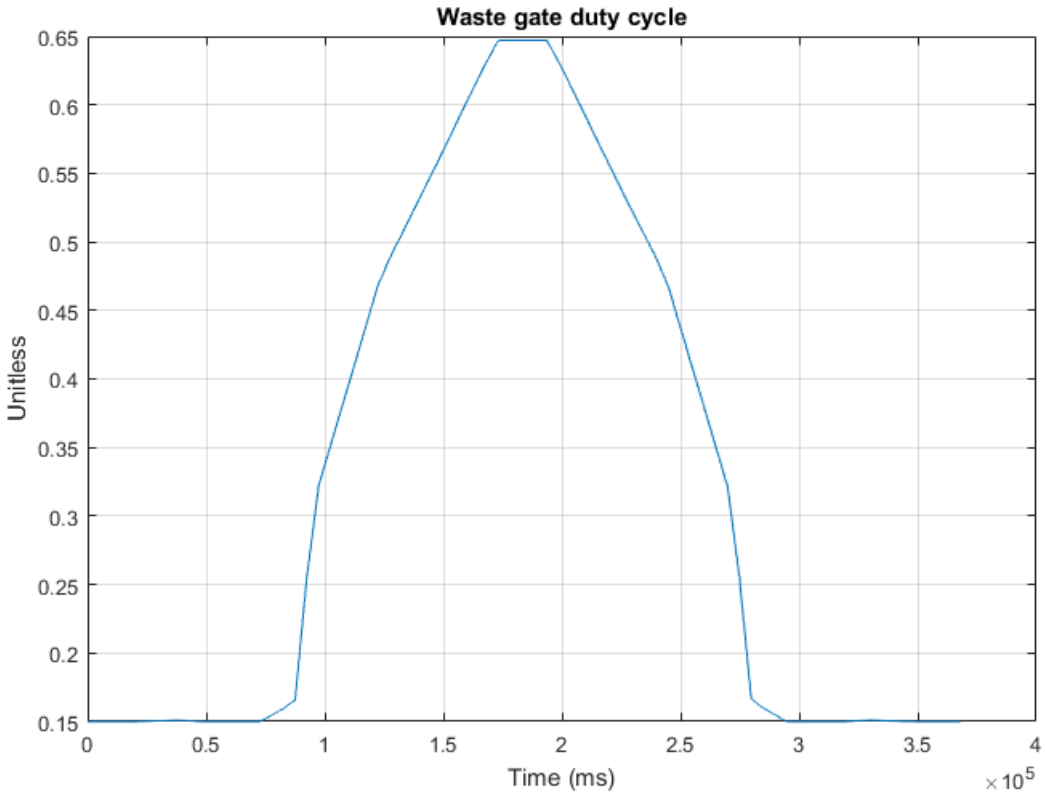


Figure 5.4 Waste gate duty cycle data

The test starts with the actuator fully open and it starts closing at about 70 seconds. It is noticeable that the automation software starts closing the actuator significantly just before 100 seconds since the test started which is the point that the throttle butterfly has no effect on inlet manifold pressure anymore since it is already almost fully open. The duty cycle graph is quite linear and that is because the duty cycle has a linear effect on the boost pressure produced by the turbocharger. The maximum value achieved in this test is 0.65 and at that point the maximum inlet manifold pressure was achieved. Looking at both of the actuator graphs it is noticeable that the line of the graph during ramping up and down is exactly the same which ensures the best possible air charge data quality and repeatability.

After looking at the above graphs it is obvious that the actuators are following the design of experiment but another important element needed to focus on is the inlet manifold temperature. It is very crucial this temperature is controlled during air charge calibration because large temperature differences can seriously affect the amount of air entering the engine due to density variations. This becomes even more critical on turbocharged applications such as the engine under test in this project due to the increase of pressure and as a result temperature of the boosted air coming out of the turbocharger. To control the temperature of the air entering the inlet manifold a water cooled intercooler is used which is controlled by a PID controller and the set point for this test is 25 degrees Celsius. In figure 5.6 the inlet manifold temperature during the test can be seen. The temperature was measured at the centre of the inlet manifold by a special thermocouple (0.08 mm diameter) specifically designed for this project which is described at chapter

4. Due to the very fast response of this thermocouple very slight variations in temperature can be captured and obtain a very accurate measurement. Looking at the graph it can be seen that the test started with a manifold temperature of about 26 degrees and dropped to 20 degrees the first 100 seconds. This happens because during that time the engine is running without any boost pressure and the increased air flow due to throttle opening is cooling down the inlet manifold. After that the boost pressure starts building up and the temperature rises to 32 degrees. Although the PID controller tries to control the temperature to 25 degrees at the intercooler outlet there are slight temperature variations at the inlet manifold due to heat conductivity from the cylinder head to the manifold. Overall the temperature control is good without massive temperature differences and this will become more obvious later when the data for the air flow into the engine is analysed.

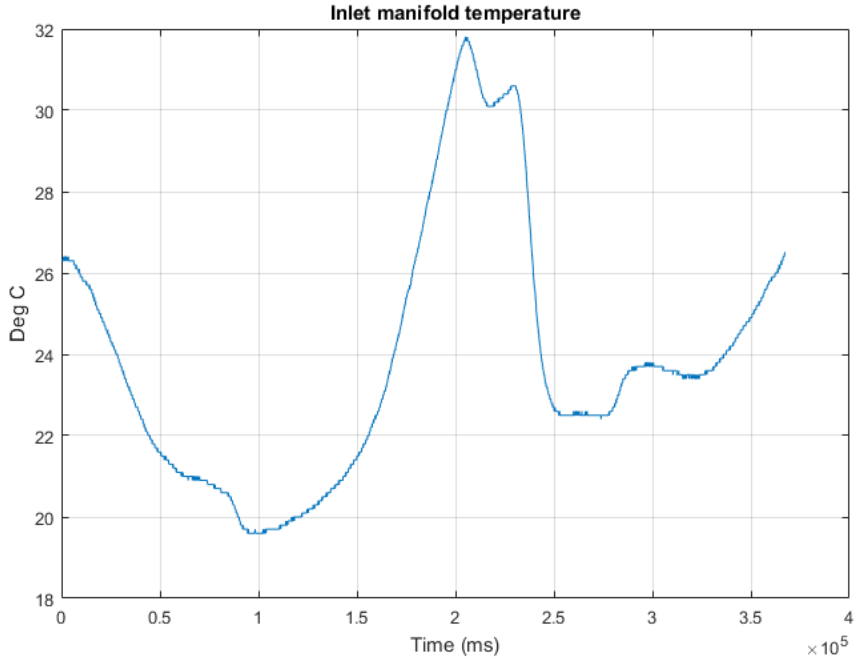


Figure 5.5 Inlet manifold temperature

The next critical channel that needs analysing is the camshafts actuator positions because this can affect the air flow into the engine if it is not kept constant during the test.

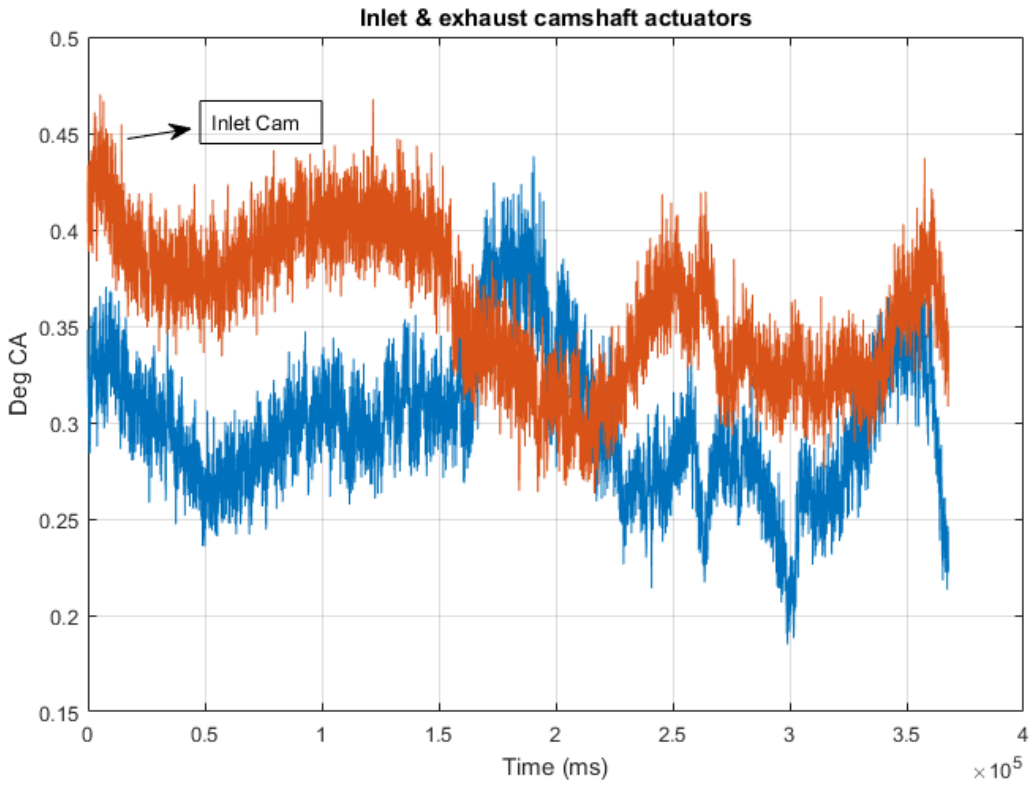


Figure 5.6 Inlet & exhaust camshaft position data

Based on the design of experiment they are set to 0 degrees crank angle (CA) for the duration of the test as explained earlier in this chapter. Looking at the above graph it can be seen that they very close to 0 for the whole duration. The slight variations up to 0.35 deg CA for the exhaust camshaft and up to 0.45 deg CA for the inlet one are due to some electrical noise between the actuators and the engine wiring loom and should not raise any concerns.

The next very crucial element for this test that needs analysing is the inlet manifold pressure. The inlet manifold pressure is directly related with the air

charge and  is necessary to make sure that during the air charge calibration the maximum intake manifold pressure is achieved so the engine can be calibrated through the whole operating envelope.

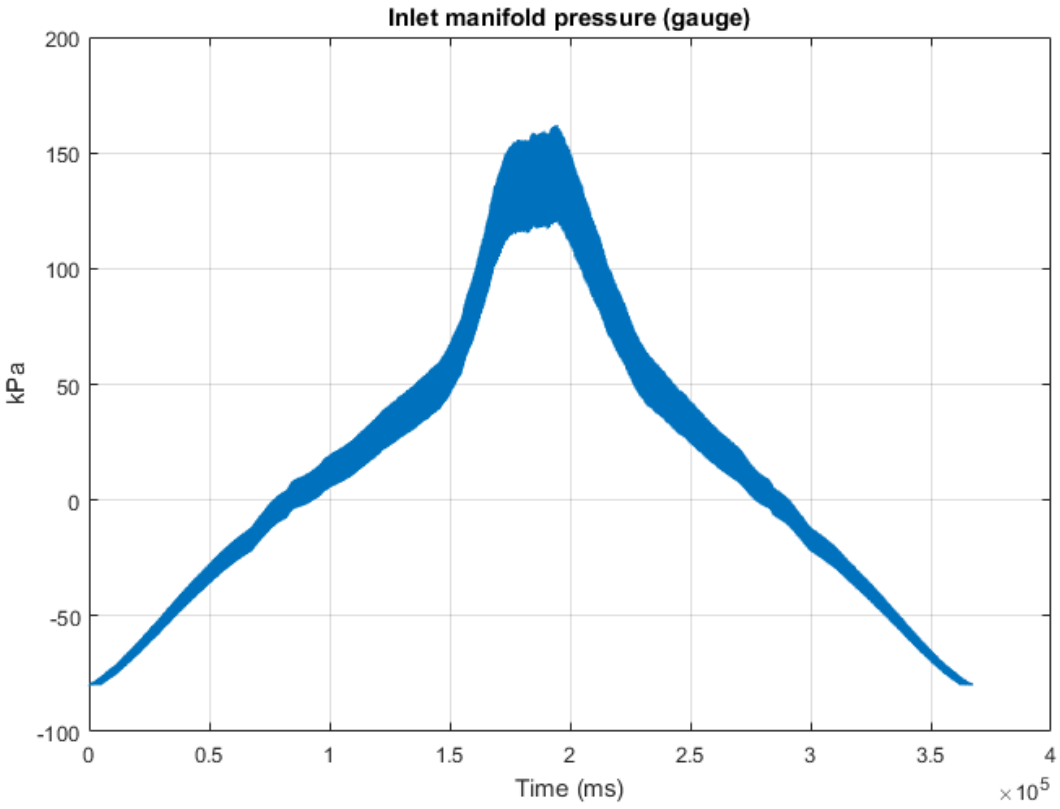


Figure 5.7 Inlet manifold pressure (gauge)

Looking at graph 5.7  it can be seen that the test starts with a manifold pressure of -80 kPa and increases linearly to a maximum value of 160 kPa. This value is 40 kPa more that the rated inlet manifold pressure of the engine which is 110 kPa and ensures that the whole operating envelope of the engine is covered. When the maximum pressure is achieved the engine is kept at steady state operation for 20 seconds for stabilisation purposes and then the pressure decreases linearly again until the minimum pressure is

achieved. It is also noticeable that the shape of the graph is almost perfectly symmetrical which shows that the test was performed flawlessly.

All the above graphs with the engine data presentation and analysis are very crucial because they allow us to explain and visualise how the air charge test was performed and also to check that it was conducted as described by the design of experiment (DoE). After proving that the test was conducted as planned now it is time to present and analyse the data for the measured engine air mass flow which is also the main reason the above test was performed. It is worth mentioning once again that the air mass flow is measured by the ultrasonic air mass flow measurement instrument described in chapter 4 and the data acquisition rate is 1 kHz.

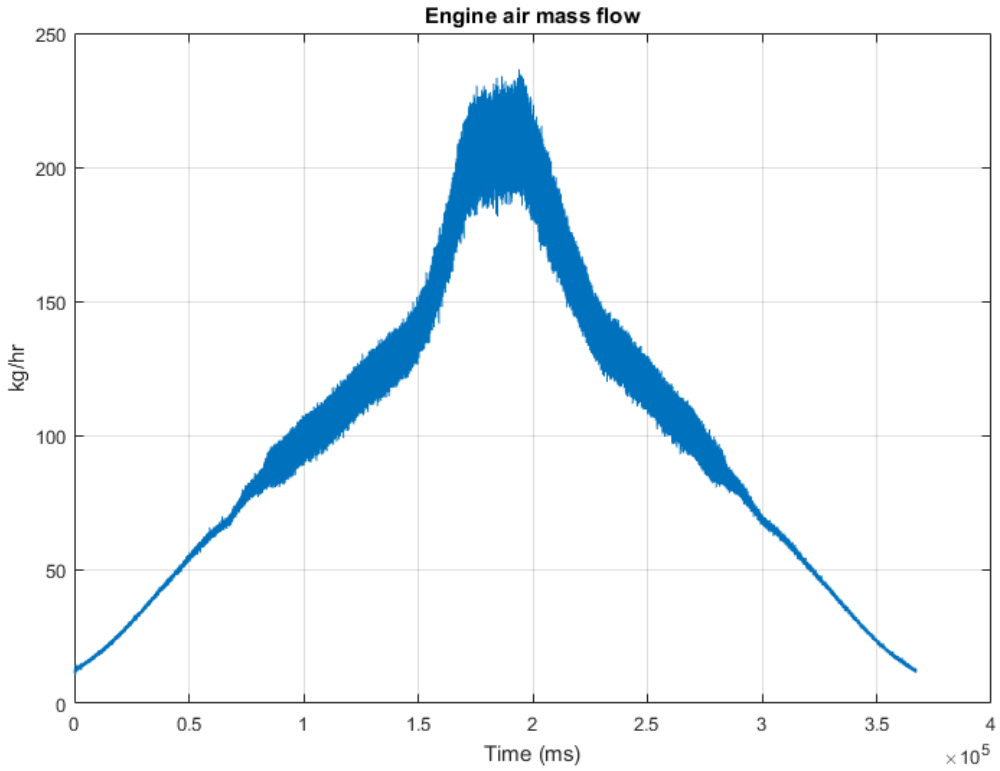


Figure 5.8 Engine air mass flow

In graph 5.8 the raw unfiltered data from the instrument can be observed. The test starts with the engine sucking approximately 20 kg/hr of air and that increases linearly as the inlet manifold pressure increases since they are directly linked to each other. At around 100 seconds the line on the graph becomes thicker and that is because the engine is entering the boosted are and there is a lot of pulsation in the inlet air path which can be captured due to the very high acquisition rate of the instrument. The maximum air mass flow of the engine is 220 kg/hr and can be seen at about 200 seconds in the middle of the steady state operation. It is also very important that the shape of the graph once again is perfectly symmetrical which shows that the air charge is linear and repeatable and also that the instrument is measuring correctly without any leaks.

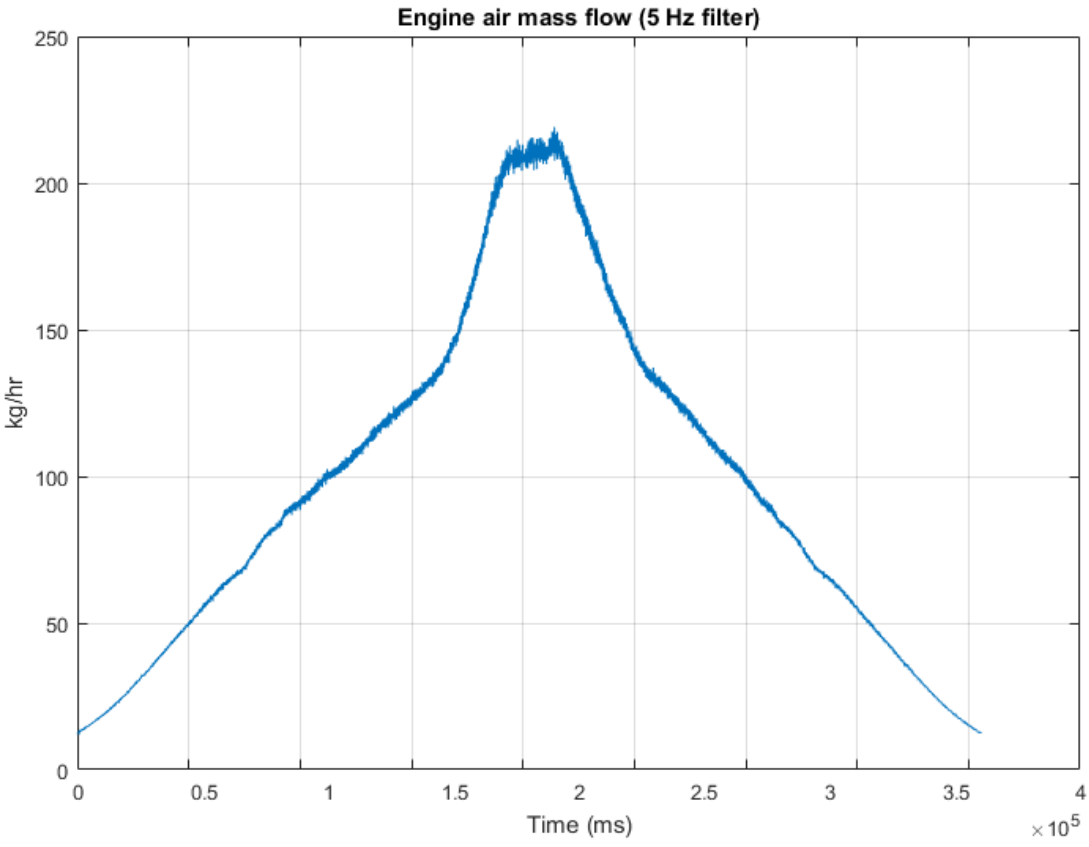


Figure 5.9 Filtered engine air mass flow (5 Hz)

In figure 5.9 a filtered version of the air mass flow data can be seen which was created by applying an electronic low pass filter at 5Hz.

## 5.4 Torque test results

In this paragraph the torque test (spark excitation) will be described starting with the operating point description and justification and followed by the data presentation and analysis.

### 5.4.1 Engine test operating point

This test was performed in order to examine how by altering the spark timing of the engine during medium- high load conditions can affect the air charge and as a result the measured air mass flow of the engine. For this test the speed of the engine was set at 3500 RPM and the throttle and Wastegate actuators were set so the load of the engine is 1. This load is a unit less ECU parameter and refers to the normalised cylinder air charge. The reason this speed was chosen is because is in the medium- high range and that ensures there is enough air flow going through the engine. The load of the engine was set to 1 because it is high enough so the engine is in the boosted region but also safe so the spark timing can be widely excited and its effects can be examined.

This test is different to the air charge one as this test is performed by setting the engine speed and the throttle and Wastegate actuators to certain values until a specific speed/load point is achieved, and then the camshaft actuators are set to locked position (index 0). Once the above are all set then the actual test is starting with the spark timing limits finding. The automation

software performs a search to find the minimum and maximum spark limits by gradually retarding the spark until combustion instability is detected by the combustion indicating software and on the other side by advancing the spark until knock is detected by the combustion indicating software. Once this search is complete two spark values should have been obtained for maximum and minimum. Based on these values the AMPRBS signal is constructed (described in chapter 4) and the test can begin.

### 5.4.2 Engine test results and analysis

Before moving on the data presentation it is important to mention that the duration of the test is 65 seconds during which the AMPRBS signal is fed into the ECU spark timing as described in chapter 4 and the data is recorded.

Like in the previous test it is important to analyse certain data to make sure that the test was performed as planned and the result are as expected before moving on to the main data analysis for this test. At first the actuator positions need to be checked and verified to ensure that the test was performed as planned.

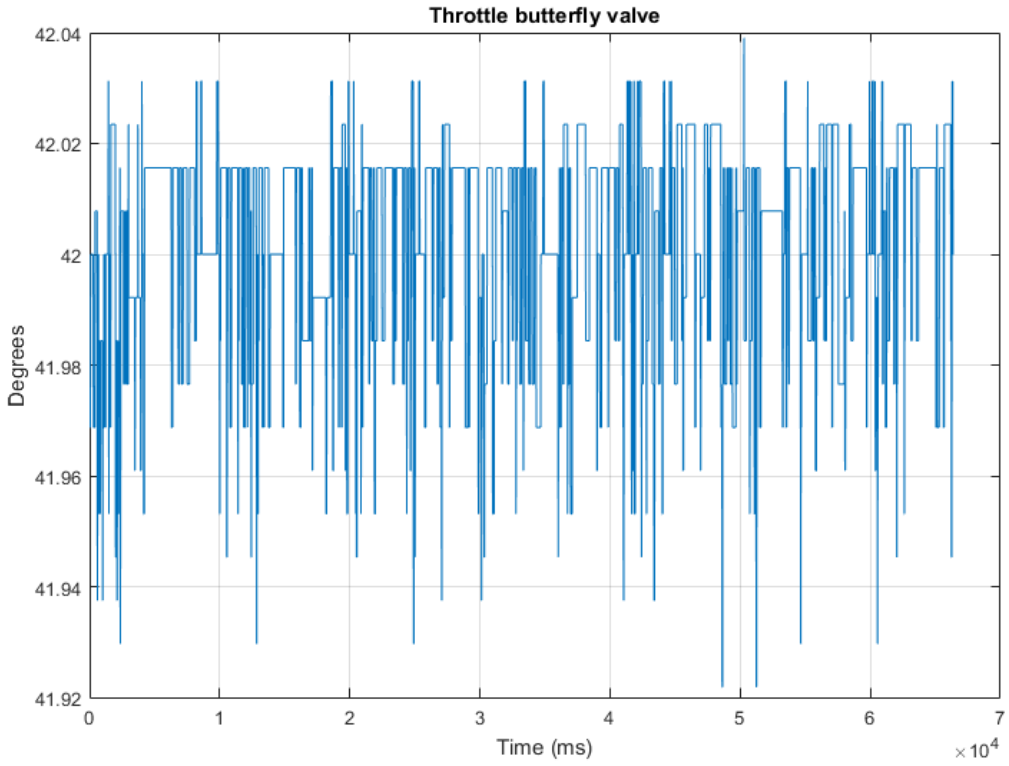


Figure 5.10 Throttle butterfly position data

Looking at graph 5.10 it is obvious that the throttle was kept at 42 degrees although the signal is quite noisy but the variation of the throttle as recorded is very minimal. The next graph shows the data from the waste gate duty cycle as recorded during the test.

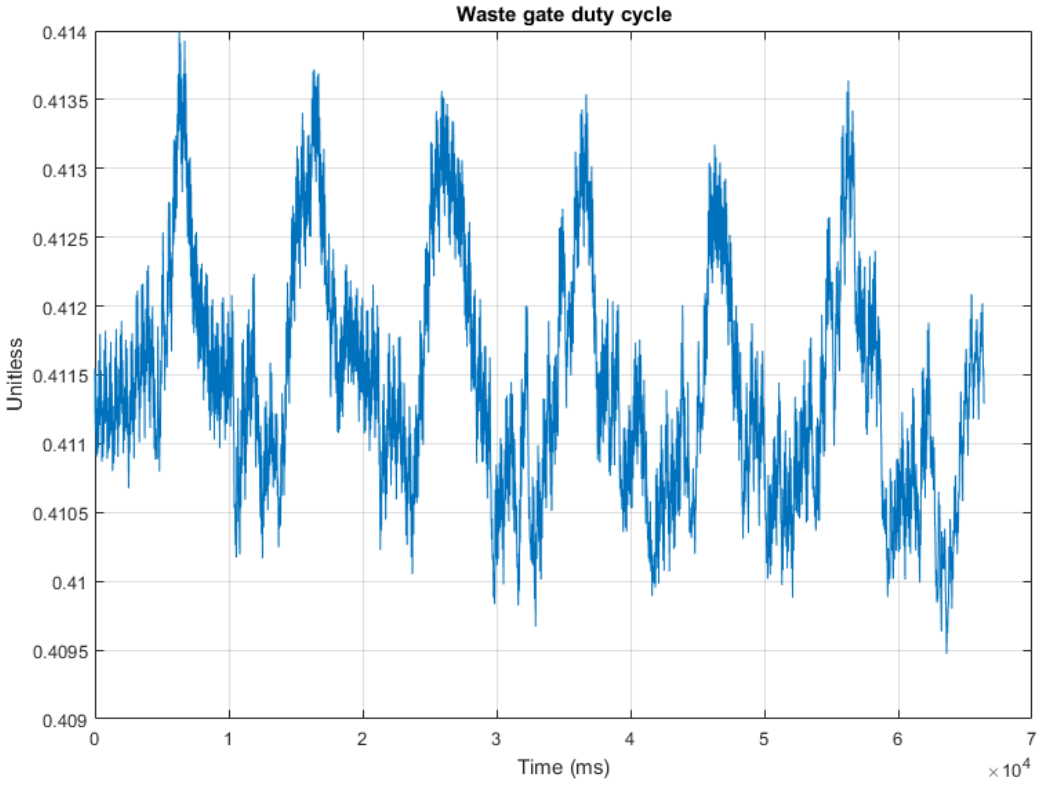


Figure 5.11 Waste gate duty cycle data

Looking at the above graph it can be seen that the required waste gate duty cycle position for this particular speed/load point was 0.41 and was kept constant during the test. Both actuator graphs ensure that the settings were correct and the test was performed as planned. One last parameter that needs checking is the camshaft actuators which were set to 0 like in the previous test. Looking at graph 5.12 it can be seen that both camshaft actuators were set to 0 as planned with a little bit of electrical noise same as in the previous test.

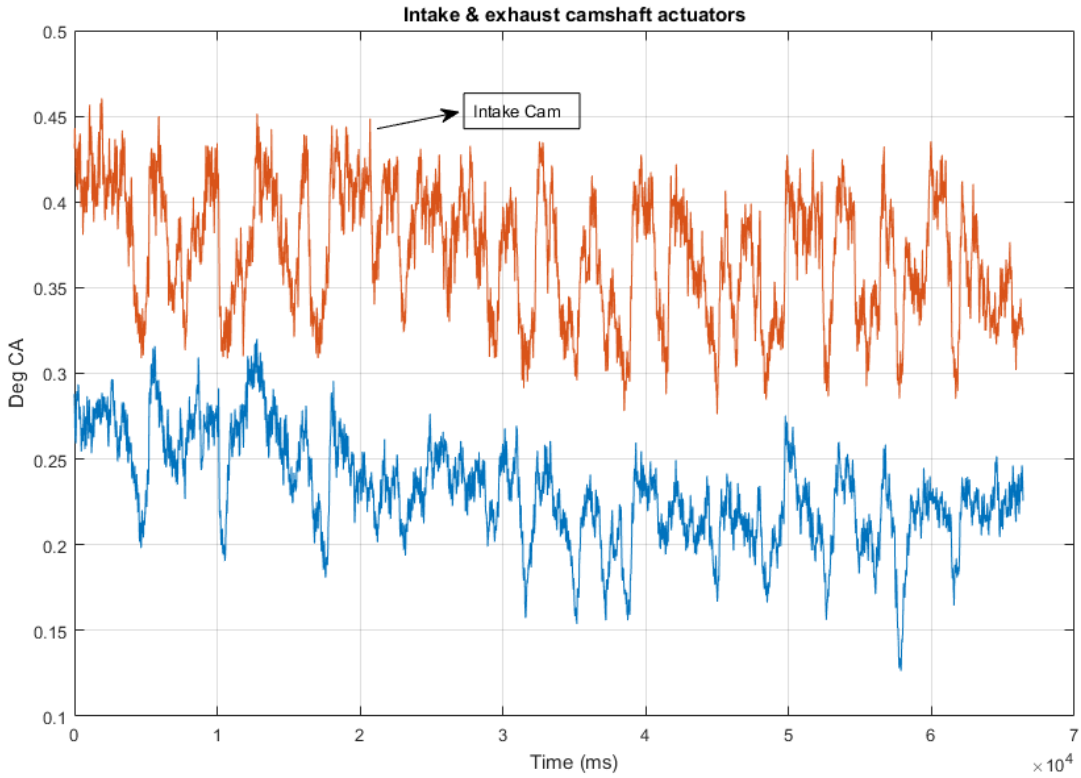


Figure 5.12 Camshaft actuators data

After ensuring that the test was conducted as planned with the engine actuators following the test design, the next step is to examine and analyse critical engine parameters and how they were affected by the spark excitation. Firstly it is important to present the data of the spark timing as measured by the ECU and see how the AMPRBS signal looks like for the first time. Figure 5.13 shows the ignition timing during this test and the random nature of the signal is immediately noticeable. The test starts with about 14 degrees spark advance before top dead centre (BTDC) followed by a random sequence of spark settings. Also having a closer look to the graph it can be noticed that the duration of each of the settings (or else called hold time) is variable and for this particular test varies between 0.1 and 1 second. The maximum spark advance achieved in this test is 15 degrees BTDC

which is the limit for knock in this particular operating point and the maximum spark retard achieved is 4 degrees ATDC. Also as can be seen in the graph the whole duration of the experiment is 65 seconds.

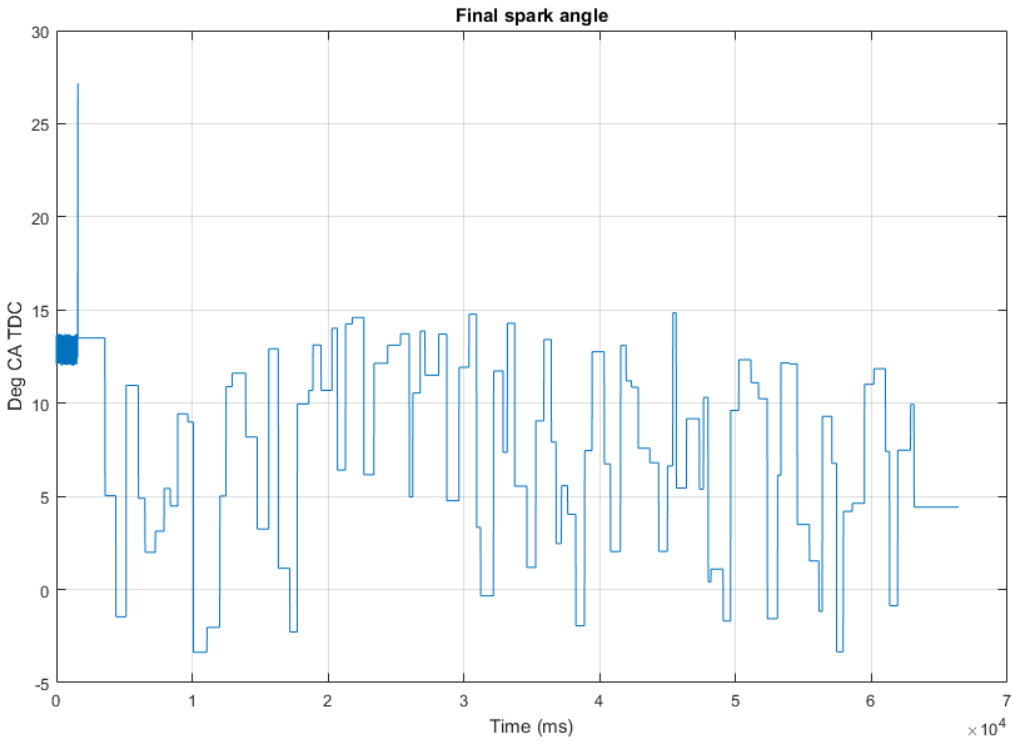


Figure 5.13 Spark timing (AMPRBS)

After presenting and analysing all the inputs of this test it is time to present the data of the critical engine outputs such as load, torque, and more importantly the engine air mass flow and see what effect the spark timing has on these. In figure 5.14 the engine brake torque can be observed. It is immediately noticeable that the torque of the engine is significantly affected by the spark timing excitation as someone would expect and in some cases can be up to 30 Nm. Also by looking at figure 5.14 and 5.15 it is obvious that the shape of the graphs follows similar pattern which confirms the above. The maximum torque produced by the engine in this test is 117 Nm and the

minimum is 79 Nm which confirms the impact the spark timing has on the engine torque.

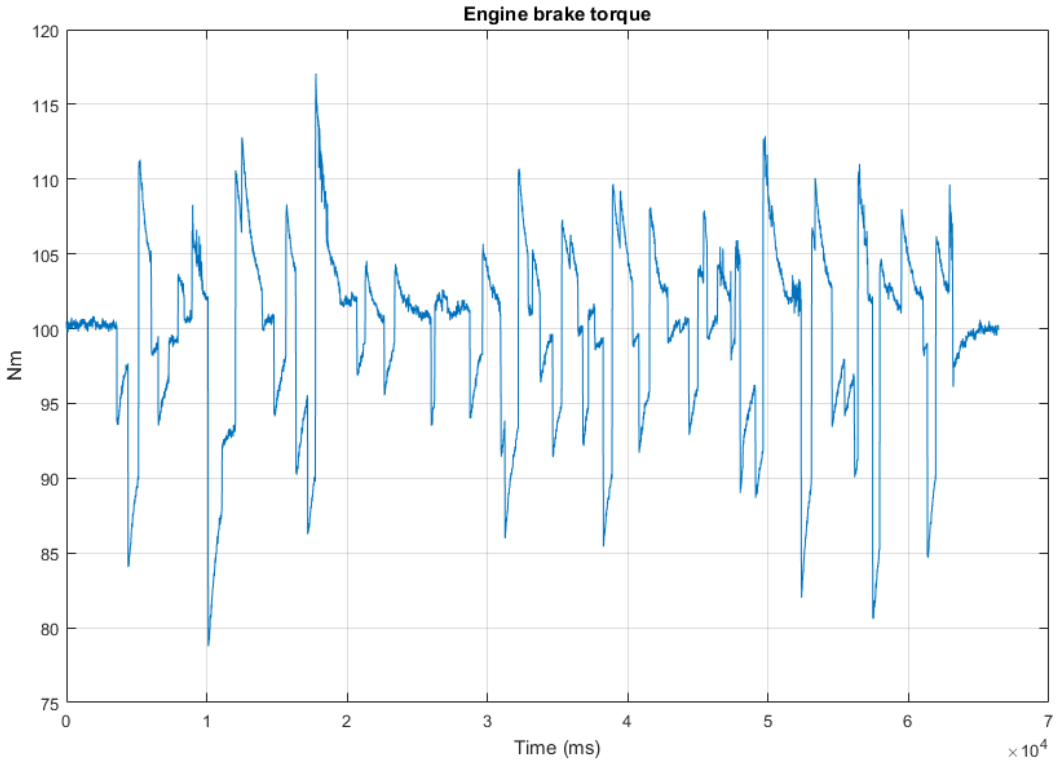


Figure 5.14 Engine brake torque

Another very interesting parameter that requires analysing is the turbocharger speed during the test. The reason this is so important is because the speed of the turbocharger is directly connected with the measured air mass flow. By having a close look at graph 5.15 it can be observed that the test start with a speed of 95000 rpm which is constantly changing and by looking at graph 5.13 it is noticeable that during the test the spark timing is mostly retarded since the maximum spark advance for this test is defined at the beginning. Every time the spark is retarded there is a significant increase in the turbocharger speed. This happens because when the spark timing is retarded the combustion is not perfect and some of the

air- fuel mixture ends up unburned in the exhaust manifold. The manifold being very hot causes the mixture to ignite and as a result additional energy is released into the turbocharger which leads to a speed increase.

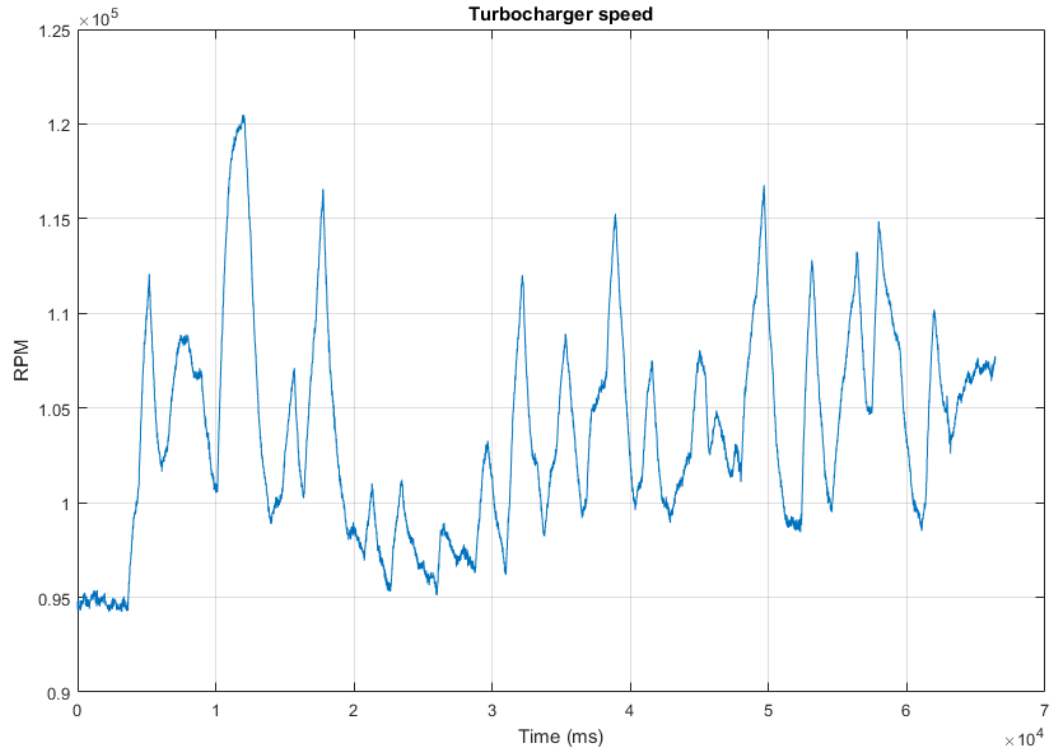


Figure 5.15 Turbocharger speed

After looking at the variation of the turbocharger speed next is analysing the effect the spark timing excitation has on load (normalised cylinder air charge). By looking at graph 5.16 it can be observed that the test starts with a load of 1 as defined in the test plan and then significant variations are occurring while the spark timing is excited. As expected since the turbocharger speed is increasing and decreasing this has similar effect on the engine load as well because they are directly linked to each other. The maximum load value is obtained at about 120 seconds since the test started and is 1.2.

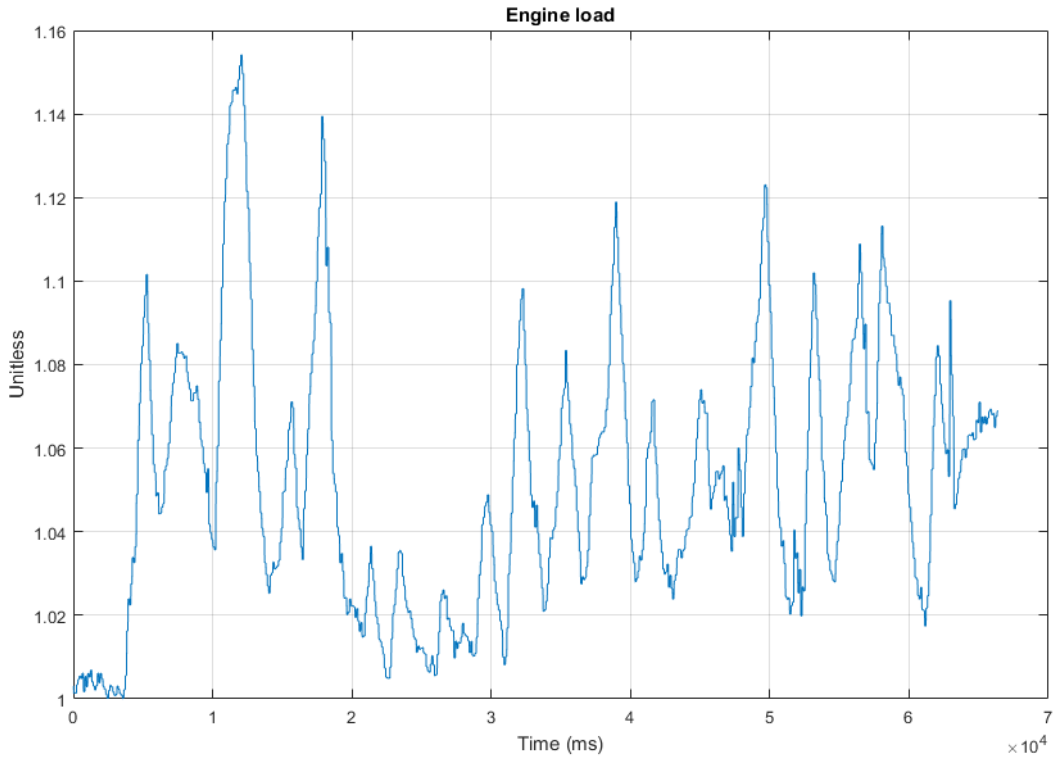


Figure 5.16 Engine load (normalised cylinder air charge)

Finally after analysing all the inputs and outputs of the engine and how they have been affected by the spark timing excitation it is crucial to examine what is the effect of spark timing excitation in the measured engine air mass flow during medium-high speed and load conditions. By looking at graph 5.17 it is observed that the test starts with an air mass flow of 130 kg/hr which is also the minimum recorded value and as soon as the spark excitation starts, large variations in the air mass flow can be observed. The maximum measured air mass flow is 157 kg/hr at about 12 seconds after the test started. It is also clear that the signal is a little noisy due to the very high acquisition rate of the instrumentation equipment and also by minor pulsation phenomena during engine operation.

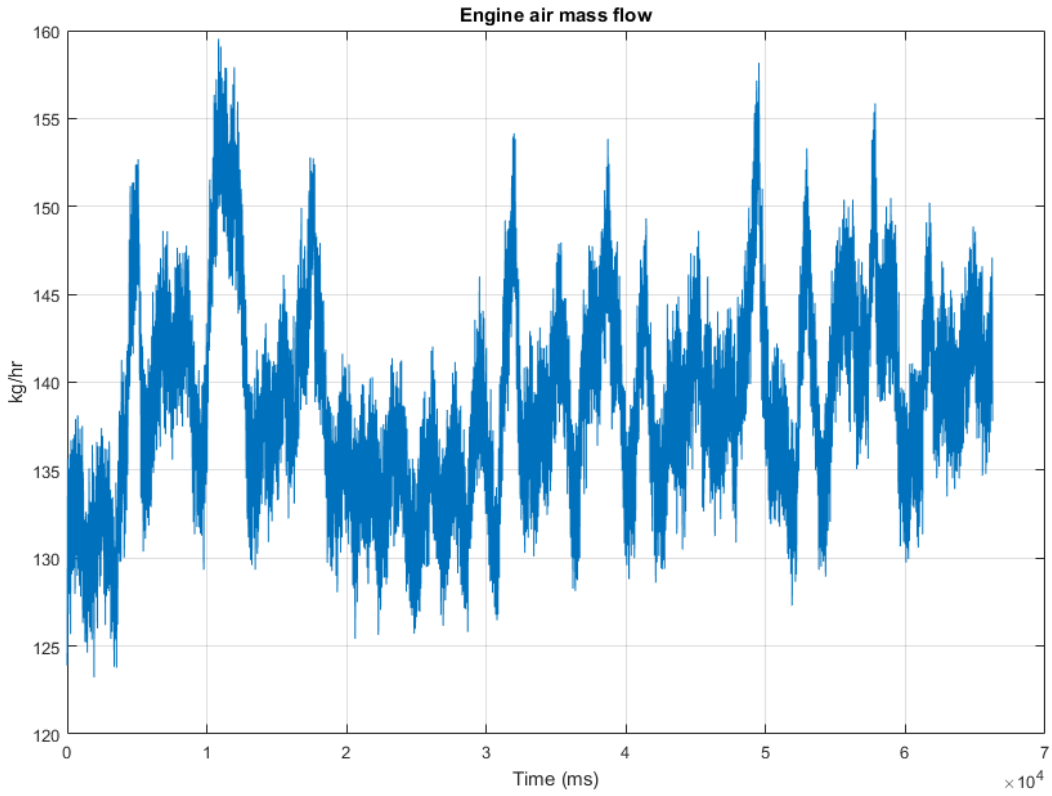


Figure 5.17 Measured engine air mass flow

## 5.5 Turbocharger test results

In this paragraph the way the test was conducted is described and justified giving details about the operating point and actuator settings followed by the engine data presentation and analysis and examining the effect this kind of testing has on certain engine parameters.

### 5.5.1 Engine test operating point

The principle behind this test is very similar to the torque test but in this case we set the test point based on engine speed and inlet manifold pressure. So the set point for starting this test is 3000 RPM and 30 inches Hg manifold pressure which is equal to 100 kPa (absolute). The reason this point was chosen is because again the speed is high enough so we have adequate air flow through the engine and the manifold pressure is high enough so the engine runs on a boosted region. After the operating point is set the AMPRBS signal is injected this time to the waste gate actuator for 70 seconds which is the whole duration of the test. The procedure for setting the operating point is the same as in the previous test by setting the throttle butterfly and the Wastegate actuator until the required speed/manifold pressure point is achieved.

### 5.5.2 Engine test results and analysis

Before moving on to the main data analysis it is crucial to ensure that the actuators are set appropriately for the test to commence. In graph 5.18 the data from the throttle butterfly valve can be observed.

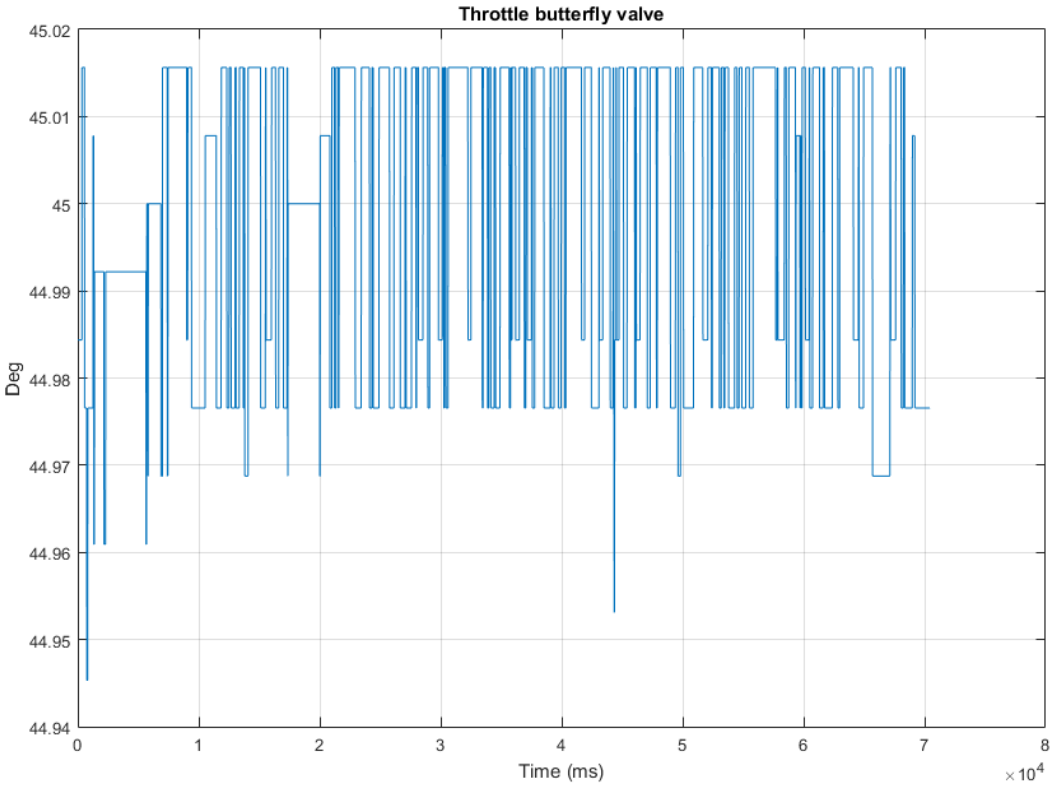


Figure 5.18 Throttle butterfly valve

From the graph above it is obvious that the butterfly valve was kept constant at 45 degrees through the duration of the test. This setting is the one required to achieve the set point for this particular test.

The next actuator which needs examination is the waste gate one which is also the one excited in this experiment. In graph 5.19 the data from the test can be observed.

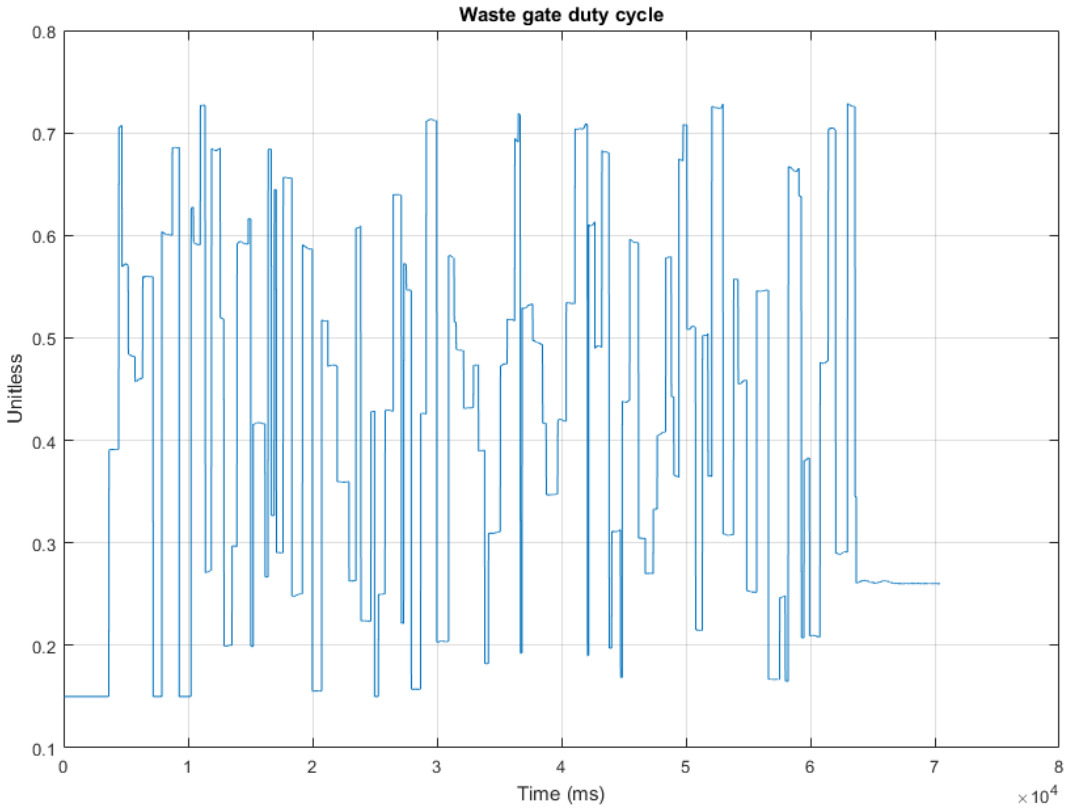


Figure 5.19 Waste gate actuator data

The test starts with a value of 0.16 which is the required for the set point to be achieved and then the AMPRBS signal is injected to the ECU with variable hold times and values. The maximum duty cycle achieved in this test is 0.72. After presenting the data for the engine actuators (inputs) it is worth looking at the outputs of the engine starting from the turbocharger speed which is directly affected from the waste gate excitation. The waste gate actuator is used to control the pressure produced by the turbo charger by directing gases away from the turbine wheel the more it opens or directing gases to the turbine wheel the more it closes. Looking at graph 5.20 it can be observed how the turbocharger speed is affected by the waste gate excitation.

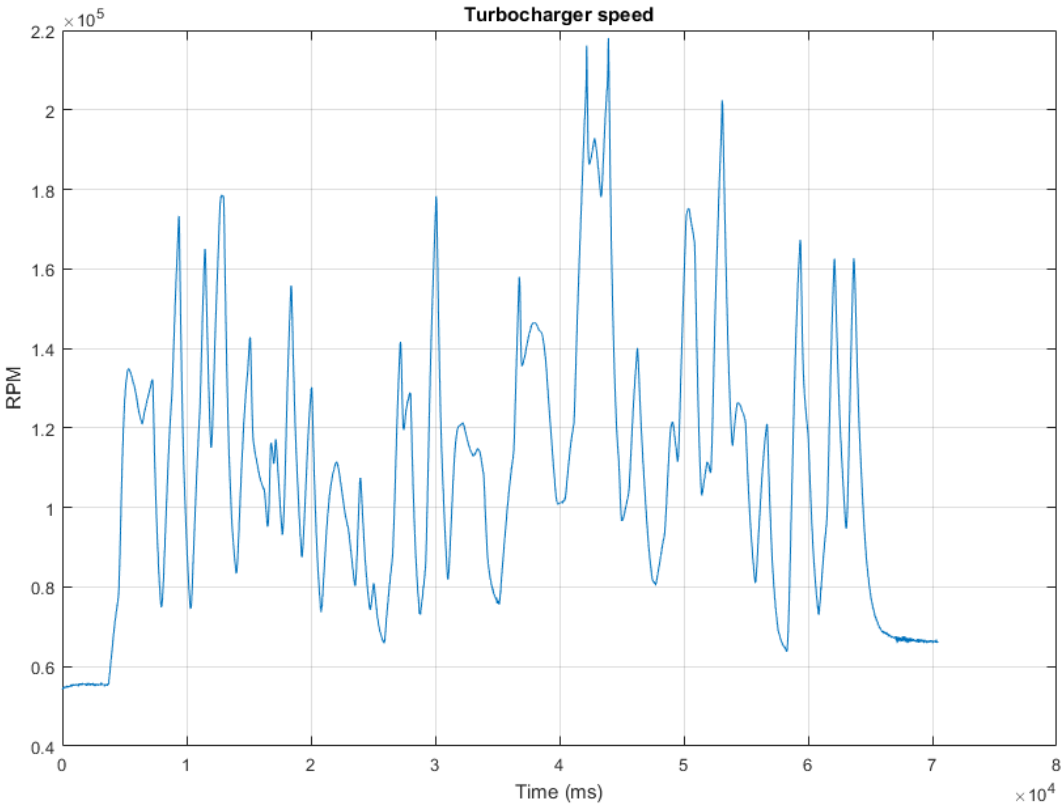


Figure 5.20 Turbocharger speed

As expected the turbocharger speed data follow similar pattern with the waste gate actuator data because the turbocharger speed is directly affected by the position of the waste gate actuator. It is also noticeable that at 42 and 44 seconds the turbo speed reaches almost 220.000 rpm which is also the component limit which clearly shows that the engine operated at maximum load for part of this test and this will have an effect on the measured air mass flow as it is presented later in this chapter. It is also very interesting to examine what happens to the exhaust gas temperatures before and after the turbocharger during the duration of the test. The reason this is important is because according to the pressure law the higher the temperatures of the gas, the higher the energy of the gas is which leads to higher turbine speed.

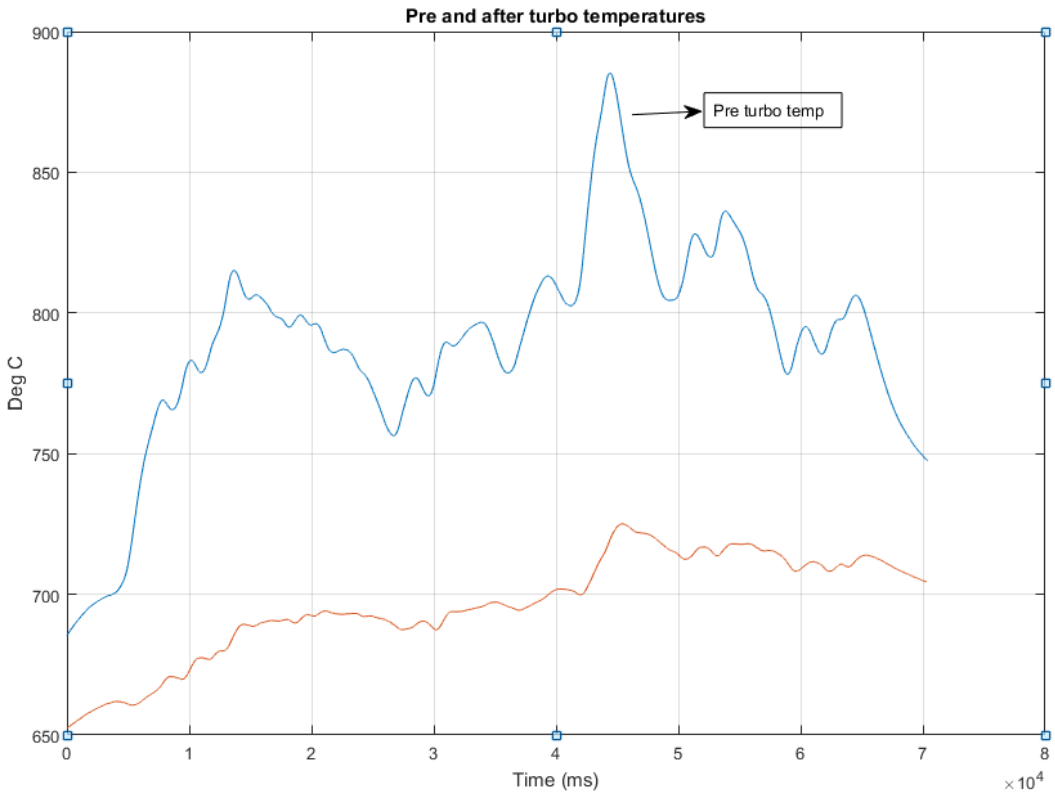


Figure 5.21 Pre and after turbocharger temperature

Looking at graph 5.21 the two temperatures can be observed. The line on the top with higher temperature is the pre turbocharger data and the line at the bottom is after the turbocharger. The temperature before the turbocharger is higher because as the gases exit the cylinder hear they have to go through the turbine wheel which itself causes a restriction. That leads to pressure increase and as a result a temperature increase. Both graph trends are increasing for most of the duration of the test due to thermal inertia accumulated in the exhaust system and particularly at around 42 seconds where a big increase in turbocharger speed occurs that leads to a big spike on both gas temperatures.

Finally looking at the last graph 5.22 it can be examined how the measured air mass flow of the engine is affected by this experiment.

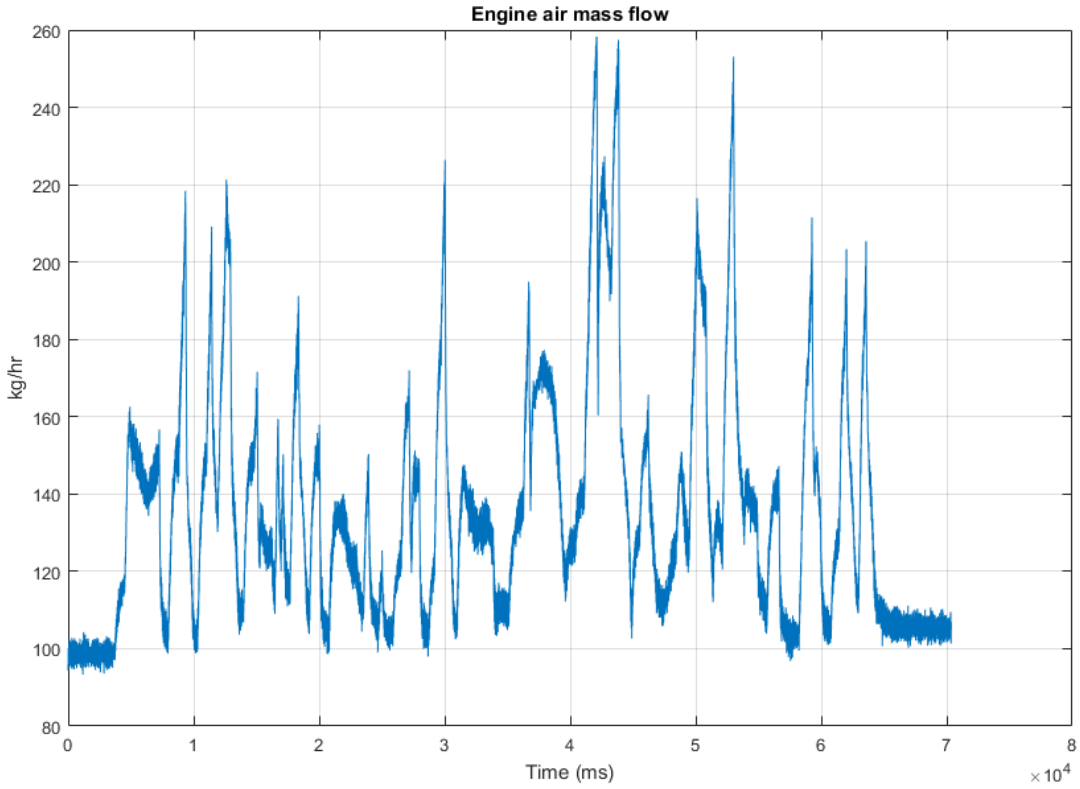


Figure 5.22 Measured engine air mass flow

In figure 5.23 it can be seen that the measured air mass flow of the engine is significantly affected by the waste gate excitation and particularly at about 42 seconds when as explained before there is a massive increase in turbocharger speed which causes the air mass flow to reach almost 260 kg/hr which is the maximum that should be expected from this engine. The minimum value of air mass flow is obtained at the start of the test and is about 100 kg/hr. These data like in the previous tests are the raw unfiltered ones and are recorded at 1 kHz.

### 5.6 Engine test results summary

Looking at all the data presented in this chapter for all three different tests the conclusion is that all tests excite the engine with completely different

ways but the common output of all is that the engine measured air mass flow is significantly affected. At first the air charge test which is used for air charge calibration increases the air mass flow linearly by ramping up the inlet manifold pressure which is the element that has the most significant effect to the air mass flow of the engine. The graph that presents the air mass flow data is very linear and repeatable on the way up and also on the way down which shows that the test was performed correctly and in a repeatable way and the data can be used in a later chapter for comparison with the modelled data. The other two tests follow different principle to the first one but by exciting the spark timing and the waste gate actuator they prove that a significant change on the measured air mass flow can be achieved. Of course in this chapter only one operating point for each test was presented but during the course of this project many different operating points were ran for each different test to ensure that the necessary repeatability is achieved and also to examine the effects of each test through the whole operating envelope of the engine.

# Chapter 6: Virtual engine model (WAVE)

This chapter is about the development and analysis of the virtual engine model which was developed for this project using Ricardo WAVE engine simulation package. At first the importance of engine modelling is presented and also justified. The next paragraph will be an introduction the WAVE software itself focusing on its main characteristics and features and explaining the necessity of using such a software for modern engine development. Then moving onto the main model starting with the model structure which will be describing the most crucial elements of the model, followed by the model building and parameterisation which explains how that particular model was built. The last paragraph of this chapter will be about the simulation and results where the data and graphs obtained by the model will be presented and analysed.

## 6.1 Why using engine modelling

Modern reciprocating engines clearly differ in many aspects from other type of engines such as gas turbines or aircraft engines. The reciprocating engines have highly transient operation during service which makes the combustion process highly transient as well with fast changes in pressures and temperatures and also all the processes that are related to the combustion process such as intake manifold pressure or air fuel ratio are never constant during engine operation. In addition to that modern engines comprise of many complex subsystems and parameters which makes the control and calibration of the above very challenging.  On top of that the

development engineers face the need their engines to comply with stricter emission legislation and fuel efficiency standards which further increases the complexity of the engine development process. All the above make the use of model based simulation approach necessary during engine development process where computer based models are used to predict and optimise various engine outputs such as torque, speed and AFR. Another very important reason why engine modelling is so popular is because it reduces the actual experimental time used for engine development. In other words it is much cheaper for automotive companies to develop virtual engine models and use them for part of the engine development process rather than focus only in experimental engine testing using real engine hardware and equipment which is very time consuming and also very expensive. [78]

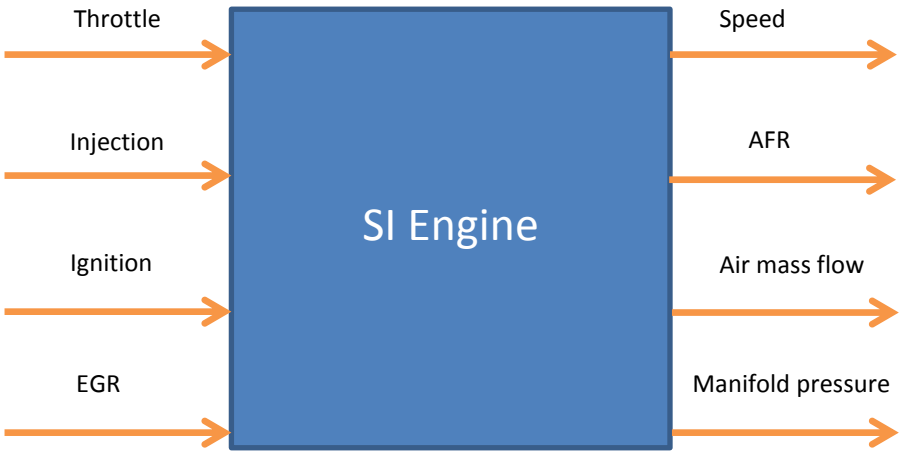


Figure 6.1 Input output signal principle in engine modelling

Figure 6.1 is a representation of how the input-output principle is used during the engine modelling procedure. The actual engine model is the “SI engine”

where the known inputs are fed and the model will produce the output parameters of the engine.

During modelling an engine in a virtual environment it is required to set clear targets and objectives about the purpose of the simulation and what is expected to be produced as an output. Different objectives and targets would need different engine design, parameterisation etc. so it is very important for the model developer to understand the details and choose the right model type accordingly. [79], [80]

### 6.2 Introduction to Ricardo WAVE software

The virtual engine model required for this project was developed using the Ricardo WAVE software package. WAVE is one of the market leading 1D gas dynamics and simulation package and is widely used from the automotive manufacturers worldwide. Its computer aided code is capable of analysing the dynamics of pressure waves, air mass flows and energy loses in all the subsystems of the engine during operation. When additional detailed analysis is required it can be coupled with various industry standard software packages such as CFD analysis or statistical analysis programs to carry out simulation of almost every process during engine operation. However WAVE is not limited only to simulating the internal combustion engine as it includes an extensive library of machinery elements such as piston compressors and pumps which make it suitable for also simulating other compressible fluid flow systems. [81], [82]

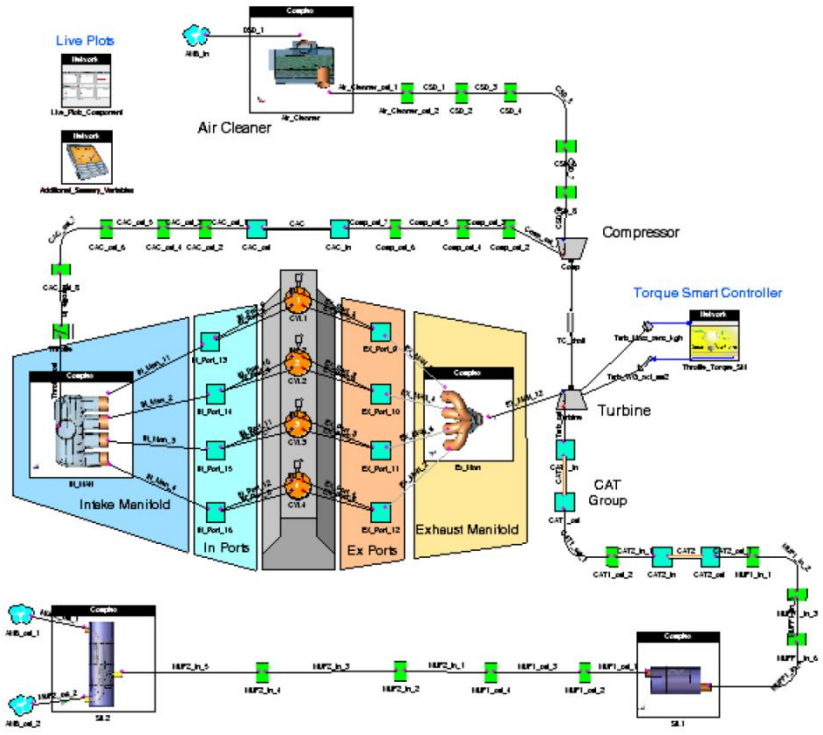


Figure 6.2 Engine model in WAVE

Typical applications where WAVE is used include:

- Engine performance

WAVE is widely used through the engine design process from the early concept studies to detailed investigation of production ready engines and offers solutions to applications such as fuel consumption prediction, valve train design, turbocharger and waste gate design, EGR studies etc.

- Combustion process and emissions

WAVE incorporates advanced combustion models both for gasoline and diesel engines and also exhaust after treatment models which can be used for combustion system design, after treatment system design, emission studies etc.

- Acoustics and noise

WAVE is used by automotive manufacturers worldwide for acoustic prediction of the intake and exhaust noise produced by the engine either for developing a cost effective exhaust system or for developing a more premium sound for upmarket vehicles. It offers big selection of intake system components for design purposes as well as exhaust systems components and also offers the capability of designing a specific noise signature for special applications.

- Thermal analysis

The software includes a 2D structural conduction model which provides accurate prediction of the heat extraction and is also capable of performing exhaust warm- up transient tests. The above can be used for exhaust – catalysts light off and also intake and exhaust system component temperature prediction for failure.

After describing the main applications where the software can be used, next is to describe the main programs which combined together make WAVE. WAVE is the generic name of an entire suite of software which comprises of the following three software types:

1) Pre- processors
2) Solvers
3) Post- processors

All three software types above are employed in that particular order for any simulation work within WAVE software and they are available both for Windows and Linux operating systems.

The pre- processors are programs which are used to set up the simulation work. They have a graphical user interface (GUI) where the engineer is able to select a series of values and inputs which are required to describe the simulation work needed and perform the analysis. The clever design of the pre- processors is what makes WAVE software relatively straight forward to configure and parameterise. The solvers receive the data in an appropriate format by the pre- processors and are used for the analysis of these data. They are mainly non interactive and just give the user a text print about the progress of the simulation. As expected they require substantial computational power and they are the ones which dictate the performance characteristics of the hardware used to run the simulations. Lastly the post-processors are used to view and interpret the results provided by the post-processors and they are primarily GUI based and they require some inputs from the user to produce 2-D or 3-D graphs or numerical arrays. [83]

### 6.3 WAVE model structure

In this paragraph the basic elements which form the structure of the model will be described and analysed before moving on to the model building and parameterisation in the next paragraph.

The complete WAVE engine model developed for this project was discretised into sub systems which make the development of the model easier and eliminate the possibility of wrong parameterisation. WAVE offers a library of objects which represent the actual engine components from where the user chooses the right parts. All the parts are linked together using connection

lines and junctions which if parameterised correctly mirror the gas flow paths. The main components of the model can be split into two main categories:

- Air flow elements (manifolds, pipes, throttle body etc.)
- Engine elements (engine block, turbocharger, fuel injectors etc.)

The air flow elements represent the components of the engine from which air flow passes through to the engine and from the engine. It is very important these are picked from the library wisely and parameterised correctly as they can significantly alter the simulation results. The airflow elements are connected with each other and to the engine using ducts, orifices and Y-junctions. The ducts are used to represent all the sections of pipework which have one dimensional flow and they have a specific diameter in each length and a given length. On the contrary the orifice element has no length or diameter and is used to connect to adjoining ducts which don't have the same diameter. Finally the Y- junctions are used to define a junction of the model with two or more openings and are used to model complex geometries such as intake manifolds' air filters and exhausts collectors. The throttle body is not represented by any of the above as it is used to model a butterfly plate in an orifice. The user can reference to a butterfly valve sub model which allows specifying the butterfly open area as a function of butterfly plate angle.

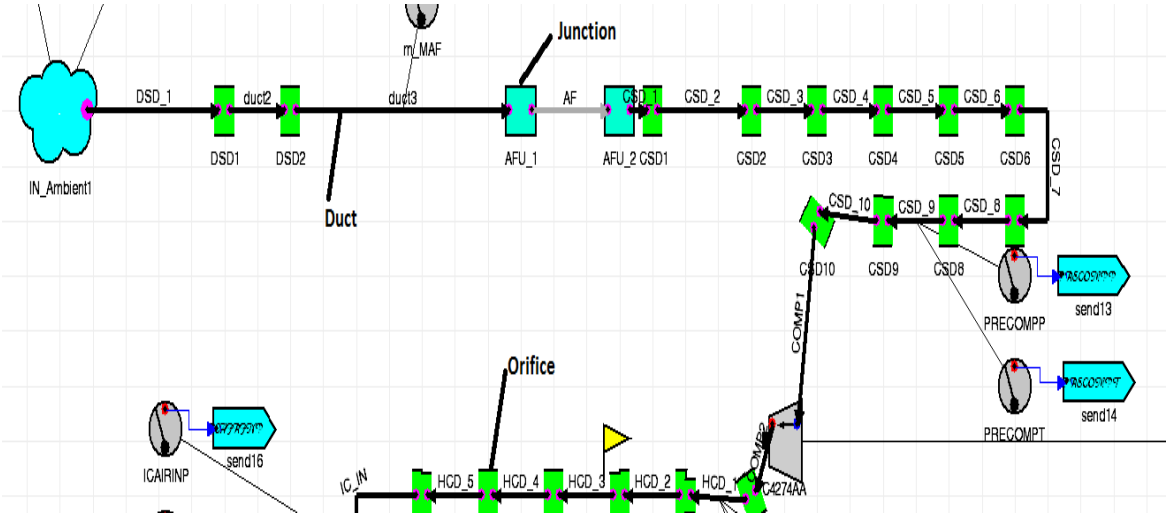


Figure 6.3 WAVE model air flow elements

In figure 6.3 part of the air intake system of the WAVE model can be observed. Some of the air flow elements and how they are connected in the model can be seen.

The engine elements are the basic mechanical components the engine consists of and they are used to describe the base engine in a virtual environment. The most important of these elements is the engine block which contains all the crucial design information about the engine. The engine block element is used to characterise the mechanical arrangement between the pistons, connecting rods and crankshaft and also supply all the necessary information to the software about the engine type, cylinder dimensions, firing order etc. as it will be described in the next paragraph. Also the turbocharger element which exists in our model is used to represent the complex machinery of turbine and compressor setups and it has no volume but changes the condition of the flow based on the parameterisation by the user. Lastly the injectors are the last of the major engine elements and they are used to characterise the fuel mass flow required for the combustion

process. The user can specify a target variable based on the engine operating point and WAVE can control all other variables to achieve this target.

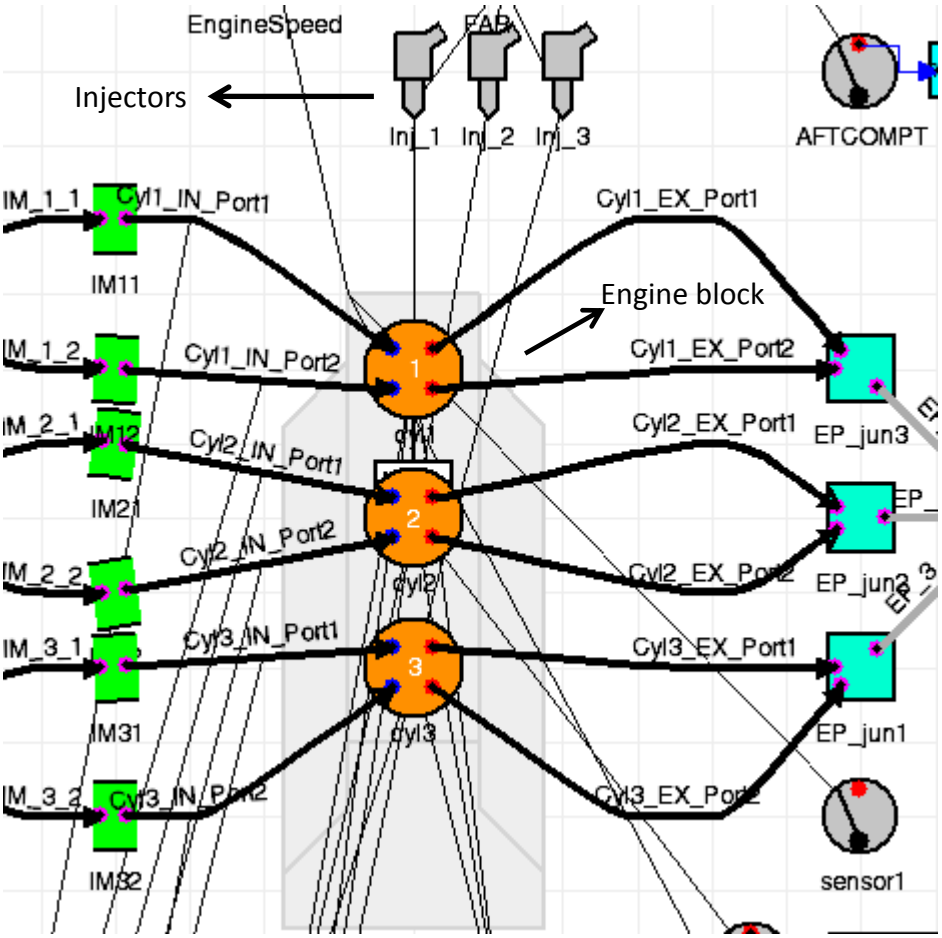


Figure 6.4 WAVE model engine elements

In figure 6.4 the engine elements of the WAVE model can be seen. In the next paragraph a detailed analysis of how the model is built and parameterised will be given.

## 6.4 WAVE model building- parameterisation

Building an engine WAVE model from the ground up is a lengthy process which requires high level of accuracy and planning in order to obtain the desired results from the model simulation.

For this project the model building process and parameterisation was divided into the following main steps:

- Gathering data
- Preparing data
- Building the model

During engine model building in WAVE or any other simulation software the engineers need to become very familiar with all the aspects of the system (engine) and access to the real hardware is invaluable for measurements and data collection. Building the model in WAVE is the last part and WAVE being just a tool for calculating physical and mathematical models, the result will be as good as the inputs and assumptions made when preparing the model.

### 6.4.1 Gathering data

Before the model starts being built there is a wide range of prerequisite information related to the system which needs to be collected. This information can be split into three main categories:

- Geometric data
- Engine data
- Operating parameters

The geometric data is the most time consuming part during model building because for an engine all the dimensions of the intake and exhaust systems including the intake and exhaust ports are required. The accuracy required while modelling these systems is very high because they can significantly affect the engine outputs during simulation. The geometric data can usually be found from engineering design drawings which are confidential for each engine manufacturer but in this project have full access to the engineering drawings of the engine was provided. In figure 6.5 the CAD drawing of the whole inlet air path can be seen from which the dimensions were obtained.

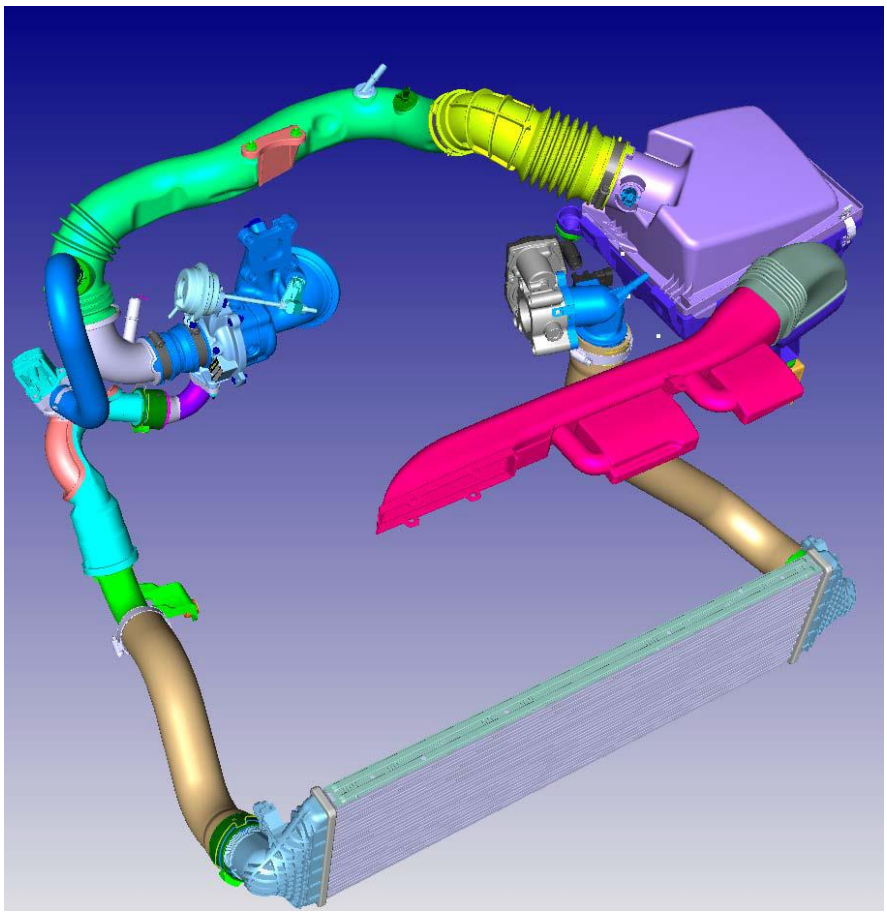

Figure 6.5 Fox Upgrade intake system CAD drawing (courtesy of Ford Motor Co)

It is very useful to also have access to the parts that need modelling especially the air cleaners, throttle bodies and connecting ducts as these parts can be examined and their dimensions can be compared with the drawings. As a general rule it is best to gather as much information and as many components as possible to ensure building the most accurate model possible

Next step is the engine data which refers to all dimensions and characteristics associated with the actual engine itself. This includes the cylinder head and inlet and exhaust ports while for the base engine only information such as bore, stroke, connecting rod length, compression ratio and firing order are required. All the information for the base engine is available as presented in chapter 4. For the cylinder head the data required make the process a bit more complicated since port flow coefficients, valve diameter data and valve lift and cam profiles are required. In this project direct access to this data from the cylinder head component engineers was provided. In table 6.1the table with all the engine and cylinder head data can be seen which was provided by the base engine department of Ford Motor Co.

**Fox-Upgrade Engine Specifications**

| | |
|---|---|
| Engine installation angle (East / West) | 7° (turbo-side down) |
| No of flywheel teeth | 112 |
| Crankshaft Pulley Teeth (CPS) | 60 – 2 |
| PCM Prime route | Bosch Multi Core |
| PCM (Interim with SPAM or AFCM PCM as at XM) | Bosch MEDG17 |
| ECOM_3 | 162324 |
| Maximum engine speeds | *Continuous* *6450rpm*<br>*Intermittent* *6675rpm*<br>*Injector Cut* *6800rpm* |
| Max Power | 125PS (92KW) @ 6000 rpm |
| Max Torque | 170 Nm @ 1400-4500rpm |
| Max Torque (Over Boost) | 200Nm @ 2000-2500rpm |
| Idle Speed | 860 rpm |
| Bore | 71.9 mm |
| Stroke | 82.0 mm |
| Total Engine capacity | 999 $cm^3$ |
| Capacity of each cylinder | 333 $cm^3$ |
| Con rod length | 137.0 mm |
| Nominal compression ratio | 10.5:1 (±0.1 EPD spec) |
| Firing order | 1-2-3 |
| Spark plug gap | 0.7mm (+0mm -0.1mm) |
| Turbocharger compressor blades | 12 |
| Turbocharger maximum rpm | 252700 rpm (244500 rpm cal limit) |
| Program Fuel | 95 RON |
| Crank offset | 8mm |
| Piston offset | 0.5mm (0.4mm ???) |
| Total offset | 7.5mm |
| Intake Valve Diameter (inner seat) | 23.8 mm |
| Exhaust Valve Diameter (inner seat) | 19.3 mm |
| IVO (with lock-pin) | 20°ATDC |
| EVC (with lock-pin) | 0° TDC |
| Intake valve peak lift | 140°atdc(±2°or ±1° for EPD) |
| Exhaust valve peak lift | 124°abdc(±2°or±1° for EPD) |
| Intake /Exhaust duration | 240° / 248° |
| Intake /Exh Cam ROA | 60° |
| Tappet clearance – Intake | Hydraulic RFF |
| Tappet clearance – Exhaust | Hydraulic RFF |

Table 6.1Data used in the WAVE model (courtesy of Ford Motor Co)

Finally the last part of the data gathering is about the operating parameters. They refer to conditions at which the simulation will be run, typical parameters required for an engine simulation are the inlet and exhaust temperatures, the engine operating range, the air fuel ratio and ambient conditions. These are the minimum parameters required to get a model running and they are normally obtained through experimental data in an engine test bed. At this point it is worth mentioning that it is very crucial to have temperature data in various locations at the exhaust system as the temperature varies significantly and has a big effect on predicted

performance. For this project the real engine exhaust system was instrumented as shown in figure 6.6 so the experimental data can be obtained to be used in the model.

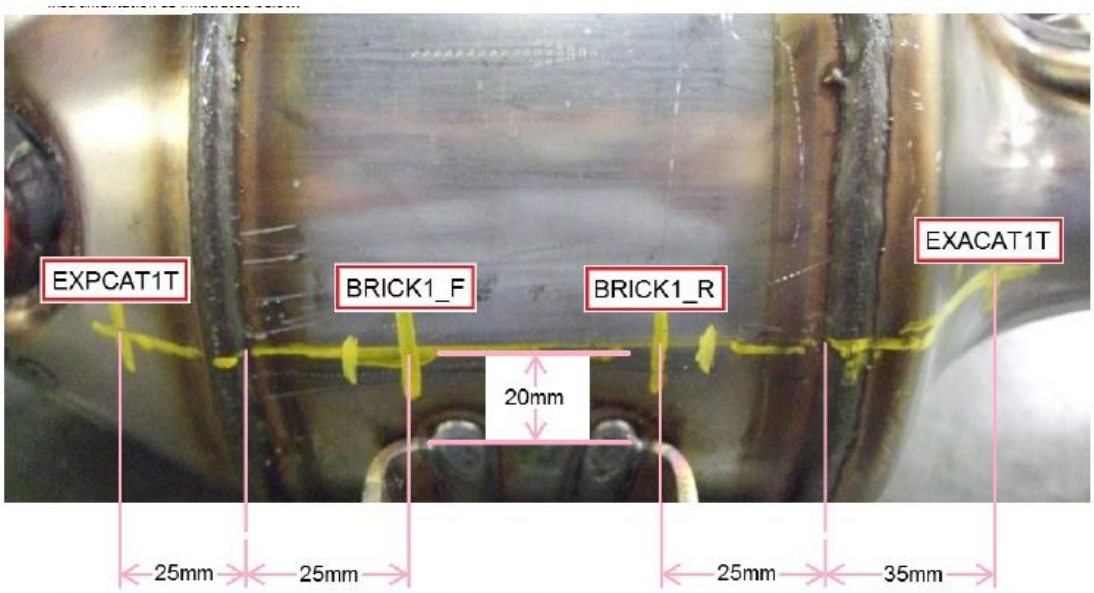


Figure 6.6 Exhaust hot end instrumentation

In figure 6.7 the hot end (catalyst) of the engine can be observed with accurate instrumentation instructions. This component was used during actual engine testing and the data obtained where used as inputs in the WAVE engine model.

### 6.4.2 Preparing data

Before entering the data into WAVE model it is very helpful to organise how the geometry of the real system is going to be split and modelled. It was found the best way to achieve that is to create a simple sketch as shown in figure 6.8 which will show all the sub components of the model including piping and is representative of how the model will look like when it is built. If

this procedure is followed then it is anticipated that the steps of the building process described later will be easier and without errors.

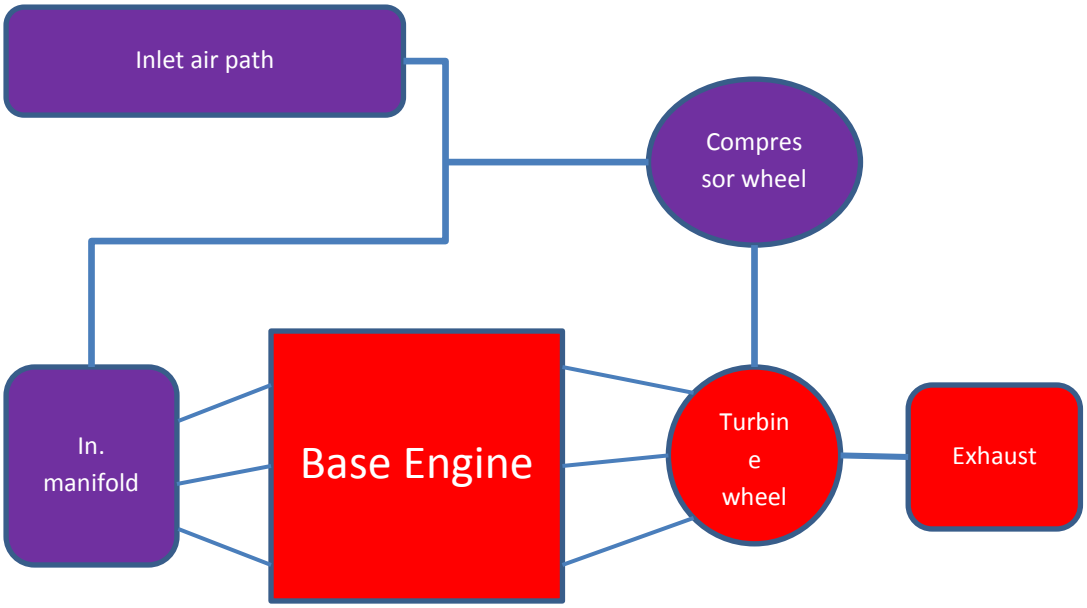


Figure 6.7 Sketch of the system as it will be modelled

### 6.4.3 Building the WAVE model

This paragraph will describe in as much detail as possible the model build and parameterisation process of the main model components and also describe some generic modelling rules and conventions. Also views of the model as shown within WAVE software will be presented.

The model was built using WAVEBuild which is the pre-processor used to build the geometric models and also add the data to the physical models required for the simulation. WAVEBuild has a large library of objects which each one of them represents actual components of the engine. These objects can be edited by the user so they represent as accurately as possible the real system. Before we start showing the model build it is worth

mentioning a few modelling rules regarding the ducts and the junctions which are used to join the main components of the model so a better understanding can be gained. The junctions are used for mainly connecting different ducts and also modelling elements that are made up of large volumes such as the air cleaner. When joining a duct to a duct where only the duct diameter changes an orifice junction should be used. When joining a duct to an atmospheric condition an ambient junction should be used. Finally when a complex shape volume is modelled then a combination of Y-junctions should be used. The ducts are primarily used to model pipe geometry and also to connect sub-volumes together. The ducts appear differently on the model depending on their state for example if they are defined or undefined or in case of a massless duct.

After understanding some simple modelling rules, the model building procedure and parameterisation follows. The first component that needs building is the engine block because it is the core of the engine and every other sub-component attaches to it.

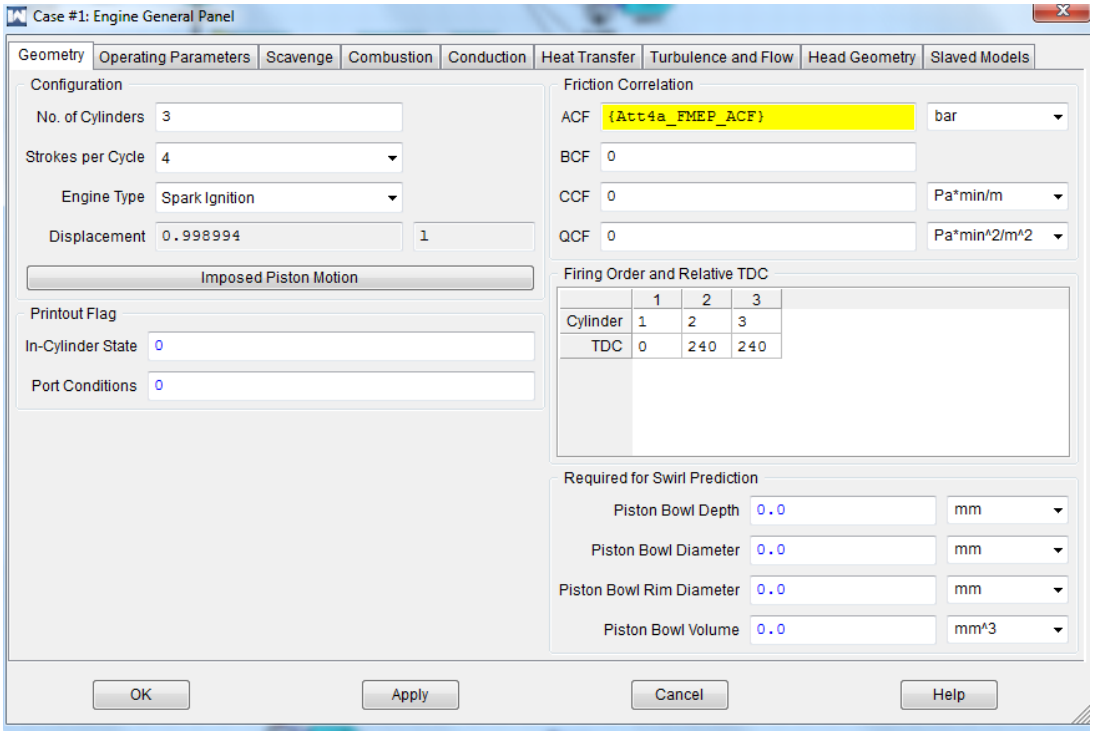


Figure 6.8 Engine block parameterisation

In figure 6.8 the parameterisation window within WAVE for the engine block can be seen. In this window the user needs to input all the main parameters of the engine such as geometry, firing order and type of engine. Highlighted in yellow the friction data of the engine have been inserted into the model in a table form and they have been obtained from the development engineers of the engine. Once the block has been parameterised it appears in the software as shown in figure 6.12 below.

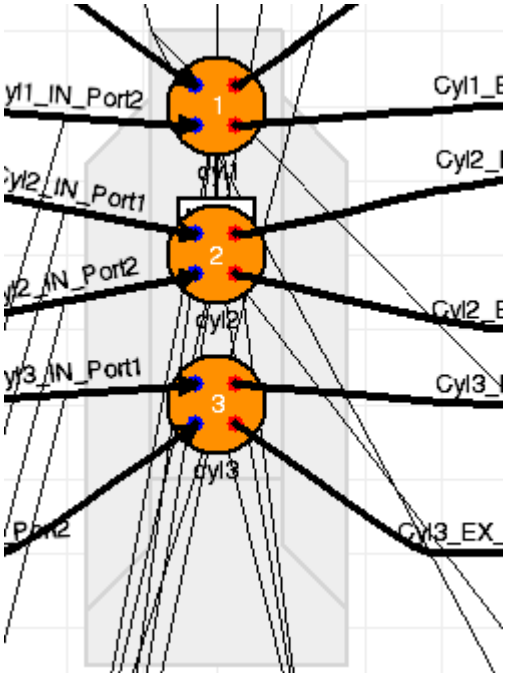


6.9 WAVE engine block

After configuring the engine block the next component is the engine cylinder. The cylinders are located inside the engine block as it can be seen on figure 6.9 but they are parameterised separately. This particular engine has three cylinders so the process for all three is similar and in figure 6.10 the parameterisation window in WAVE can be observed. The software requires all the geometrical information of the cylinder as shown and also which cylinder is within the engine and how many valves the cylinder head has for this particular cylinder

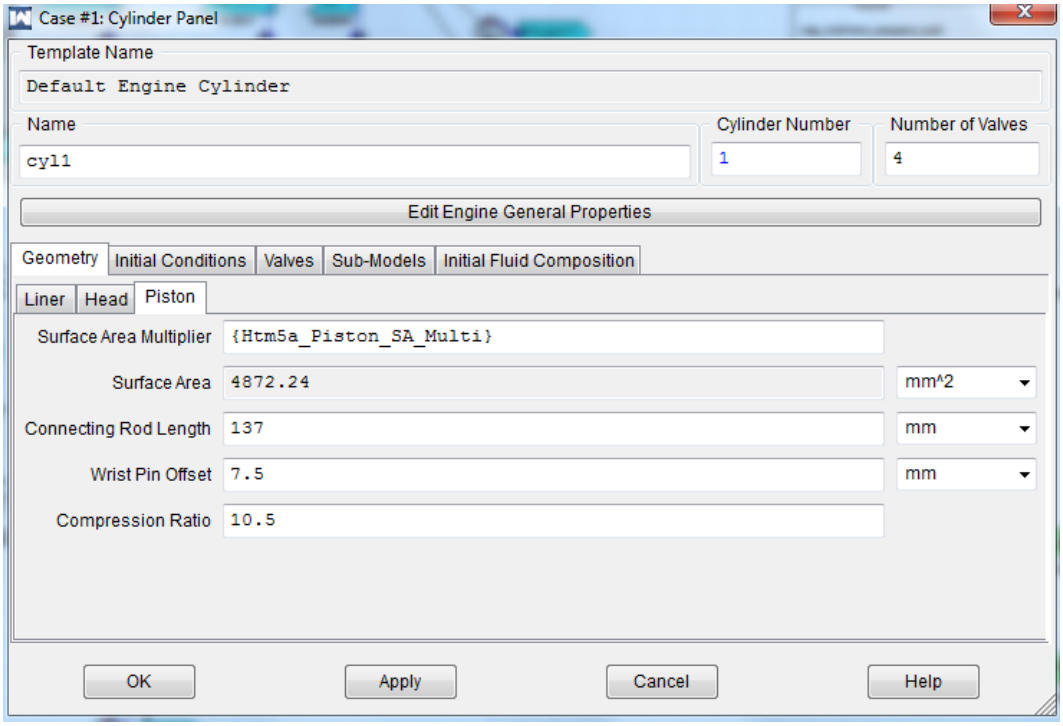


Figure 6.10 Engine cylinders parameterisation

The next crucial model parts that follow are the intake manifold, the manifold runners and the cylinder head intake ports.

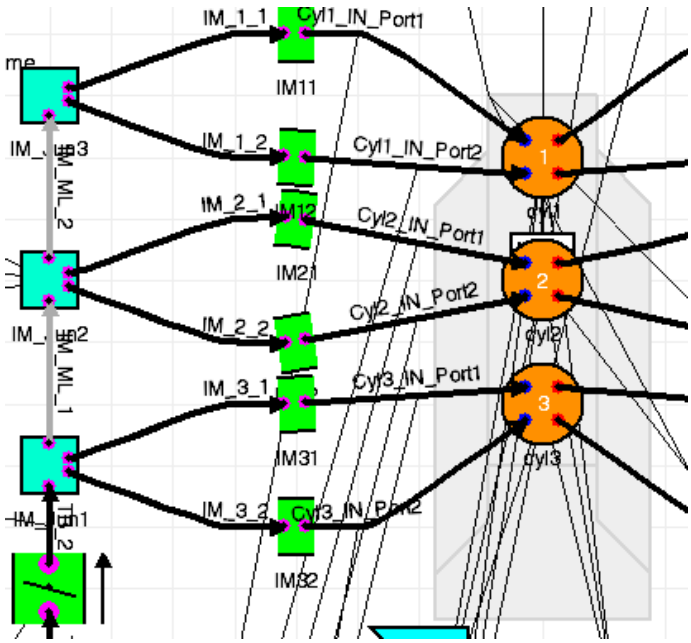


Figure 6.11 Inlet manifold, manifold ports, cylinder head inlet port

The intake manifold being a complicated part shape wise, it was modelled using three Y- junctions as explained earlier to achieve the maximum model accuracy. In figure 6.11 the inlet manifold junctions on the left can be observed and also attached to each junction are two inlet manifold runners for each cylinder. These are being modelled using ducts and they are parameterised similarly to the cylinder head inlet ports which will be explained later. In figure 6.12 the parameterisation of one of the inlet manifold Y- junctions can be seen.

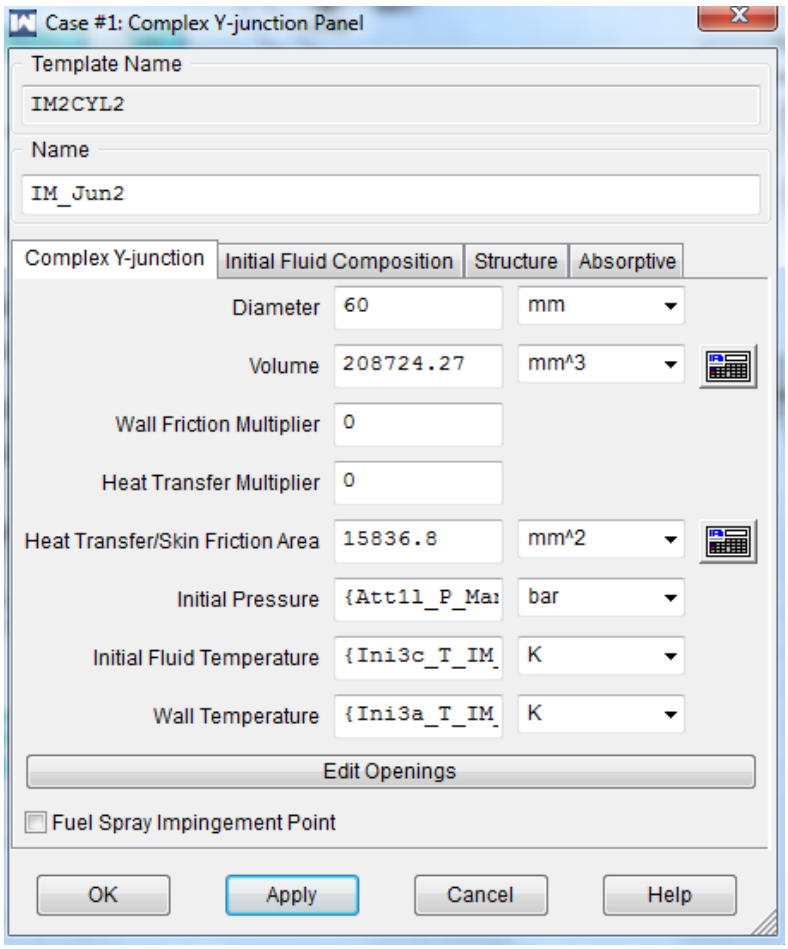


Figure 6.12 Inlet manifold parameterisation

During building and parameterising the inlet manifold, WAVE needs to know the total volume of the manifold as well as the diameter. The rest of the

conditions such as initial pressure or fluid temperature are default settings recommended in the WAVE manual for this type of simulation and were left unchanged. After the intake manifold is built and parameterised the next part is the cylinder head inlet ports which can be seen in figure 6.13 between the inlet manifold and the engine block. As mentioned above these are just ducts and they are parameterised as shown in figure 6.13 below.

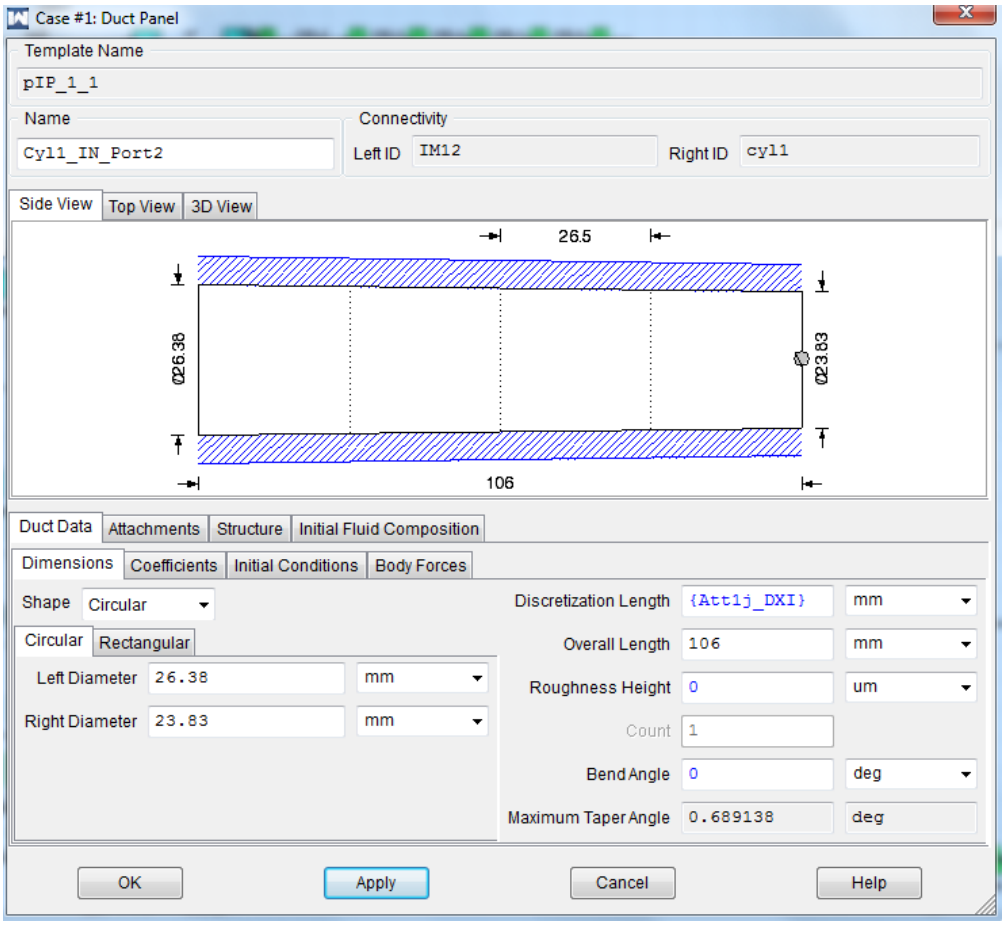


Figure 6.13 Cylinder head inlet port parameterisation

The cylinder head inlet ports are two per cylinder as shown in figure 6.13 and WAVE needs to know the exact dimensions and length of these ducts for accurate modelling of the part. At this point it is important to mention that the cylinder head exhaust ports and the exhaust manifold were built and

parameterised identically to the inlet side with the only difference being the dimensions.

The next important component that follows is the catalyst parameterisation which can be seen in figure 6.14.

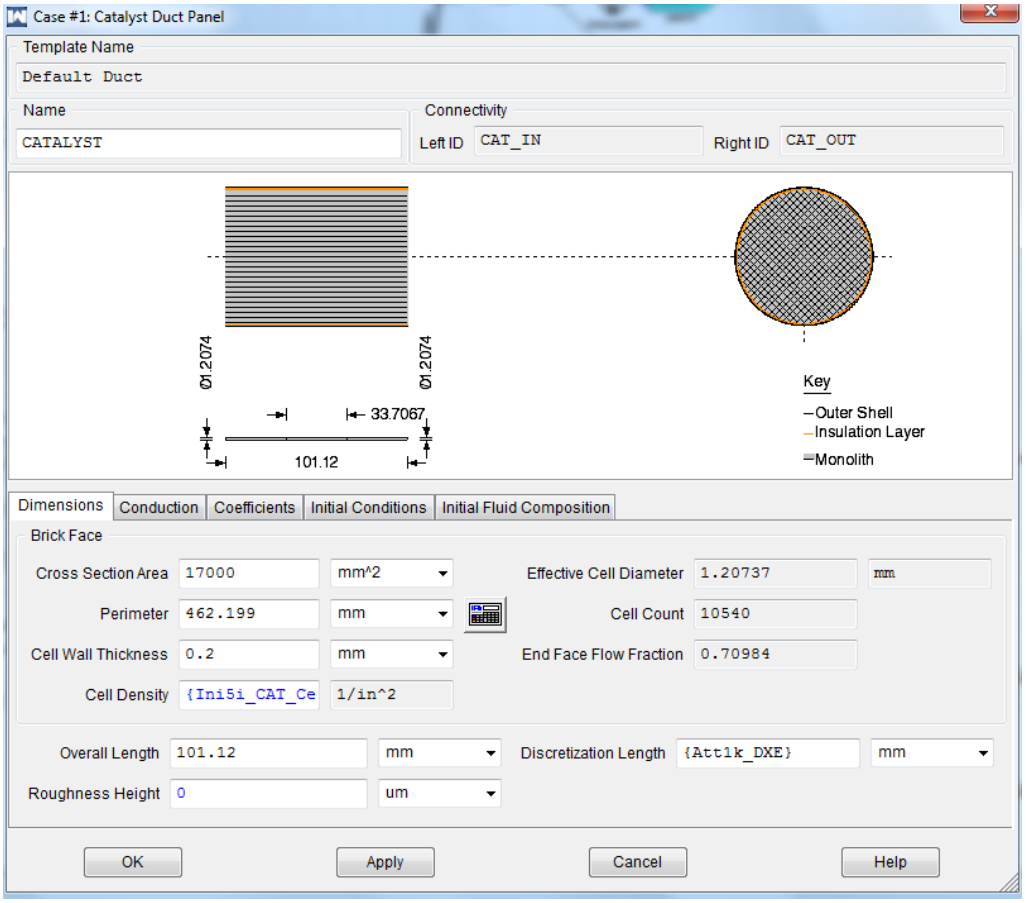


Figure 6.14 Catalyst parameterisation

During this process the user needs to input all the critical dimensions of the catalyst in the software such as overall length, cell wall thickness and cross section area. The catalyst is a critical component as its design can affect exhaust temperatures and pressures which in turn can lead to different simulation results so a lot of effort was put in order to obtain the accurate components dimensions to ensure the best possible modelling of the part.

After finishing with the exhaust the next step is the inlet air path and the compressor wheel of the turbocharger which can be seen modelled in figure 6.15. On the left of the air cleaner a sensor was located for providing the engine air mass flow data during simulation which will be presented in the next chapter.

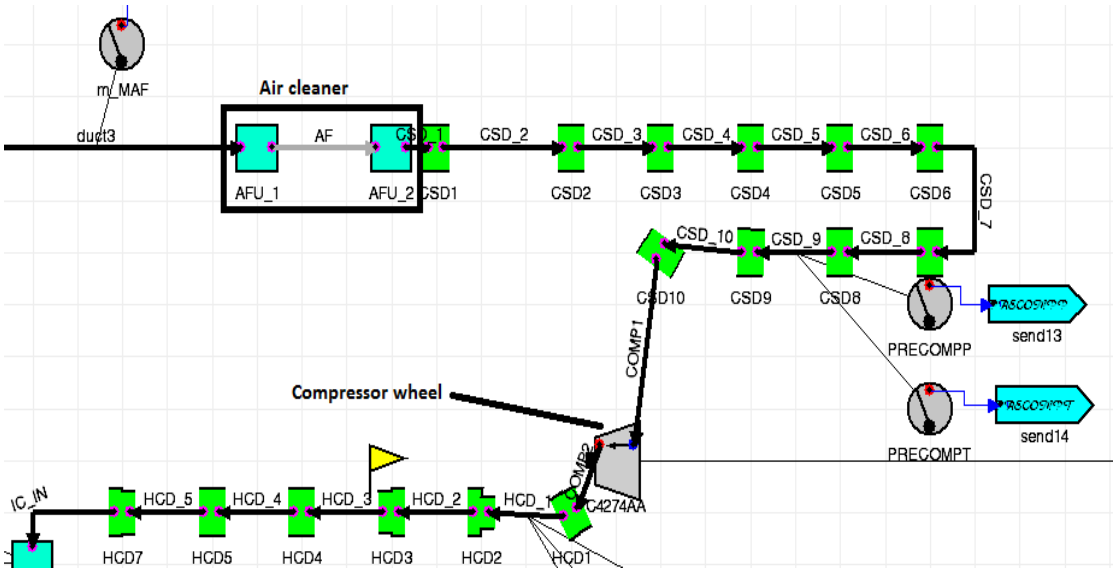


Figure 6.15 Inlet air path and compressor wheel

The inlet air path mainly consists of ducts of different length and diameters which makes it very challenging to model and in figure 6.16 below one of these ducts can be seen as parameterised in the WAVE software. During this process the user needs to input into WAVE all the dimensions of the duct such as diameter, overall length and bend angle. After the dimensions are inserted, the software creates a 3D view of the component for easier visualisation as shown in figure 6.19. The same steps are followed until all the different ducts of the inlet air path system have been parameterised. The air cleaner being a complicated shape component is modelled using Y-

junctions in a similar way to the inlet manifold modelling described earlier in this paragraph.

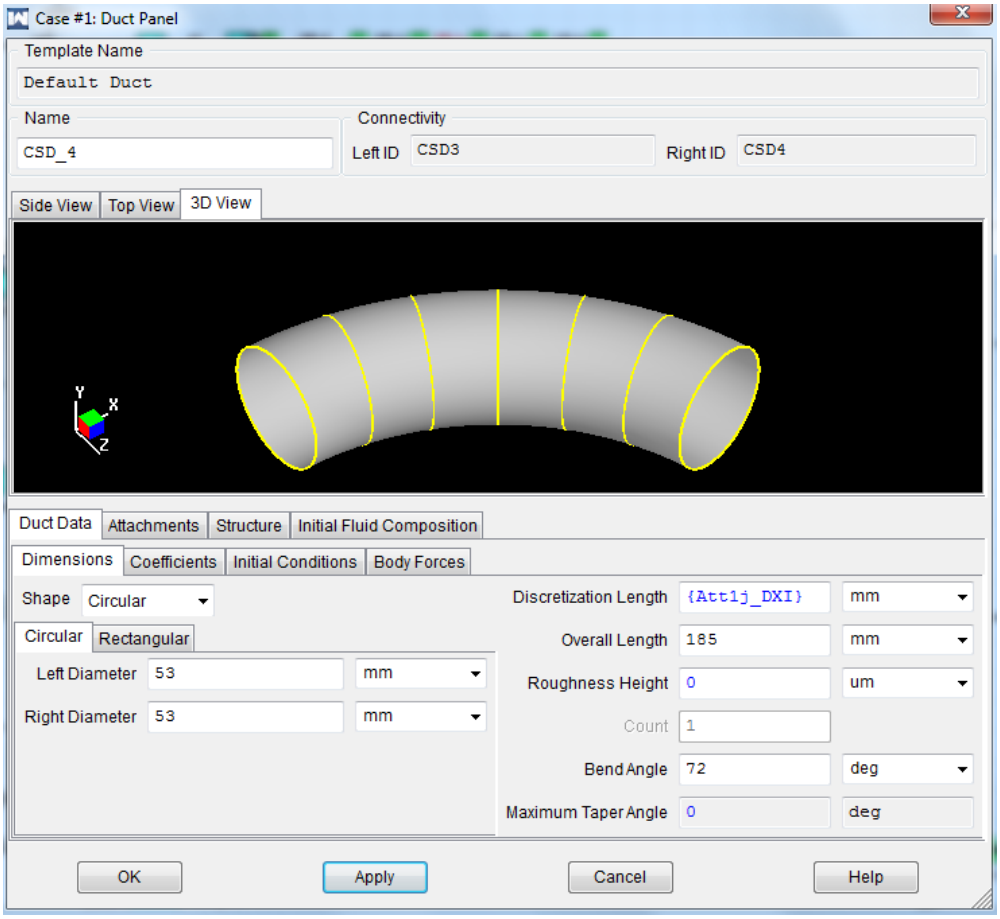


Figure 6.16 Inlet air duct parameterisation

Having modelled and parameterised the entire air path of the engine the last item related to the air path that needs modelling and parameterisation is the turbo charger compressor. During compressor parameterisation the user needs to input to WAVE the compressor map efficiency data which are obtained by the component manufacture as shown in figure 6.17 at the bottom. The rest of the settings such as diameter and efficiency are default values within WAVE and is recommended to use these for this type of

compressor. The turbine wheel of the turbocharger which is mechanically connected with the compressor but is located on the exhaust side, is parameterised with exactly the same way but with different efficiency map data again from the manufacturer.

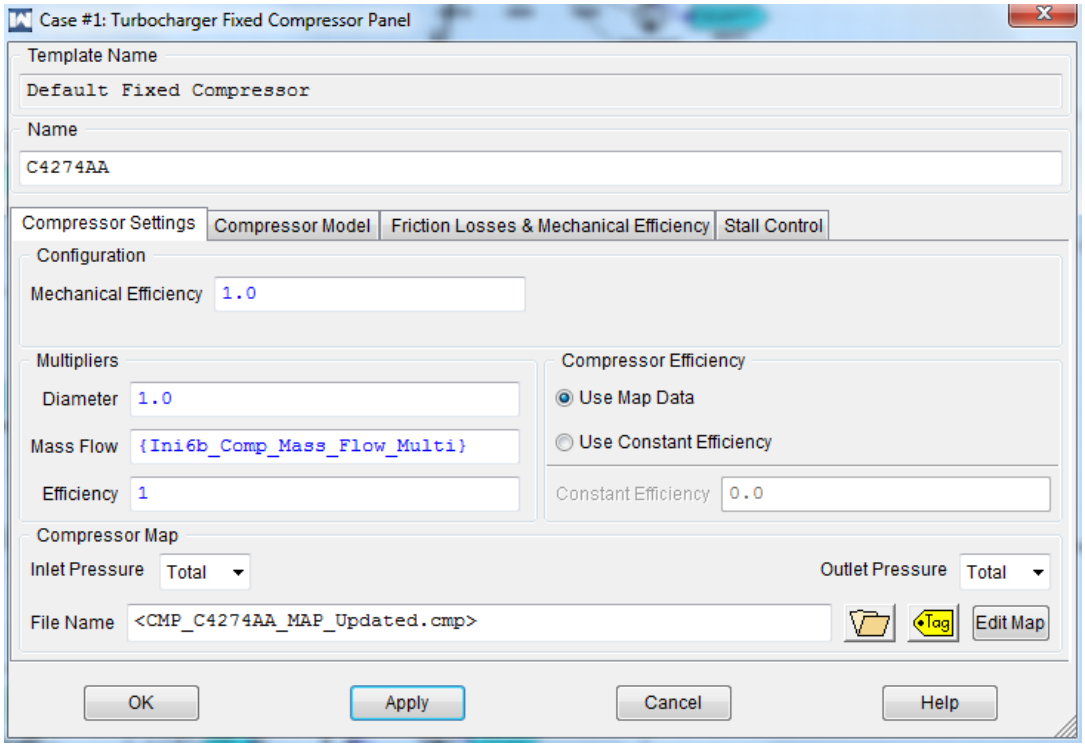


Figure 6.17 Compressor parameterisation

The last major part that needs modelling and parameterisation is the exhaust system after the catalyst. This part as shown in figure 6.18 consists of ducts and orifices and is modelled and parameterised identically to the air inlet path described earlier but with different dimension characteristics.

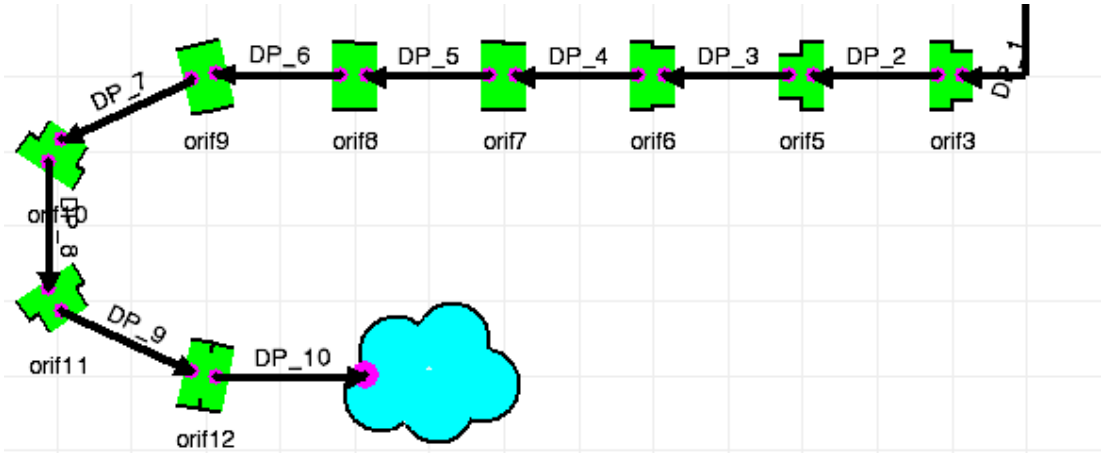


Figure 6.18 Exhaust system modelling

## 6.5 WAVE model simulation

For the simulation of the developed model the WAVE-RT (real time) solver was used. WAVE-RT is the primary solver for all the 1D simulations of fluid dynamic systems and contains special algorithm for flow dynamics simulation and optimisation. It is also designed to provide a link between WAVE and other testing environments such as Matlab/Simulink for software in the loop or hardware in the loop testing platforms. It is also designed to be generic which ensures its compatibility with various engine layouts which offers great simulation flexibility.

The objective of this simulation is to run the virtual engine model and perform exactly the same air charge characterisation test as described in chapter 5.

| Parameter | Value | Units |
|---|---|---|
| Control mode | Closed loop | - |
| Index | 0 | - |
| Engine speed | 2905 | RPM |
| Ramp time | 360 | seconds |
| Minimum MAP | 20000 | Pascal |
| Maximum MAP | 260000 | Pascal |
| AFR | 14.7 | - |
| IC wall temperature | 300 | Kelvin |
| Cyl. Wall temperature | 373 | Kelvin |
| Mfb50 | 8 | Degrees CA |
| Combustion duration | 31 | milliseconds |
| Actuator values | Model | - |
| Ramp type | Dual ramp | - |
| Signal smoothing | On | - |
| Smoothing factor | 0.3 | - |
| DoE name | DOE_SF | - |

Table 6.2 Simulation input table

To achieve that a parameter input table was created which can be seen in table 6.2 with elements that WAVE requires in order to perform an engine simulation study. In this table set parameters such as engine speed, camshaft index, ramp time and min and max MAP are set exactly the same as in the test performed on the dynamometer to replicate the test conditions. On the other hand parameters such as AFR, intercooler wall and cylinder wall temperature, actuator values and ramp type are parameters that WAVE needs to know in order to perform the study and in the real engine test would be controlled either by the ECU or the test automation software. The last three parameters are user defined and enable WAVE to produce data which will give a bit smoother graphs by slightly filtering the outputs of the model

and also give a name to the design of experiment so the user can access the data after the simulation is finished. The total simulation time for this model was 360 minutes because being a crank angle based model requires very high computational power.

In the following chapter the data from the WAVE model simulation will be presented and validated by comparing the virtual engine model data and the actual engine data presented in chapter 5 for the air charge experiment.

# Chapter 7: Validation of the virtual engine using the engine test results

This chapter focuses on the validation of the virtual engine data developed in WAVE with the data collected from the actual engine in the test room environment. The first paragraph is describing the reasons why data validation is important and is followed by the actual data validation and analysis and how do they compare with the actual engine data. The last part of the chapter discusses some arising conclusions after comparing and validating the data from the virtual and the actual engine.

## 7.1 Importance of data validation- validation method

After building and simulating an engine model in any software, it is very crucial to have a method to make sure that the simulation data are accurate. This is the so-called model validation process and it is the only method to ensure that the outputs of the model are realistic and accurate so the engineers can rely on them. In this project, the chosen validation method is to compare the virtual engine model data directly with the real engine data from the dynamometer, as according to the author's opinion this is the most accurate method. The reason it is believed to be the most accurate method is because the simulation data are directly compared with the data collected from a state of the art facility used in an industrial environment for engine development and calibration. Furthermore, all the equipment used to record data in this facility is regularly checked and calibrated so if the data from the engine model are similar to the real engine test then we can make the safe assumption that the engine model was built and parameterised correctly and the results are as accurate as they can be. The engine test data that will be

compared with the model data are from the air charge test, which was described in chapter 5. The reason this test is chosen is because it is the main test used for air charge characterisation and the one affecting the engine air mass flow most. As explained in chapter 6 the model simulation was run identically to the air charge test on the dynamometer so it will be a direct data comparison between these data.

### 7.2 Validation results

Before moving on to the actual data validation it is necessary to check that the test was performed as planned and in order to do that the main inputs to the model for this test have to be checked which are the throttle butterfly and the waste gate actuator.

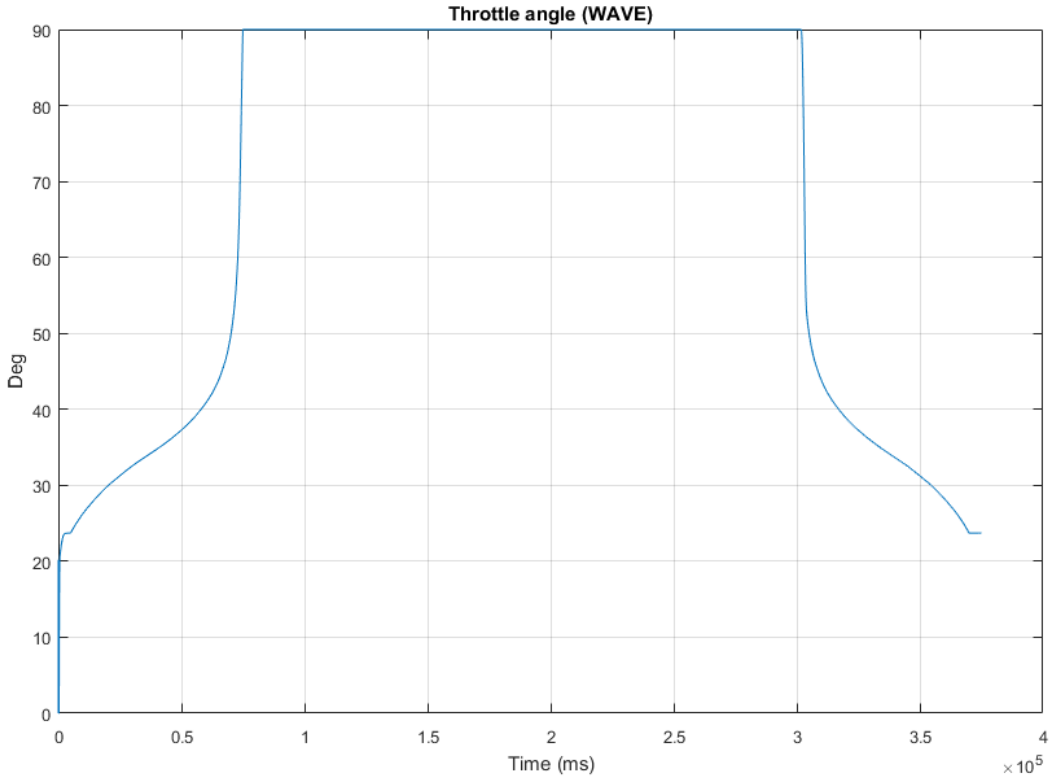


Figure 7.1 Throttle angle data from WAVE

In figure 7.1, the data from the throttle butterfly can be observed. The test starts with just over 20 degrees of butterfly opening and reaches to 90 degrees, which is the maximum value. It is worth mentioning that during the simulation the throttle angle reaches 90 degrees which is the maximum angle that can be achieved which compared to the actual engine data (presented in chapter 5) is slightly higher. The reason is that in the actual engine, the component limit is 81 degrees (figure 5.4) and is the maximum opening allowed. Based on the above graph it is certain that the throttle butterfly in WAVE was simulated correctly and the values shown in the graph are the expected ones.

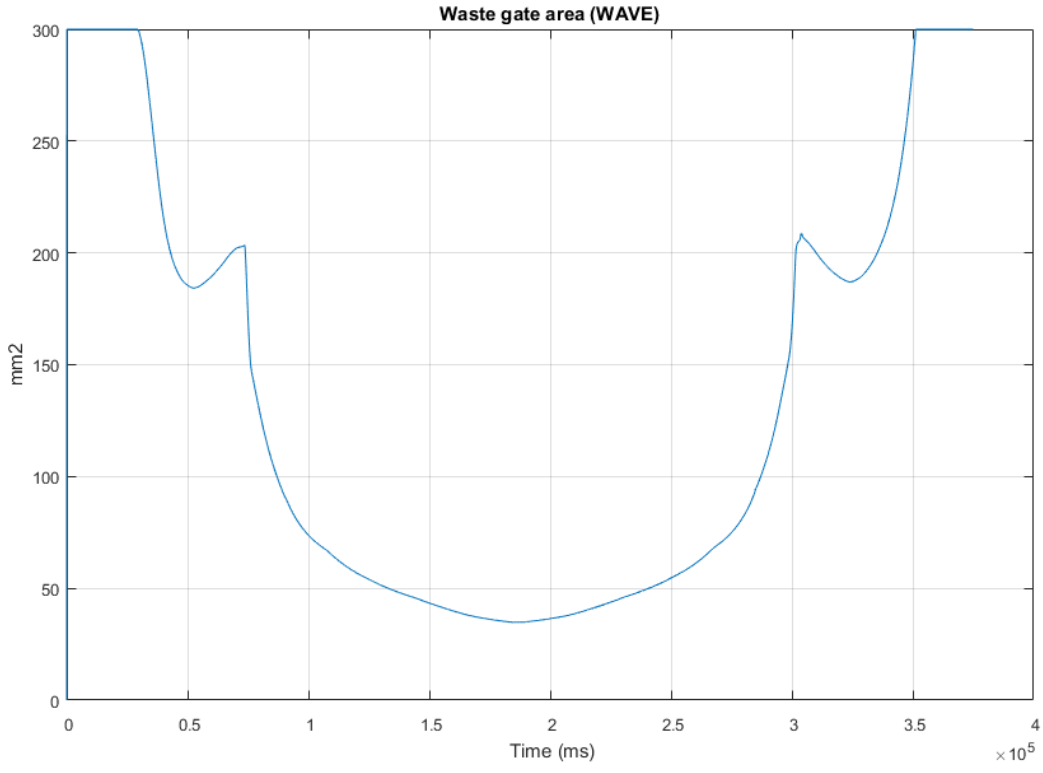


Figure 7.2 Waste gate area data from WAVE

In figure 7.2, the waste gate opening area data can be seen. The test starts with the waste gate fully open where the opening area is 300$mm^2$ and

gradually reduces to about $30mm^2$. The Wastegate opening values are controlled by WAVE model so that the target MAP can be achieved. At around $200mm^2$ of opening area a small oscillation can be noticed and that is because the model was unstable at that point. The model does not give waste gate duty cycle as an output because that is specific to the ECU but from figure 7.2 it is certain that the actuator is simulated correctly. After making sure that the most important actuators to perform this simulation are set correctly, it is time to see how the most important data from the model for this particular test compare with the equivalent test data from the actual engine in the dynoThe focus will mainly be on the inlet manifold pressure and temperature because these are primarily the factors that affect the engine air mass flow and finally the air mass flow from both tests will be compared. In figures 7.3 and 7.4 the inlet manifold temperature from WAVE and actual engine dyno data can be observed.

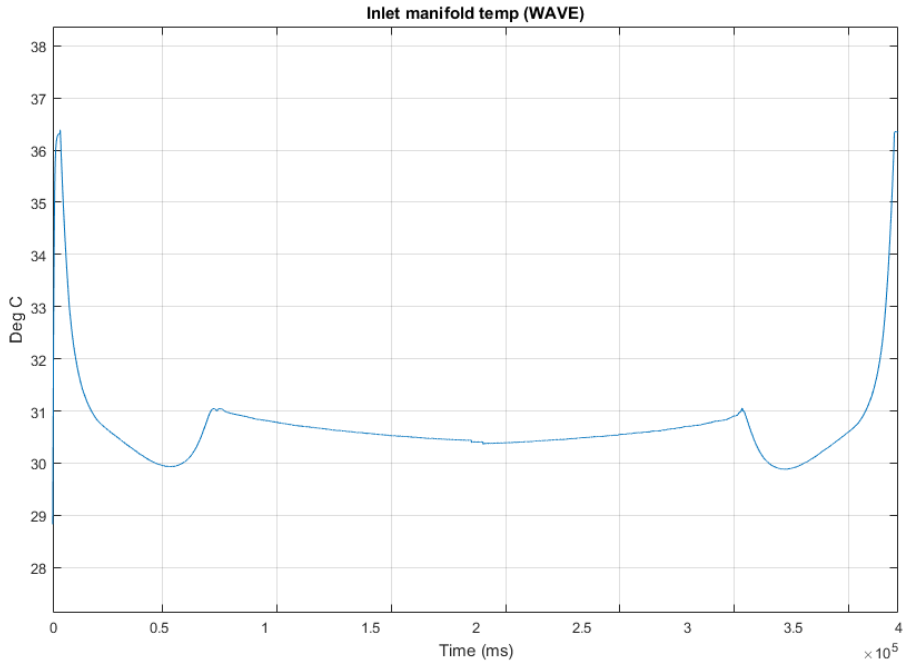


Figure 7.3 Inlet manifold temperature data from WAVE

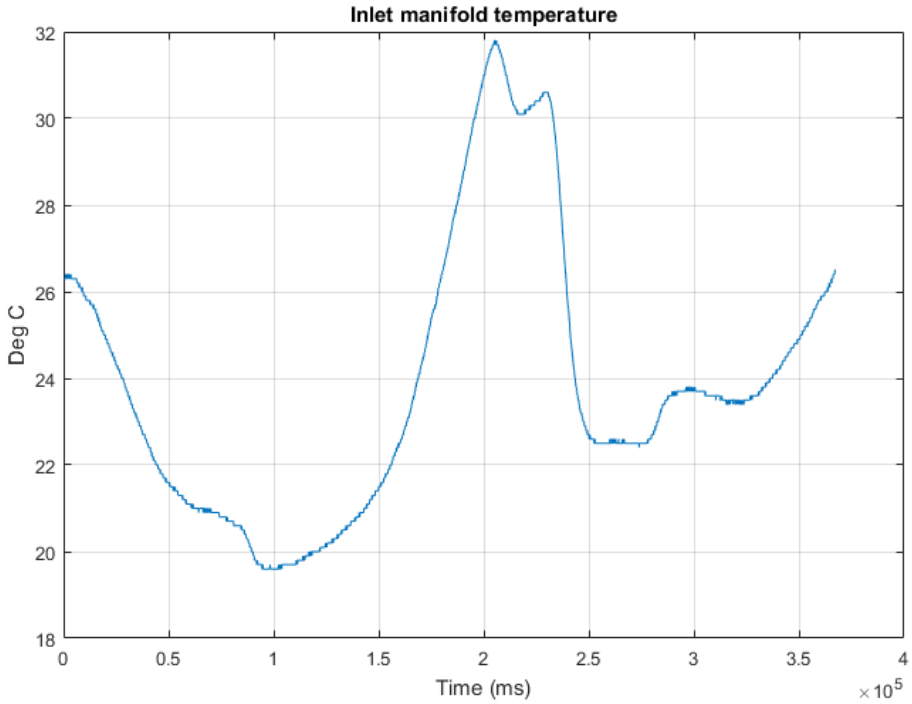


Figure 7.4 Inlet manifold temperature data from dyno

Looking at both the above figures it is noticeable that the shape of the graph is different and that is because the inlet manifold temperature model in WAVE is slower to react compared to the actual thermal events that take place in the actual engine. Looking closer to the graph though, it can be seen that for the majority of the duration of both tests the temperature in the inlet manifold was between 25-31 degrees Celsius, which confirms that WAVE can predict the inlet manifold temperature quite accurately. Because of that, any serious fluctuations in the inlet manifold pressure data from WAVE are not expected.

After the inlet manifold temperature validation, next parameter to check is the inlet manifold pressure. It is a very important parameter because it is directly linked with the engine air mass flow. The higher the manifold pressure is, the

higher the air mass flow of the engine. Figures 7.5 and 7.6 are showing the inlet manifold pressure data from the real engine and WAVE model.

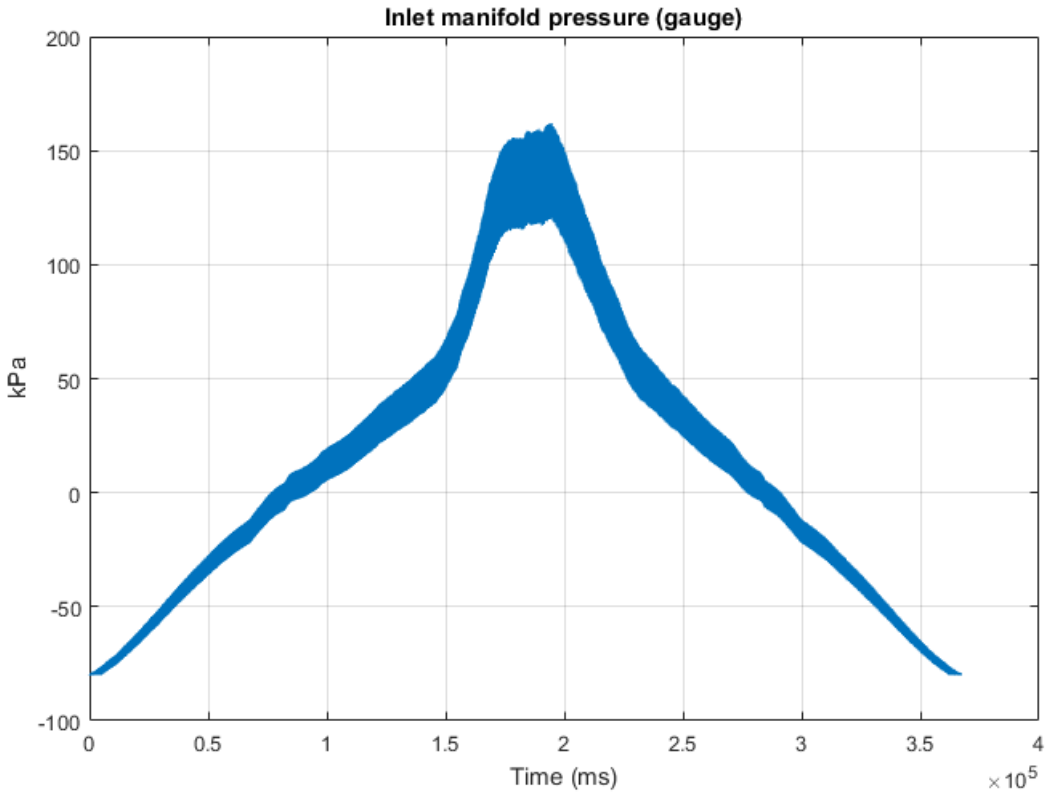


Figure 7.5 Inlet manifold pressure data from dyno

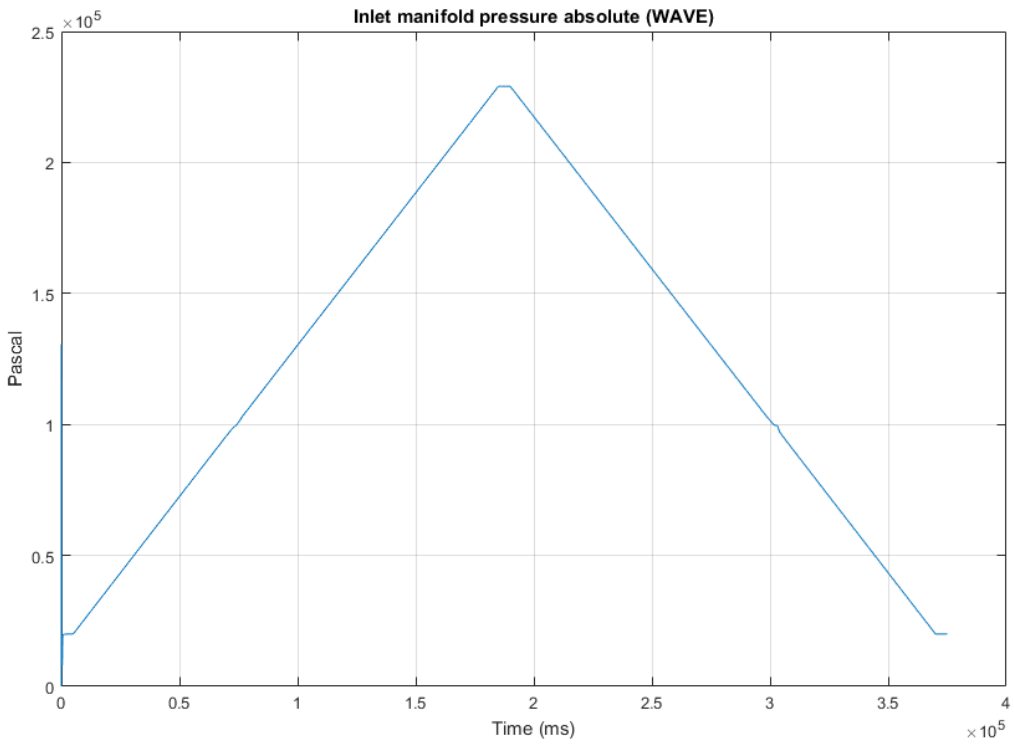


Figure 7.6 Inlet manifold pressure data from WAVE

Looking at both inlet manifold pressure graphs it is immediately noticeable that they look almost identical. At first, the inlet manifold pressure achieved by the virtual engine is the same as the one from the real engine at 260 kPa. In addition, the trend of the graph is the same with the only difference that the engine data are a little bit noisier due to the dynamics of the real engine. In figure 7.5 at around 150 kPa a slight change on the pressure increase rate can be observed due to the waste gate dynamics which is not noticeable in the WAVE data because the model ramps up the pressure linearly. Taking into account all the above it can be assumed that the simulation results are very good and directly compare with the real engine data and it is certain that WAVE can simulate the inlet manifold pressure for this engine very accurately.

The last and most important part of the validation process is to compare the measured engine air mass flow from the real engine and compare it with the predicted air mass flow data from WAVE simulation. In the following figures, 7.7 and 7.8 the air mass flow data are presented. Again, it is immediately noticeable that the shape of the graphs is almost identical with the simulation data being more linear as expected due to WAVE having a linear controller during a simulation. In terms of accuracy, for the engine data the maximum air mass flow measured id 220 kg/hr while for the model the prediction is 210 kg/hr. Taking into account that and comparing simulation data with real experimental data the result is very encouraging with a difference of about 5%, which is very good. By analysing the data from these graphs, it can be assumed that WAVE is very accurately predicting the air mass flow of that engine.

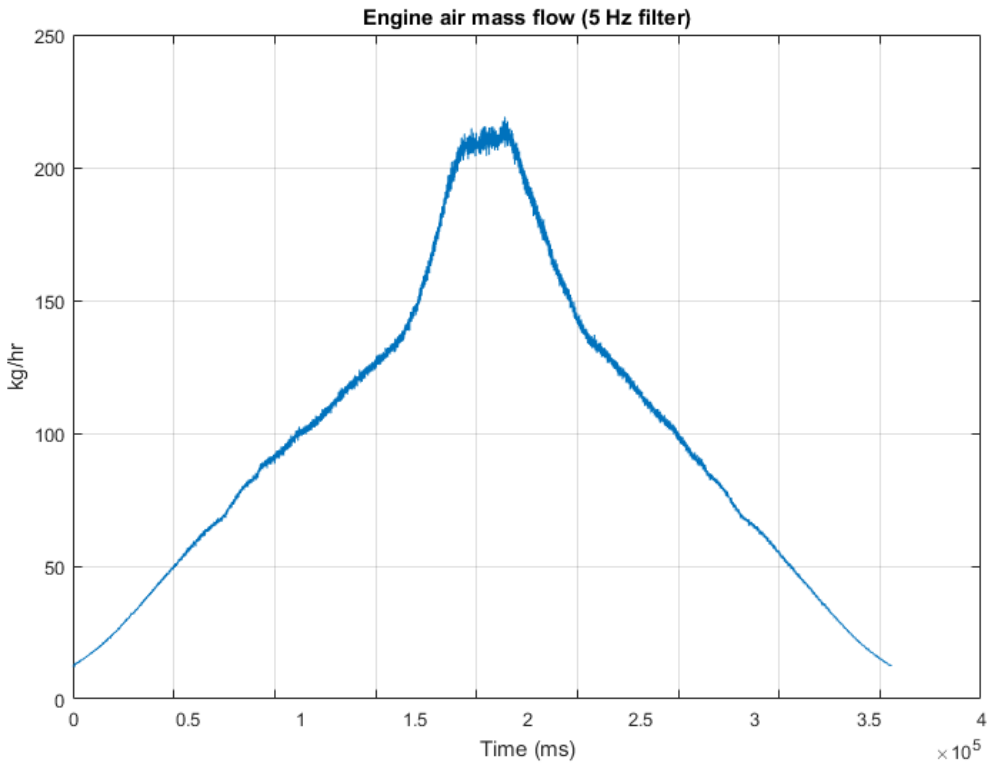


Figure 7.7 Air mass flow data from dyno

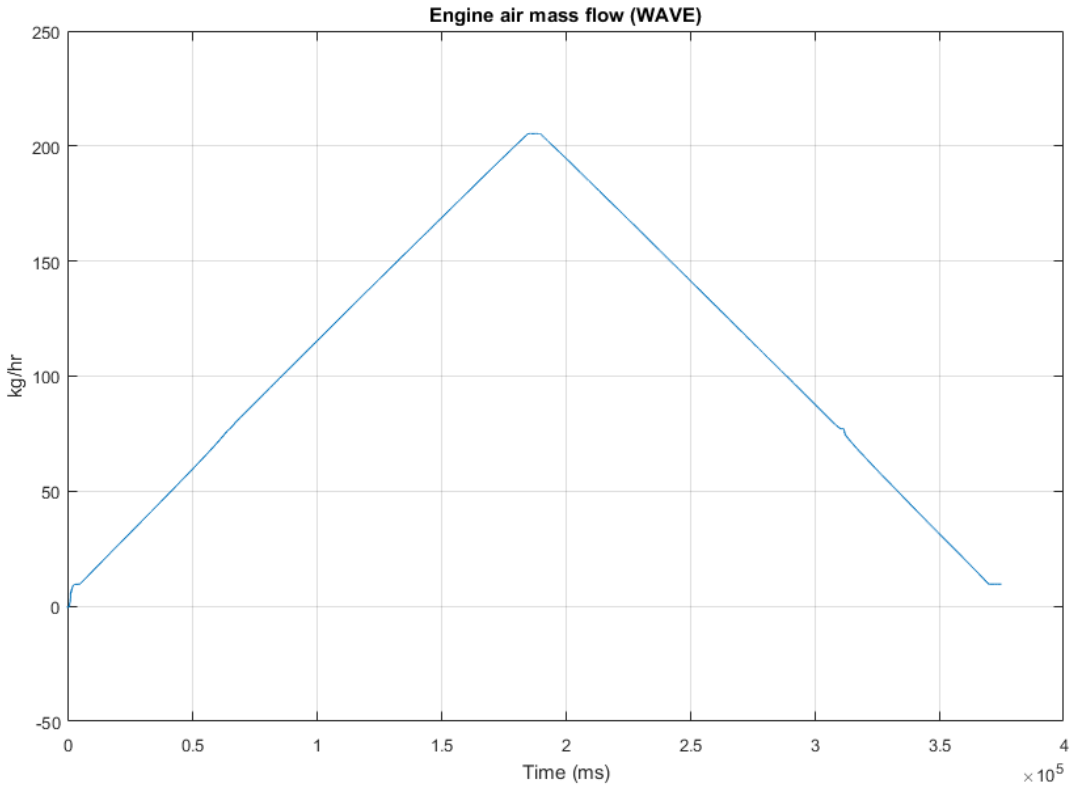


Figure 7.8 Air mass flow data from WAVE

### 7.3 Validation conclusions

Comparing the WAVE model data and the real engine data leads to the conclusion that they are almost identical. This chapter proves that firstly the simulation test was performed as designed and also all the important data such as the inlet manifold temperature and pressure that directly affect the engine air mass flow are very close between simulation and real engine tests. For the air mass flow data now between the WAVE model and the real engine as shown earlier, they are almost the same with an error no more than 5%. This means that the WAVE engine model can accurately predict the air mass flow of the engine and that is because it was build and parameterised correctly taking into account all the important data and information collected from the real engine.

## Chapter 8: The response of a distributed parameter model

In this chapter a distributed-lumped model of one dimensional gas dynamics equations are used for model the flow through the inlet manifold comprising of a series of interconnected elements is presented in a way that the distributed parameter elements are connected to a lumped parameter element. After deriving the theoretical analysis of the distributed lumped model of the system (DL or port based model) a CFD model is represented to show the accuracy of the DL or port based model which is the virtual sensor developed in this thesis.

The topology used in this type of modelling is similar to port based modelling procedure with a well-defined input-out structure as shown in figure 8.1. The derivation for a distributed parameter pipe of length $l$ , with diameter d will be considered. The inlet comprises an infinite series of infinitesimal elements dx, in length, which are subjected, at a distance x along the pipe, to input and output flows, respectively.

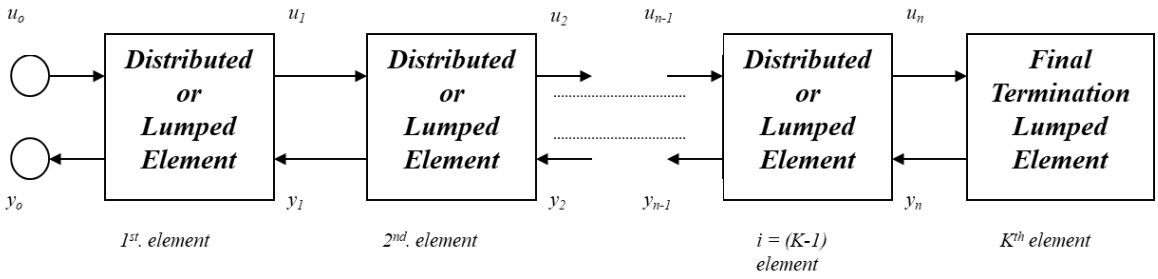


Figure 8.1 Port based modelling structure

## 8.1 Model parameters

The principle schematics of the investigated airpath are presented in figure 8.2. The intake system consists of an airbox with air filter, compressor, intercooler and intake manifold. The airbox is connected to the atmosphere through an inlet pipe from which air is sucked.

The simplified 3D geometrical model of the engine intake system is shown in figure 8.3. To reduce the computational time and cost most of the 3D model geometrical details have been disregarded. The compressor and the intercooler are represented as simple cylindrical expansion sections along the airpath. Simplifying the 3D model of the intake system resulted in a “cleaned” geometry model, which is more favourable regarding the computational mesh generation. The basic technical specifications of the intake system components are presented in Table 8.1.

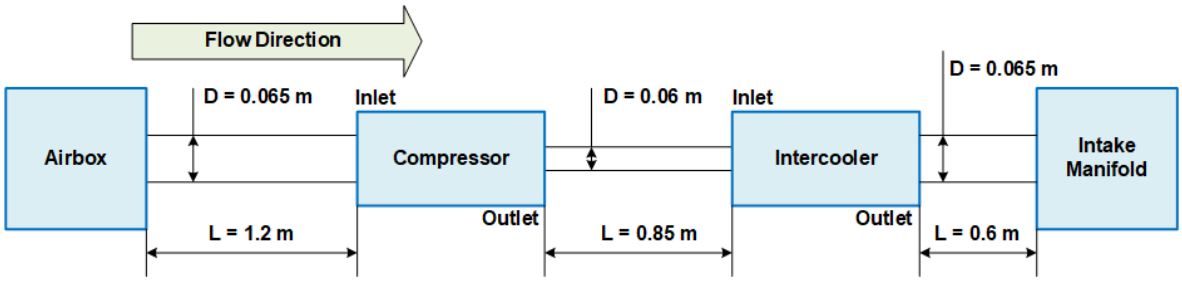


Figure 8. 2 Principle Schematics of the Engine Intake System

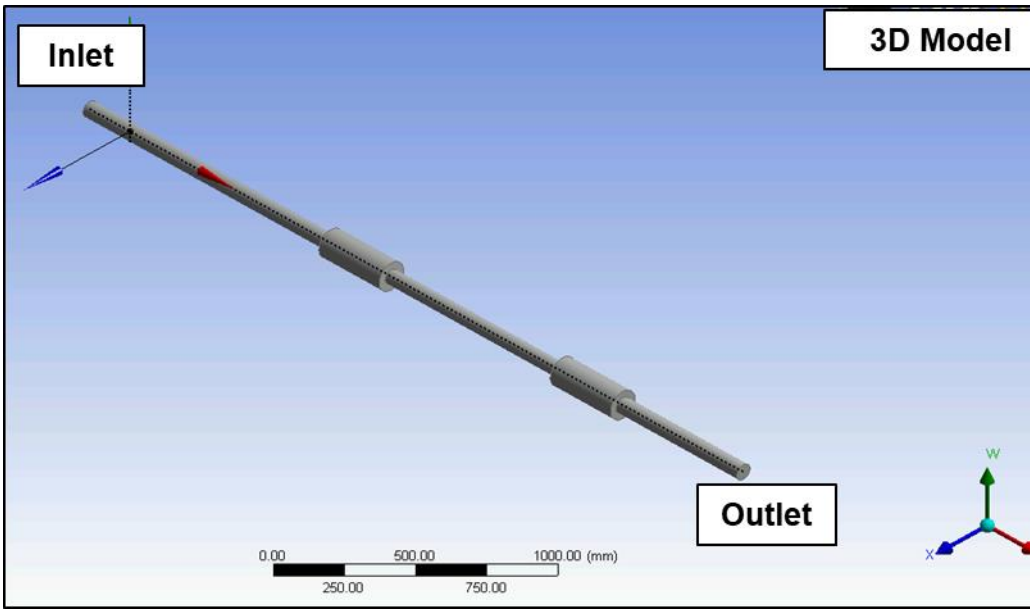


Figure 8.3 Simplified 3D Geometrical Model of the Intake System

| Table 8.1 Technical specifications of the Intake System | | |
|---|---|---|
| Mass flow rate | 0.591 | Kg/s |
| Air dynamic viscosity, $\mu$ | $1.789E^{-5}$ | Kg/m.s |
| Air density at compressor outlet | 1.468 | $Kg/m^3$ |
| Supercharging pressure | 1.5 | bar |
| Air density at intercooler outlet | 1.49 | $Kg/m^3$ |
| Engine speed | 2,000 | rpm |

## 8.2 Theoretical Analysis of Distributed Lumped Model

The system model for the complete model could be constructed deriving a distributed parameter airway of length $l$, with diameter $d$ will be considered. The intake comprises an infinite series of infinitesimal elements dx which are subjected, at a distance x along the intake, inputs and outputs of P(t,x) and P(t,x + dx), respectively [84]

For analysis purposes the shaft consists of an infinite series of elements, as shown in Figure 8.4.

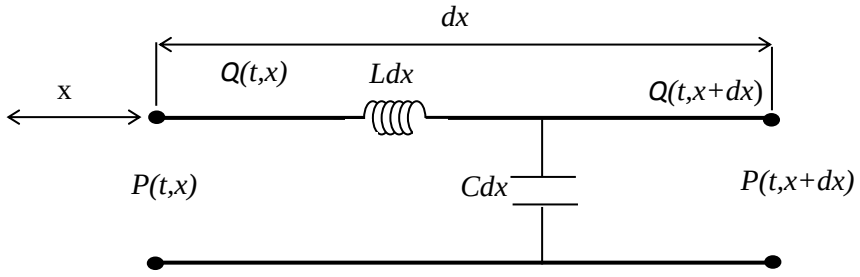


Figure 8.4 Incremental pipe elements

The corresponding volumetric flow, inputs and outputs, are *Q(t,dx)* and *Q(t,x+dx),* respectively. Each element has an associated series inductance L which is equivalent to the gas path inertia per unit length. A shunt capacitance *C*, equivalent to the air stream compliance per unit length, is also acknowledged, where, as shown in for the overall system:

$L = l_1/\pi r_1^2$ (air stream inductance)

$C = V/R\,T\,n$ (air stream capacitance)

$l$ is the length of the pipeline and r is the radius, and $= l_1 \pi r_1^2$ .

$$p(t,x+dx)-p(t,x)=-L\frac{\partial q}{\partial t}(t,x+dx)dx,$$
$$q(t,x+dx)-q(t,x)=-C\frac{\partial p}{\partial t}(t,x+dx)dx.$$

(8.1) [84]

and

$$\frac{\partial p(t,x)}{\partial x}=-L\frac{\partial q(t,x)}{\partial t}$$
$$\frac{\partial q(t,x)}{\partial x}=-C\frac{\partial p(t,x)}{\partial t}$$

(8.2) [84]

The governing equations for an infinitesimal length *dx*, are;

$$\begin{bmatrix} y(s) \\ y_{j+1}(s) \end{bmatrix} = \begin{bmatrix} \zeta_1 w_1(s) & -\zeta_1\sqrt{({w_1}^2(s)-1)} \\ \zeta_1\sqrt{({w_1}^2(s)-1)} & -\zeta_1 w_1(s) \end{bmatrix} \begin{bmatrix} u_j(s) \\ u_{j+1}(s) \end{bmatrix}$$

(8.3) [84]

By inverting 8.3 all of the outputs y(s) can be computed yielding analytical expressions for the response of the system following a change on the input, $u_j(s)$. In the theoretical development, the various parameters for the distributed and lumped elements enable spatially distributed models.

The overall model consists of the lumped and distributed element as shown in figure 8.2. [85]

The distributed parameter pipeline model is connected through a manifold. The air flow through pipelines of varying lengths and diameters could be analysed. From equation 8.2

$$\frac{d^2p}{dx^2}=LCs^2p,$$
$$\text{and } \frac{d^2q}{dx^2}=LCs^2q$$

(8.4) [84]

The above equation has the same form and a general solution.

The general solution required

$$\Gamma\,(s) = s\,\sqrt{(L\;C)} \qquad (8.5)\ [84]$$

If a propagation function is defined as

Hence:

$$T(s,x) = \mathrm{A}\,\cosh\Gamma(\mathrm{s})x + B\;cosh\Gamma(s)x \qquad (8.6)\ [84]$$

$$\omega(s,x) = \mathrm{C}\,\sinh\Gamma(s)x + \mathrm{D}\,\cosh\,\Gamma(s)x \qquad (8.7)\ [84]$$

Where in equations 8.6 and 8.7:

General frequency domain transfer function relationship of the input and output flows:

$$\begin{bmatrix} p_{j(s)} \\ p_{j+1(s)} \end{bmatrix} = \begin{bmatrix} \zeta_j w_{j(s)} & -\zeta_j\sqrt{\left(w_{j(s)}^2 - 1\right)} \\ \zeta_j\sqrt{\left(w_{j(s)}^2 - 1\right)} & -\zeta_j w_{j(s)} \end{bmatrix} \begin{bmatrix} Q_{j(s)} \\ Q_{j+1(s)} \end{bmatrix} \quad (8.8)\ [84]$$

Transformation function:

$$w_{j(s)} = \frac{e^{2\Gamma_j l_j + 1}}{e^{2\Gamma_j l_j - 1}} \qquad (8.9)\ [84]$$

$$\sqrt{(w_1^2(s) - 1)} = \frac{2e^{l_1\Gamma_1(s)}}{e^{2l_1\Gamma_1(s)} - 1}$$

Transformation functions in delay form:

$$w_1(s) = \frac{1 + e^{-2l_1\Gamma_1(s)}}{1 - e^{-2l_1\Gamma_1(s)}}$$

$$\sqrt{(w_1^2(s) - 1)} = \frac{2e^{-l_1\Gamma_1(s)}}{1 - e^{-2l_1\Gamma_1(s)}}$$

Propagation operator:

$$\Gamma_{(s)} = \frac{ls}{V_s} \qquad (8.10)\ [84]$$

Characteristic Impedance:

$$\zeta_{(s)} = \frac{\rho_0 V_S}{\pi r^2} \qquad (8.11)\ [84]$$

Where:

$Q$ is the volume flow rate ($Q = f(t)$) and $l$ is the intake length, $l = 0.3\ m$, $V_S$ , sonic velocity (air), $V_S$ = 343 m/s; s – Laplace Variable and r is the radius of the intake pipe, $r$ = 0.03 m with $\rho_0$ – air density, $\rho_0$ = 1.225 kg/m$^3$.

For $j = 1$

$$\begin{bmatrix} p_1(s) \\ p_2(s) \end{bmatrix} = \begin{bmatrix} \zeta_1 w_1(s) & -\zeta_j\sqrt{(w_1^2(s)-1)} \\ \zeta_j\sqrt{(w_1^2(s)-1)} & -\zeta_1 w_1(s) \end{bmatrix} \times \begin{bmatrix} Q_1(s) \\ Q_2(s) \end{bmatrix}$$

$$\begin{bmatrix} p_1(s) \\ p_2 \end{bmatrix} = \begin{bmatrix} \zeta_1 w_1(s) & -\zeta_j\sqrt{(w_1^2(s)-1)} \\ \zeta_j\sqrt{(w_1^2(s)-1)} & -\zeta_1 w_1(s) \end{bmatrix} \times \begin{bmatrix} Q_1(s) \\ Q_2(s) \end{bmatrix}$$

$$\begin{bmatrix} p_1(s) \\ p_2(s) \end{bmatrix} = \frac{\begin{bmatrix} a_{22} & -a_{12} \\ -a_{21} & a_{11} \end{bmatrix}}{\Delta} x \begin{bmatrix} T_m(s) \\ 0 \end{bmatrix}$$

Where,

$a_{11} = \zeta_1 w_1(s)$

$a_{12} = -\zeta_1\sqrt{(w_1{}^2(s)-1)}$

$a_{21} = \zeta_1\sqrt{(w_1{}^2(s)-1)}$

$a_{22} = -\zeta_1 w_1(s)$

$\Delta = a_{11}a_{22} - a_{12}a_{21}$

Therefore,

$$\frac{Q_1(s)}{p_1(s)} = \frac{a_{22}}{a_{11}a_{22} - a_{12}a_{21}}$$

$$\frac{Q_2(s)}{p_1(s)} = \frac{-a_{21}}{a_{11}a_{22} - a_{12}a_{21}}$$

Substituting assumptions $a_{11}$ to $a_{22}$

$\Delta = \zeta^2$

$$\frac{Q_1(s)}{p_1(s)} = \frac{-\zeta_1 w_1(s)}{\zeta^2} \qquad \Longrightarrow Q_1(s) = \frac{-\zeta_1 w_1(s)}{\zeta^2} \times p_1(s)$$

$$\frac{Q_2(s)}{p_1(s)} = \frac{\zeta_1\sqrt{({w_1}^2(s)-1)}}{\zeta^2} \quad \Longrightarrow Q_2(s) = \frac{\zeta_1\sqrt{({w_1}^2(s)-1)}}{\zeta^2} \times p_1(s)$$

### 8.3 Simulation of the DL model

Using the equation developed in previous section the block diagram model of the intake system is developed as shown in figure 8.5**.** Using the block diagram model it is possible to investigate the air flow in the intake system by developing a Simulink model as shown in figure 8.6.

The results of the simulation model are given in figure 8.7, $y_1$, $y_2$ and $y_3$ for a variety of engine speeds.

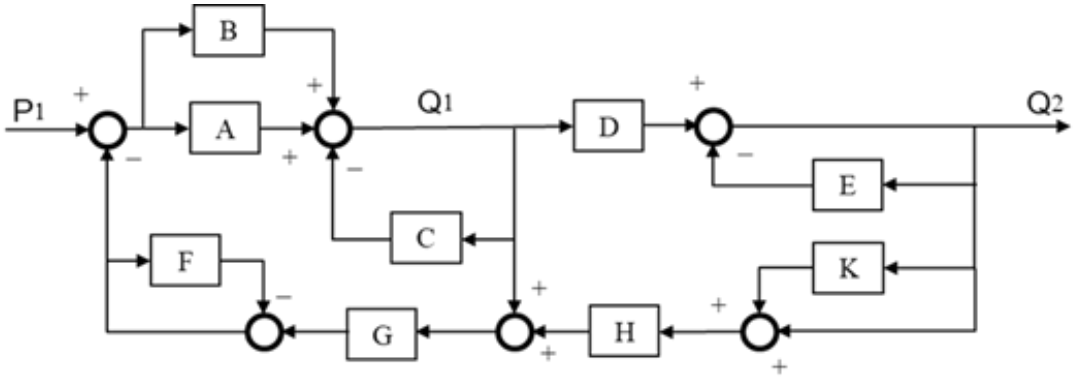


Figure 8.5 Block diagram model for simulation of the system

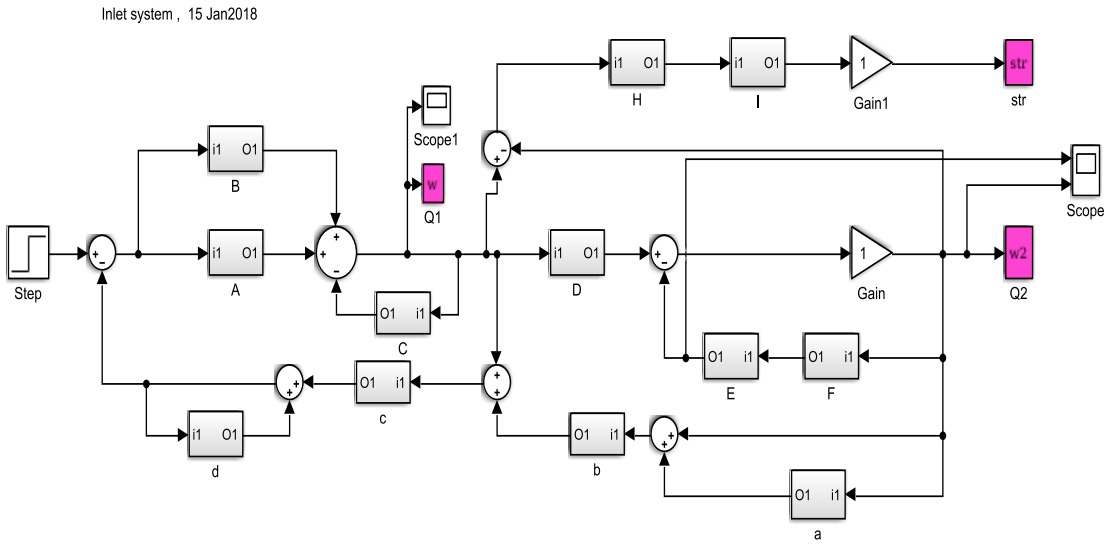


Figure 8.6 Simulink model of the system

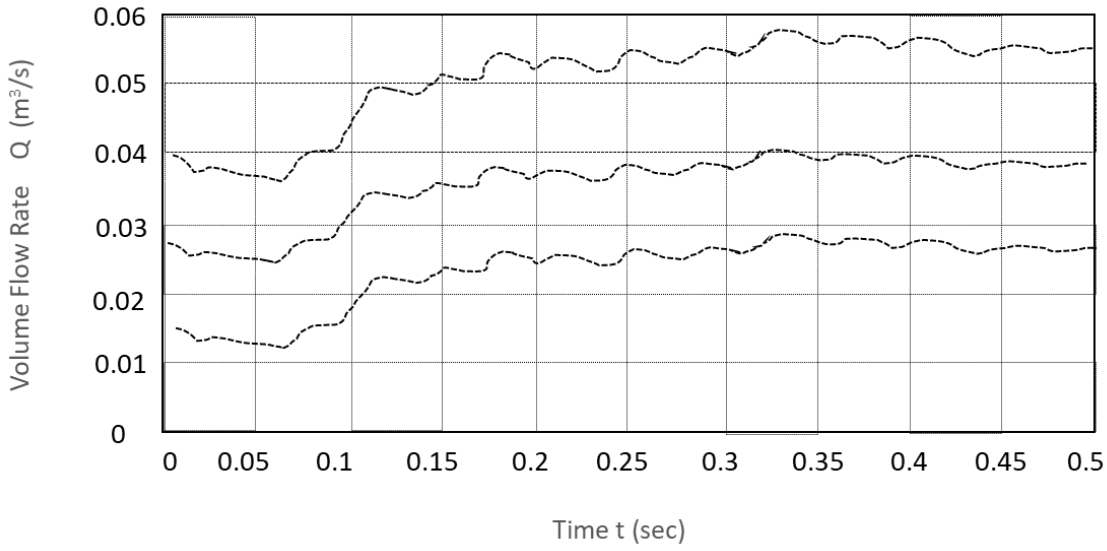


Figure 8.7 Output response of the DL model

## 8.4 CFD Modelling

In this section a computational fluid dynamic (CFD) model is presented. The Computational Fluid Dynamics (CFD) approach allows for the simulation of the intake system performance under different operational and ambient conditions in the early development stages. Thus, eliminating design variations with low performance parameters. The theoretical data obtained by the CFD simulations allow us to gain a deeper understanding of the complex mass and energy transfer processes during the intake system operation. [86]

The air intake and filter system have a significant effect over the performance and efficiency of an engine. This system directly affects the engine combustion efficiency and the emission of greenhouse gases and solid particles in the atmosphere. A major component of the system is the air filter, it removes the solid particle pollutants like dust, dirt and soot from the intake air, thus ensuring optimal performance of the engine and protecting it from damage.

The internal combustion engine intake system can be characterized by three general criteria. The first criteria encompass the intake air filtering. The intake system must provide clean, filtered air to the engine. The second and third criteria which are of importance to the intake design process are the flow and acoustic performance. The engine overall power performance and efficiency is directly influenced by the intake flow parameters. The operational cycle of a four-stroke internal combustion engine consists of four consecutive processes, namely intake, compression, combustion-expansion and exhaust. The intake and compression strokes have predominant influence over the flow distribution and parameters in the cylinder during the intake stroke and the subsequent compression stroke. Due to the high velocities of the flow during the engine operation the flow inside in the cylinder is predominantly turbulent. The maximization the air mass inducted into the cylinder during the intake stroke can be achieved by optimisation of the intake system.

To meet the Government regulated noise level emission standard the noise emitted by a vehicle must by lower than the upper limit of the allowed noise level. The flow speed in an intake system can reach high values, which can contribute to the overall vehicle noise generation. The acoustic and flow performance of the intake system are interconnected. The balance between acoustic and flow performance is the main objective of the design development stage.

The preliminary evaluation of both acoustic and flow performance can be achieved with numerical simulation procedures.

The main objective of the CFD is to provide a robust and computationally inexpensive numerical modelling approach for intake system flow aerodynamics and performance preliminary evaluation. The numerical modelling allows for the analysis of the main geometrical parameters influence over the system operation. To meet the main objective of the present study the following tasks are established:

- Development of a simplified geometrical model of the intake system;
- Generation of computational mesh with reasonable density;
- Setup of the numerical modelling procedure;
- Analysis of the theoretical results.

### 8.4.1. Computational Mesh Generation

The properties of the computational mesh have significant effect over the accuracy and reliability of the numerical results. To capture in detail the three-dimensional, unsteady nature of the intake flow the computational mesh should be refined with high quality mesh metric parameters. In the present study an unstructured tetrahedral mesh was adopted. The unstructured type of mesh is easier to generate, manipulate and apply to complex geometries in comparison with the structured type meshes. The unstructured mesh provides a good balance between reasonable modelling accuracy and mesh generation efforts.

The mesh for the current study was generated by the commercial mesh generator ANSYS Meshing. The number of mesh cells generated is around 450,000. The minimum size of the fluid cells was set to 0.001 mm, while the maximum size was set to 4 mm. The mesh has been refined and modified until the satisfactory value of 0.814 for the mesh metric parameter was

obtained. Mesh metric values closer to 1 are desirable. The generated computational mesh is presented in figure 8.8.

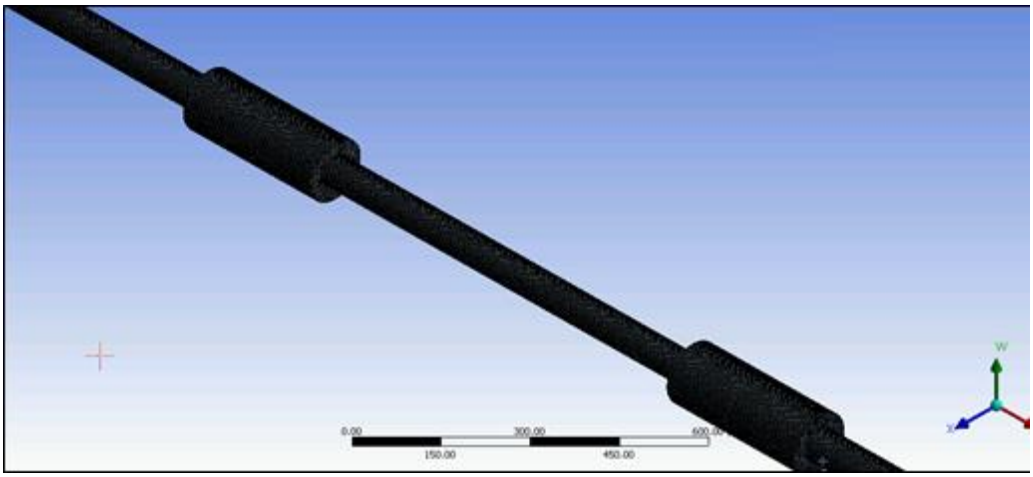

Figure 8.8 Unstructured Tetrahedral Computational Mesh

8.4.2 Governing Equations

The governing mass and impulse conservation equations for a one-dimensional compressible viscous Newton fluid flow are:

$$\frac{\partial \rho}{\partial t} + \rho_0 \frac{\partial u_i}{\partial x_j} = 0$$

$$\rho \frac{\partial u_i}{\partial t} + \rho u_i \frac{\partial u_i}{\partial x_j} = -\frac{\partial p}{\partial x_j} + \frac{\partial T_{ij}}{\partial x_j}$$

where $u_i$ is velocity component, $x_j$ is direction of a component, $t$ is time, $p$ is pressure, $\rho$ is density, $p$ is pressure and $T_{ij}$ is viscous stress tensor.

The current analysis adopts the unsteady time averaged fluid flow modelling approach or the Unsteady Reynolds Averaged Navier-Stokes (URANS) numerical modelling procedure. The URANS modelling approximates the

dynamic nature of an unsteady turbulent fluid flow through time averaging of the flow velocity components fluctuations. Thus, the flow turbulence is not directly calculated through the governing equations, but rather its averaged effect over the mean flow is modelled.

### 8.4.3 Turbulence Model

The turbulence closure models are introducing additional transport terms to the governing equations (URANS), thus introducing the turbulent fluctuations caused by the vortex structures of different sizes to the main flow. The turbulence model is bringing the governing system of equations to a numerically solvable state.

The turbulence model adopted in the present study is the standard $k$-$\varepsilon$ turbulence model. The $k$-$\varepsilon$ model uses a set of two additional equations to estimate the turbulence kinetic energy and dissipation. The standard $k$-$\varepsilon$ model provides reasonable accuracy results in a relatively wide range of fluid flow regimes. The standard wall function was chosen for the near-wall boundary layer treatment. The standard wall function is applicable for a broad spectre of internal fluid flows with high Reynolds number.

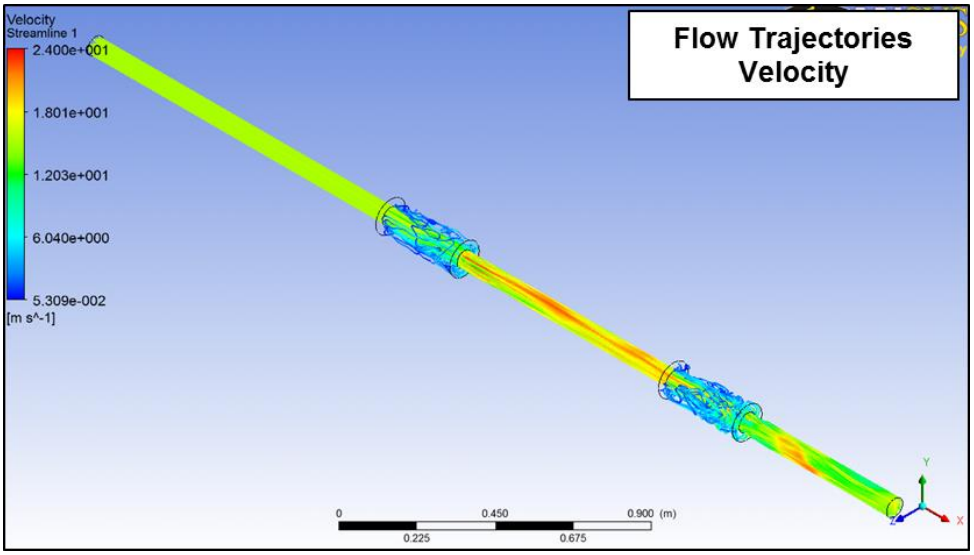


Figure 8.9 CFD model of the inlet system showing the air flow trajectories

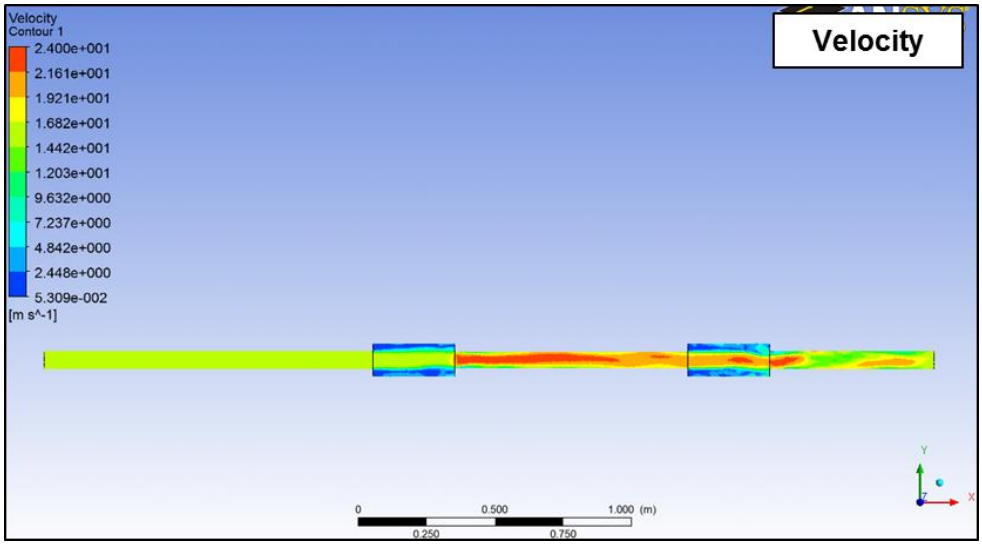


Figure 8.10 CFD model of the inlet system showing the air flow velocity profile

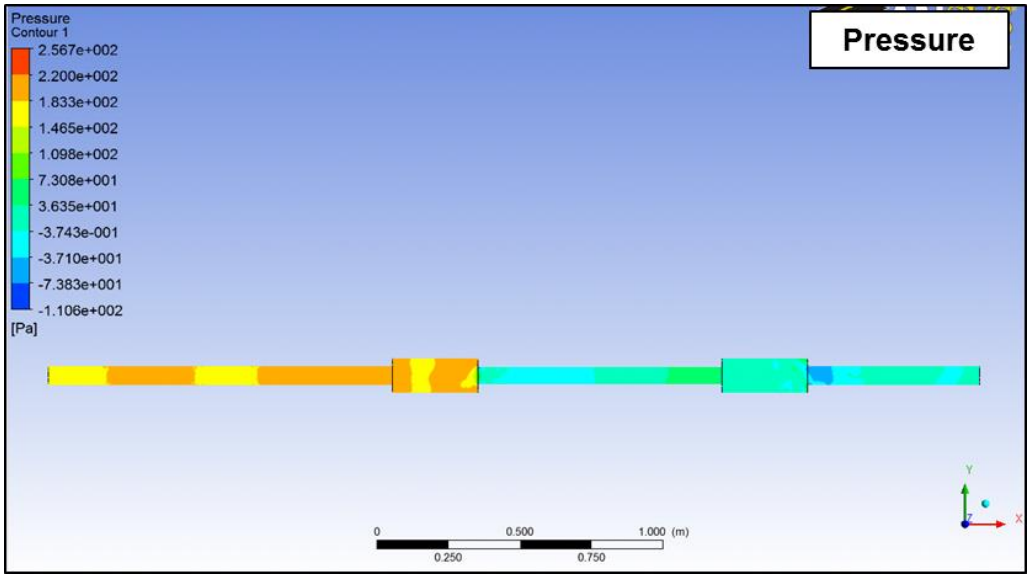


Figure 8.11 CFD model of the inlet system showing the pressure changes

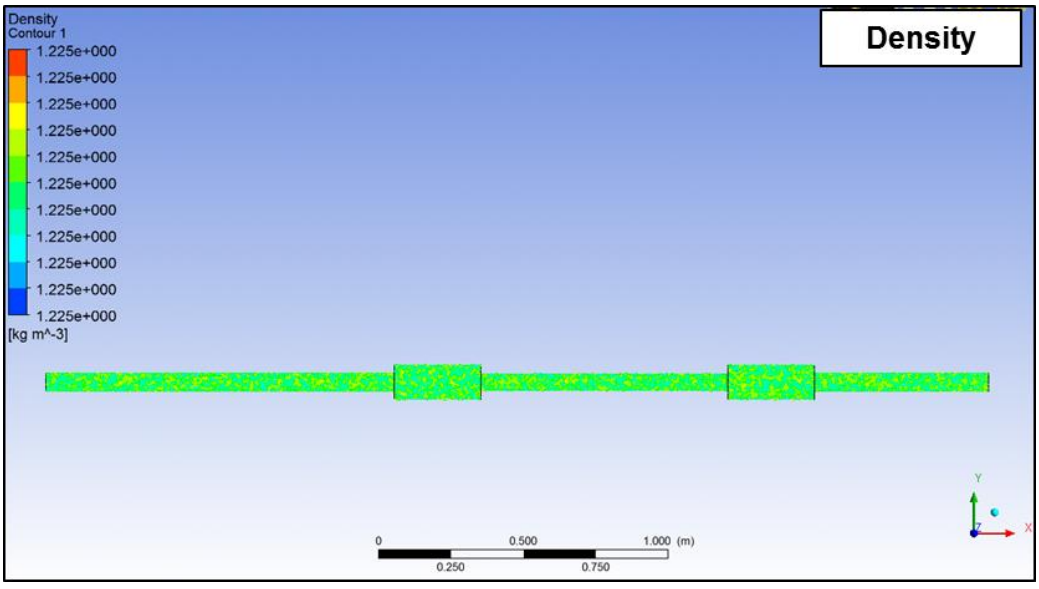


Figure 8.12 CFD model of the inlet system showing the variation in density

To validate the virtual sensor the distributed lumped model is validated against the CFD model derived in this section and the result is shown in figure 8.13. As it can be seen from the results a good correlation exists

between the results from the CFD simulation and the DL (virtual sensor) simulation result. The main difference being in the computational time for the results. The CPU time for the CFD computation was as much as 10 times greater than the computation time for the DL model. This shows that it is possible to use the virtual sensor for realtime applications as suggested in this thesis. The results further indicate as the number of the mesh (smaller mesh size) in the CFD model is increased the results tend to move closer to the DL model therefore they have higher accuracy. Consequently the increase in the number of mesh in the CFD directly results in computational time, which indicates that the CFD could not be used as a virtual sensor (realtime) in the engine control unit.

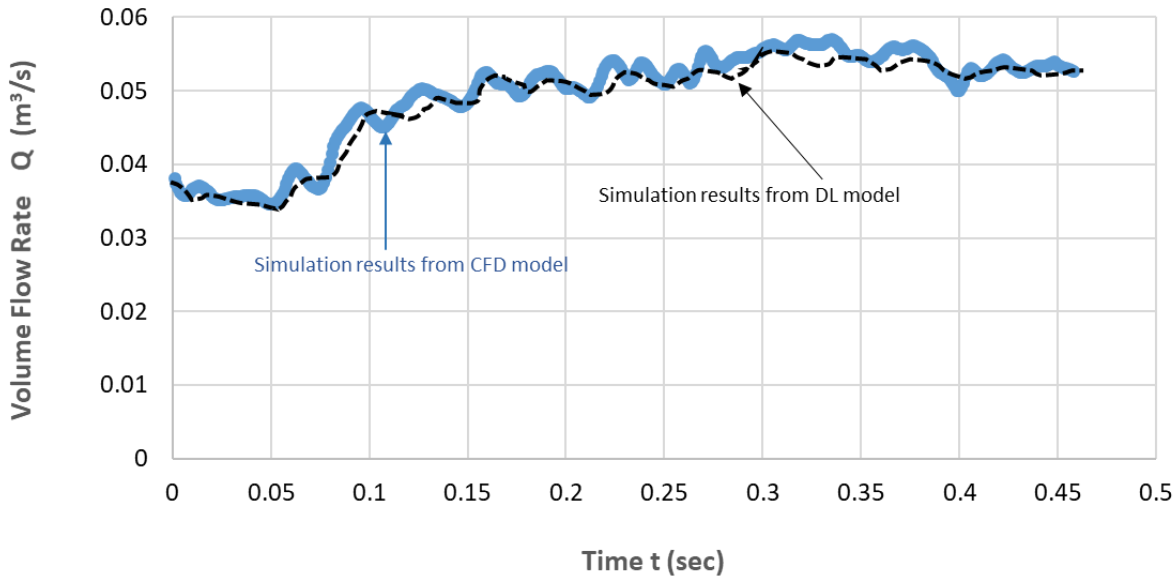


Figure 8.13 Validation of the DL model against the CFD model

### 8.5 Quantification of the results – Summary

This chapter showed the theoretical analysis for the distributed lumped model of the intake system which is the base of the virtual sensor proposed in the thesis. The developed model was validated against the CFD model which is simulated in ANSYS software. Looking at figure 8.13 it can be seen that the flow rate for the D-L model is around 0.052 $m^3$/s and by multiplying that with the density of air at 20 degrees which is 1.2 kg/$m^3$ the result is 0.062 kg/ s or 223 kg/hr. Similarly the CFD model predicts 0.055 $m^3$/s or 237.6 kg/hr. By comparing these numbers it can be observed that the CFD model over predicts the air mass flow of the engine by 6.55% compared to the D-L model. Now comparing these two simulation results with the actual data from the dyno which is 220 kg/hr (figure 7.7) it can be seen that the D-L model is extremely close to the real engine data over predicting the engine air mass flow only by 1.36% while the CFD simulation data show an increase of 8% compared to the real engine data. The above quantification is very encouraging because it proves that the virtual sensor (D-L model) is very close to the actual engine air flow and below the 5% error which is the measure of success within the sponsor's organisation (Ford Motor Company).

# Chapter 9: Conclusions and future work

## 9.1 Conclusions

The main contributions of this thesis can be summarised below as:

- Literature review on engine air mass flow measurement emphasising on different methods of engine air mass prediction such as mathematical modelling
- Explaining the importance of air mass flow measurement for the operation of a SI internal combustion engine.
- Development of state of the art transient testing methodology for engine air mass flow characterisation
- Development of 1D engine WAVE model for engine air mass flow prediction
- Development of D-L model in SIMULINK for determining the air mass flow into the cylinder of an engine.

The literature review clarified the main problem which exists with the current air mass flow measurement techniques which mainly is inaccuracy and long modelling and testing process for engine calibration which also justifies why the method described in this project is more accurate and efficient as it can run on real time during engine operation.

## 9.2 Future work

The next step after completion of this work is to implement the developed model into the engine's ECU. This can be achieved by using rapid control prototyping software. Rapid control prototyping software gives engineers the ability to modify ECU functionality without modifying the original ECU's source code (strategy). It is mainly used for control development purposes. The key features of such a technique are:

- Can be implemented using the current ECU calibration software as described in chapter 4
- No need for recompiling the source code (ECU strategy)
- No modification to the original source code needed

The key advantages of such a technique are:

- Shortens the development cycle
- Can be directly implemented to the development ECU used in this project since there is plenty of memory available
- Is compatible with Matlab which is the software used for model development
- Simulates sensor or actuator faults to check if the system reacts correctly

In figure 9.1 below a schematic representation of how rapid control prototyping works can be seen.

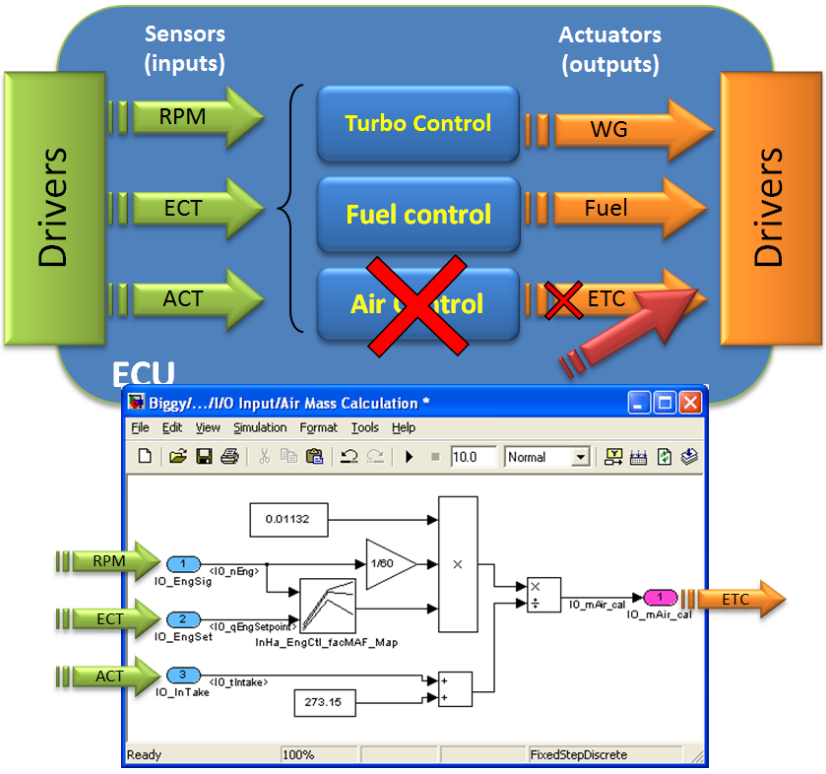


Figure 9.1 Rapid control prototyping schematic representation

As shown in figure 9.1 for controls development, rapid prototyping enables users to bypass the original ECU code and create their own calculations, models which can be implemented into the ECU in real time. The reason this step is considered very important is because it gives the opportunity to take the output of this work which is the D-L model and directly implement it into the ECU of the development engine. By doing that, the model will be running real time during engine operation. This means that the ECU's strategy air mass flow prediction, which is based on the speed-density, will be by-passed and the D-L model will be used instead. If the results are as accurate as they are expected to be, then the mapping process of the engine will be more efficient and more accurate than the current process. This will hopefully lead to an improvement on the overall performance of the engine.

## References

[1] Bosch group, Automotive electrics and automotive electronics. Springer, 2014. ISBN: 978-3-658-01784-2

[2] M. Kaiser, Bosch Group, Gasoline engine management systems and components. Springer, 2015. ISBN: 978-3-658-03964-6

[3] Bosch group, Gasoline fuel injection system K- Jetronic. Robert Bosch GmbH, 2000

[4] Denso Group, A history of engine management systems according to Denso article. Denso Automotive, 2014

[5] N.F. Benninger, G. Flapp, Requirements and performance of engine management systems under transient conditions. SAE 910083, 1991

[6] I. Kolmanovsky, P. Moral et al, Issues in modelling and control of intake flow in variable geometry turbocharged engines. IFIP TC7 Conference, Detroit USA, 1997

[7] P. Anderson, Air charge estimation in turbocharged spark ignition engines. PhD thesis, Linkoping University, 2005

[8] N.P. Fekete, U. Nester et al, Model- based air fuel ratio control of a lean burn multi cylinder engine. SAE 950846, 1995

[9] J. Grizzle, J. Cook and W. Milam, Improved cylinder air charge estimation for transient air fuel ratio control. American control conference (ACC), 1994

[10] M. Vojtisek, M. Kotek, Estimation of engine intake air mass flow using a generic speed- density method. Journal of middle European construction and design of cars, issue 1, pp 7-15, 2014

[11] M. Nyberg, L. Nielsen, Model based diagnosis for the air intake system of the SI engine. SAE 970209, 1997

[12] J. Adida, D. Claude, Spark ignition engine and pollution emission: New approaches in modelling and control. International journal of vehicle design, vol 15, 1994

[13] C.H. Onder, C.A. Roduner and H.P. Geering, Model identification for the a/f path of an SI engine. SAE 970612, 1997

[14] A. Di Gaeta, L. Glielmo et al, An extended Kalman observer for the in-cylinder air mass flow estimation. International conference on nonlinear dynamics in process engineering, Italy, 2002

[15] E. Hendricks, J. Poulsen et al, Alternative observers for SI engine air/fuel ratio control. Conference on decision and control, Japan, 1996

[16] E. Hendricks, T. Vesterholm et al, Nonlinear closed loop SI engine control observers. SAE 920237, 1992

[17] P. Anderson, L. Eriksson, Air to cylinder observer on a turbocharged SI engine with waste gate. SAE Conference, number: 2001-01-0262, 2001

[18] A. Chevalier, C.W. Viglid and E. Hendricks, Predicting the port air mass flow of SI engines in air- fuel ratio control applications. SAE 2000-01-0260, 2000

[19] E. Hendricks, M. Jensen et al, Transient air fuel ratio errors in conventional SI engine controllers. SAE 930856, 1993

[20] E. Hendricks, A. Chevalier et al, Modelling of the manifold filling dynamics. SAE 960037, 1996

[21] E. Hendricks, A. Chevalier et al, Event based engine control: practical problems and solutions. SAE 95008, 1995

[22] T.C. Cheng, W.K. Cheng, An adaptive air fuel ratio controller for SI engine throttle transients. SAE 1999-01-0552, 1999

[23] J.A. Cook, B. Powell, Modelling of an internal combustion engine for control analysis. IEEE, 1988.

[24] J.J Moskwa, J.K. Hendrick, Modelling and validation of automotive engines for control algorithm development, ASME journal of dynamic systems, measurement and control, vol. 114, pp. 278-285, 1992

[25] J.J. Moskwa, J.K. Hendrick, Automotive engine modelling for real time control applications. ACC, 1987

[26] E. Hendricks, S.C. Sorenson, Mean value modelling of spark ignition engines. SAE, 1990. ISSN: 0148-7191

[27] E. Hendricks, S.C. Sorenson, SI engine controls and mean value engine modelling. SAE 910258, 1991

[28] R.W. Weeks, J.J. Moskwa, Automotive engine modelling for real time control using MATLAB/SIMULINK. SAE, 1995. ISBN: 1560916303

[29] Y. He, C. Lin, Development and validation of a mean value engine model for integrated engine and control system simulation. SAE, 2007. ISBN: 0148-7191

[30] C. Onder, H.P. Geering, Engine management without air mass flow meter. FISITA world automotive congress, Korea, 2000

[31] A. Chevalier, M. Muller, E. Hendricks, On the validity of mean value engine models during transient operation. SAE world congress, Detroit USA, 2000

[32] S. Yurkovich, M. Simpson, Crank angle domain modelling and control for idle speed. SAE 970027, 1997

[33] S. Amphlett, T. Fickenscher et al, Crank angle resolved real time engine simulation for the optimisation of control strategies. MTZ Worldwide, Volume 69, pp 50-55, 2008

[34] P. Casoli, A. Gambarotta et al, Development and validation of a crank angle model of an automotive turbocharged engine for HIL applications. Elsevier, 2014

[35] X. Yang and G.G. Zhu, A mixed mean value and crank based engine model of a dual stage turbocharged SI engine for hardware in the loop simulation. American control conference, Baltimore, USA, 2010

[36] J.A. Cook, J. Sun et al, Opportunities in automotive powertrain control applications. IEEE 7th Conference on control applications, Glasgow, UK, 2002

[37] A.G. Stefanopoulou, J.A. Cook et al, Control oriented model of a dual equal variable cam timing SI engine. ASME journal of dynamic systems, Vol. 120, pp 257-266, 1998

[38] M. Jankovich, F. Frischmuth et al, Torque management of engines with variable cam timing. IEEE control systems magazine, Vol. 18, pp34-42, 1998

[39] E.P. Brandt, Y. Yang and J.W. Grizzle, Dynamic modelling of a three way catalyst for SI engine exhaust emission control. IEEE transactions on control system technology, Vol. 8, pp 767-776, 2000

[40] J.B. Heywood, Internal combustion engine fundamentals. McGraw- Hill, 1988

[41] C.F. Taylor, The internal combustion engine in theory and practice, volume 1. The M.I.T press, 2nd edition, ISBN: 0262700263, 1994

[42] S.B. Choi, M. Won and J.K. Hendrick, Fuel injection control of SI engines. CDC Conference, Florida, USA, 1994

[43] E. Achleitner, H. Werner et al, Electronic engine control system for gasoline engines for LEV and ULEV standards. SAE 940479, 1995

[44] G. Banish, Engine management: Advanced tuning 1st edition. CarTech, 2007 ISBN: 1932494421

[45] C. Hardie et al, Automated tuning of an engine management unit for an automotive engine. IMechE, journal of automobile engineering, Vol. 215, pp 841-849, 2002

[46] J. Turner, Automotive sensors. Momentum press, 2009. ISBN: 1606500090

[47] E.F.Brooks, G.D.Barnicoat, Air flow measurement techniques for air fuel ratio control. IEEE, 1981. IEEE: 10.1109/VTC.1981.1622906

[48] P.Zylka, P.Modrzynski, P.Janus, Vortex anemometer using MEMS cantilever sensor. IEEE, 2010. IEEE: 10.1109/JMEMS.2010.2079916

[49] R. Stone, Introduction to internal combustion engines. Palgrave – Macmillan, 1999. ISBN: 10:0-333-74013-0

[50] Lei X. et al, Airflow estimation control strategy based on speed density method. SAE- China, 2014. ISBN: 978-3-662-45042-0

[51] T. Mukawa, Y. Goto et al, Development of a plastic inlet manifold. SAE Japan, 1995. ISBN: 10.1016/0389-4304

[52] Mann –Hummel group, Air intake system and modules, systematic tuning of all aspects of air induction. Mann – Hummel GmbH sales automotive, 2011

[53] W. J. Fleming, Overview of automotive sensors. IEEE, 2001. ISBN: 10.1109/7361.983469

[54] Robert Bosch GmbH, Bosch automotive handbook 9th edition. 2014. ISBN: 0837617324

[55] K. Hirschfelder et al, The first continuously variable intake system in the new eight cylinder BMW engine. BMW AG, 2002

[56] J. Halderman, Automotive fuel and emission control systems 4th edition. Pearson, 2015. ISBN: 0133799492

[57] R. Isermann, Engine modelling and control, modelling and electronic management of internal combustion engines. Springer, 2014. ISBN: 978-3-642-39934-3

[58] P.E. Moraal, J. A. Cook and J. W. Grizzle, Modelling the induction process of an automobile engine. Control problems in industry, pp253-270, Birkhauser, 1995

[59] I.V. Kolmanovsky, J. Sun and M. Druzhinina, Charge control for direct injection SI engines with EGR. American control conference, Chicago, 2000

[60] G. Smith, Ford Fox Upgrade GTDI dynamometer debug procedure to support engine dynamometer testing. Ford Motor Company, 2015

[61] J. Killedar, Dynamometer: Theory and application to engine testing. Xlibris, 2012. ISBN: 1477120068

[62] AVL List, AVL Flowsonix air product guide. AVL List GmbH, 2015

[63] H. Klingenberg, Automobile exhaust emission testing. Springer, 1996. ISBN: 978-3-642-80245-4

[64] A.J. Martyr, M.A. Plint, Engine testing, the design, building, modification and use of powertrain test facilities. Butterworth- Heinemann, 2012. ISBN: 0080969496

[65] AVL List, AVL Puma open 2012 release notes. AVL List GmbH, 2012

[66] K. Hupp, ATI Vision calibration and data acquisition user manual. Accurate technologies Inc., 2015

[67] AVL List, AVL IndiCom 2015 exploration guide. AVL List GmbH, 2015

[68] P. Schaal, S. Filippou et al, Robust methodology for fast crank angle based temperature measurement. SAE, 2016. ISBN: 10.4271/2016-01-1072

[69] ATI EMX data acquisition module series user manual. Accurate technologies Inc., 2016

[70] AVL List, AVL X-ION acquisition platform product guide. AVL List GmbH, 2016

[71] A.M. Gallacher, W.H. Krebl, Dynamic engine testing: Why? SAE- Brazil, 1995. ISBN: 0148-7191

[72] E.W. Hislop, Dynamic testing of internal combustion engines, PhD thesis, University of London, 1978

[73] K. Hupp, ATI Vision API command reference guide. Accurate technologies Inc., 2014

[74] S.J. Chapman, MATLAB programming for engineers 5th edition. CL engineering, 2015. ISBN: 1111576718

[75] B. Liu, J. Zhao et al, Design and analysis of test signals for system identification. ICCS, 2006. ISBN: 978-3-540-34383-7

[76] M. Paulweber, K. Lebert, Powertrain instrumentation and test systems. Springer, 2016. ISBN: 978-3-319-32135-6

[77] R.D. Atkins, An introduction to engine testing and development. SAE International, 2009. ISBN: 0768020999

[78] L. Guzella, C.H. Onder, Introduction to modelling and control of internal combustion engines. Springer, 2009. ISBN: 978-3-642-10774-0

[79] S. Moraitis, Model based ECU mapping and calibration test rig using hardware in the loop. University of Bradford, MSc Thesis, 2009

[80] L. Eriksson, L. Nielsen, Modelling and control of engines and drivelines. Wiley, 2014. ISBN: 978-1-118-47999-5

[81] D. Cordon, C. Dean et al, One- dimensional engine modelling and validation using Ricardo WAVE. University of Idaho, US department of transportation, 2009

[82] K. Chan, A. Ordys et al, Comparison of engine simulation software for development of control system. Kingston University, 2013. ISBN: 10.1155/2013/401643

[83] Ricardo software, WAVE user manual version 2016.2. Ricardo Inc., 2016

[84] Whalley. R, The Response of Distributed—Lumped Parameter Systems Proc. IMechE Vol 202 No (4) C6 (1988) 422–431. pt. C.

[85] Ebrahimi K.M., Filippou S, Athanasiou P and Ahmedov, A., Port Based Modelling of Intake and Exhaust System, Submitted to IMechE Part D.

[86] Whalley R., Ebrahimi M. Optimum Wind Tunnel Regulation, Proc. IMechE 215 (4) (2001) 241–252. pt. G.

# Appendix A: Combustion indicating software code

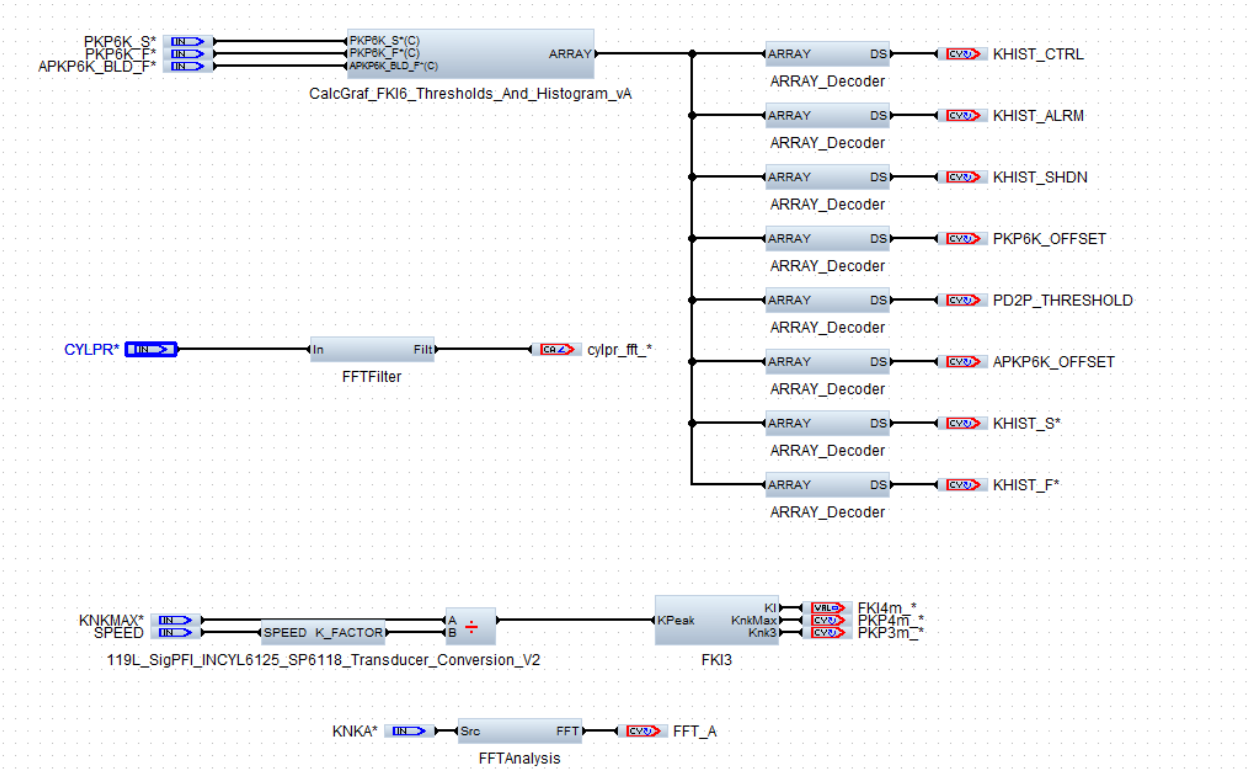

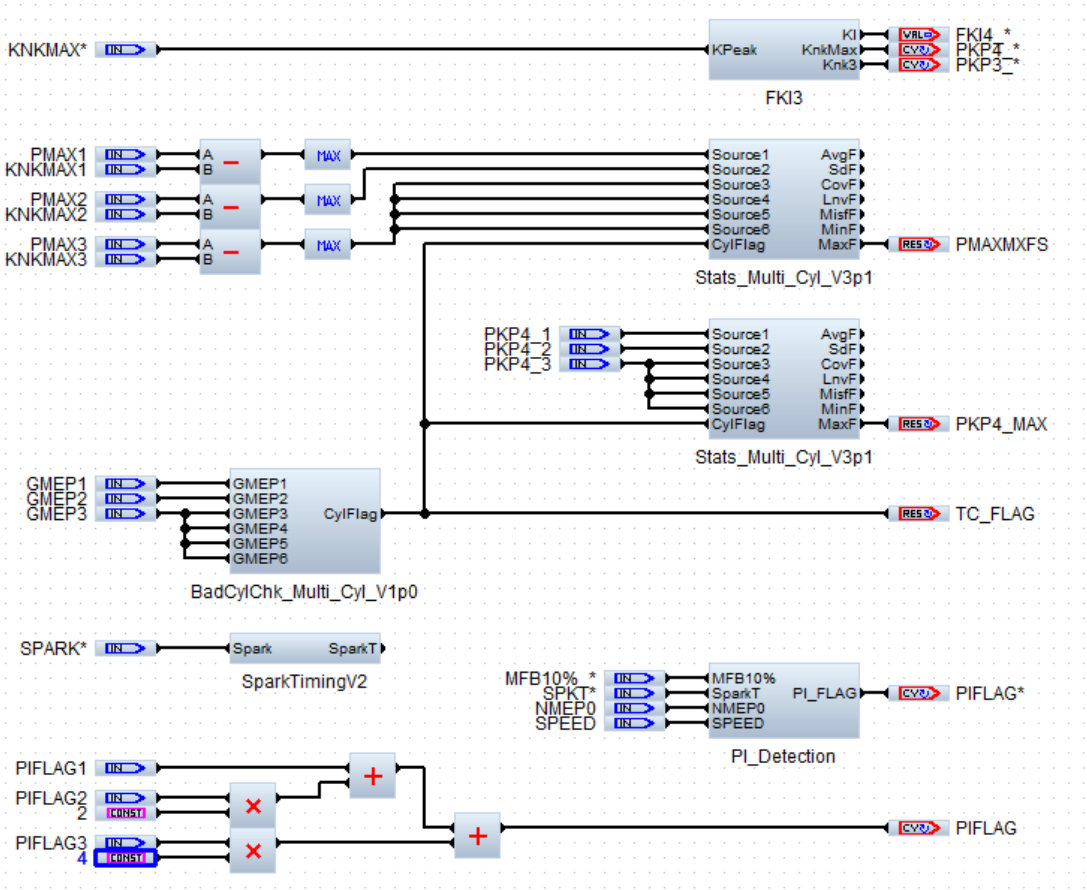
KNKMAX*
KPeak
KI
KnkMax
Knk3
FKI4_*
PKP4_*
PKP3_*
FKI3
PMAX1
KNKMAX1
PMAX2
KNKMAX2
PMAX3
KNKMAX3
A
B
MAX
Source1
Source2
Source3
Source4
Source5
Source6
CylFlag
AvgF
SdF
CovF
LnvF
MisfF
MinF
MaxF
PMAXMXFS
Stats_Multi_Cyl_V3p1
PKP4_1
PKP4_2
PKP4_3
PKP4_MAX
Stats_Multi_Cyl_V3p1
GMEP1
GMEP2
GMEP3
GMEP4
GMEP5
GMEP6
CylFlag
TC_FLAG
BadCylChk_Multi_Cyl_V1p0
SPARK*
Spark
SparkT
SparkTimingV2
MFB10%_*
SPKT*
NMEP0
SPEED
MFB10%
SparkT
PI_FLAG
PIFLAG*
PI_Detection
PIFLAG1
PIFLAG2
2
PIFLAG3
4
CONST
PIFLAG

# Appendix B: Matlab software code

```
%% randomly generated signal


start_time = 0;
end_time = 20;          %seconds
duration = end_time - start_time;
sample_time = 0.05;

time = [start_time:sample_time:end_time];

min_val = 0.15;
max_val = 0.5;

min_hold = 0.1;
max_hold = 1;

n = duration/min_hold;

%generate hold times
holds = (max_hold-min_hold).*rand(n,1) + min_hold;
cumholds = cumsum(holds);

%generate amplitudes
amps = (max_val-min_val).*rand(n,1) + min_val;
total = sum(amps);

%align amps with holds
count = 1;

for i = 1:length(time)              %checks to see if time(i) has been exceeded
    if time(i) < cumholds(count)
        value(i) = amps(count);
    else
        count = count + 1;          %if it has the counter is incremented
        value(i) = amps(count);
    end
end
```

```
% Automated  test via MATLAB - ATI VISION communication
% Torque (Spark) Experiment
% Created by  S. Filippou
% Version 1.0 (23-05-2016)

% Camshafts are set to Automatic !!
```

```
%% Initialise Programme

clear;clc; % Clear Command Window and Workspace
```

```
%% MATLAB - ATI VISION Communication
OP = 1;
%Create the Project object
Project = actxserver('Vision.ProjectInterface');

%Go Online
Project.Online = 1;

%Find PCM and set it to Device
Device = Project.FindDevice('PCM');

%Create a screen object
Screen = Project.ScreenOpen('MATEC');

% Find the Recorder1 Object in ATI Vision
% Recorder1 = Screen.FindControl('Recorder1');

% Settings
(refer to VISION API Command Reference Guide)

Recorder1 settings
Recorder1.PreTriggerPeriod = 0;
Recorder1.PreTriggerPeriodUnits = 2;
Recorder1.PostTriggerPeriod = 60;
Recorder1.PostTriggerPeriodUnits = 2;
Recorder1.DefaultSamplePeriod = 6;
Recorder1.RecorderFileDirectoryPath = ...
    'C:\Users\Application PC\Desktop\MATEC_Tests';
Recorder1.AutoExport = 1;
Recorder1.ExportFormat = 1;
```

```
%% Define and Set PCM Calibration Variables

% Define
SPK_MUL = Device.FindScalar('SPK_MUL');
SPK_ADD = Device.FindScalar('SPK_ADD');
```